

Dissertation zur Erlangung des Doktorgrades der Naturwissenschaften
der Fakultät für Biologie
der Ludwig-Maximilians-Universität
München

Analysis of genomic alterations in malignant melanoma

vorgelegt von

Henrike Körner

am 02.05.2007

Die Arbeit wurde am Max-Planck Institut für Biochemie (Martinsried)
in der NWG Molekulare Onkologie angefertigt.

First examiner:

PD Dr. Heiko Hermeking

Second examiner:

Prof. Dr. Thomas Cremer

Additional examiners:

Prof. Dr. Michael Boshart

Prof. Dr. Heinrich Leonhardt

Date of the oral examination:

05.12.2007

Erklärung

Hiermit erkläre ich, dass ich die vorliegende Dissertation selbstständig verfasst habe und keine anderen als die von mir angegebenen Quellen und Hilfsmittel benutzt habe. Sämtliche Experimente sind von mir selbst durchgeführt worden, außer wenn explizit auf dritte verwiesen wird. Ferner erkläre ich, dass ich nicht anderweitig versucht habe, eine Dissertation oder Teile einer Dissertation einzureichen bzw. einer Prüfungskommission vorzulegen oder mich einer Doktorprüfung zu unterziehen.

München, den 07.12.07

Henrike Körner

TABLE OF CONTENT

1	INTRODUCTION.....	1
1.1	Cutaneous malignant melanoma.....	1
1.1.1	Germ line mutations in melanoma	3
1.1.1.1	CDKN2A	3
1.1.1.2	CDK4	5
1.1.2	Pigmentary traits.....	6
1.1.3	Somatic mutations in melanoma.....	7
1.1.3.1	Mitogen-activated protein kinase signaling pathway.....	7
1.1.3.2	HGF/SF-MET signaling pathway	8
1.1.3.3	PTEN-AKT signaling pathway.....	8
1.2	Methods for cytogenetic and whole-genome analyses.....	9
1.2.1	Fluorescence <i>in situ</i> hybridization.....	10
1.2.2	Comparative genomic hybridization.....	11
1.2.3	Digital karyotyping	12
1.3	Dystrophin	15
1.3.1	<i>DMD</i> gene and isoforms	15
1.3.2	Dystrophin protein.....	17
1.3.3	Duchenne and Becker Muscular Dystrophies.....	18
1.3.4	Mutations in <i>DMD</i>	19
1.3.5	Dystrophin-glycoprotein complex.....	20
2	AIM OF THE STUDY	22
3	MATERIALS	23
3.1	Chemicals	23
3.2	Enzymes	24
3.3	Commercial kits and other materials	24
3.4	Buffers and stock solutions	25
3.5	Antibodies	28
3.5.1	Primary antibodies	28
3.5.2	Secondary antibodies	29
3.6	DNA constructs	29
3.7	Oligonucleotides.....	30

3.8	Bacteria strains	31
3.9	Cell lines and cell culture media	32
3.10	Equipment	32
4	METHODS	33
4.1	Chromosome metaphase spreads	33
4.2	Comparative genomic hybridization	33
4.3	7-Fluor M-FISH	34
4.4	Digital karyotyping	35
4.5	Isolation of genomic DNA from cell lines and paraffin-embedded tissue sections	40
4.6	RNA isolation and RT reaction	40
4.7	RT-PCR analysis	40
4.8	qPCR analysis	41
4.9	PCR analysis of genomic DNA	41
4.10	DNA sequencing	42
4.11	Western blot analysis	42
4.12	Generation of stable cell lines	42
4.13	Cell growth in matrigel	43
4.14	Cell migration assays	44
4.15	Cell proliferation assay	44
4.16	Analysis of apoptosis by flow cytometry	45
4.17	Senescence-associated β -galactosidase staining	45
4.18	Immunofluorescence staining and confocal microscopy	46
4.19	Statistical analysis	46
5	RESULTS	48
5.1	Characterization of malignant melanoma cell lines	48
5.1.1	General characteristics	48
5.1.2	M-FISH analysis of malignant melanoma cell lines	49
5.1.3	CGH analysis of malignant melanoma cell lines	58
5.2	Digital karyotyping analysis of malignant melanoma cell lines	63
5.2.1	Validation of the digital karyotyping results	63
5.3	Analysis of DMD in malignant melanoma	67

5.3.1	Deletion of <i>DMD</i> in malignant melanoma cell lines.....	67
5.3.2	Expression of <i>DMD</i> isoforms in primary melanocytes.....	68
5.3.3	Expression of dystrophin isoforms in melanoma cell lines.....	70
5.3.4	Functional analysis of dystrophin.....	75
5.3.4.1	Analysis of the components of the dystrophin-glycoprotein complex	75
5.3.4.2	Knockdown of <i>DMD</i> in melanoma cell lines.....	81
5.3.4.3	Re-expression of dystrophin in melanoma cell lines.....	83
6	DISCUSSION.....	86
6.1	Cytogenetic characterization of melanoma cell lines.....	86
6.2	Digital karyotyping of melanoma cell lines.....	89
6.3	Down-regulation of <i>DMD</i> in melanoma cell lines.....	90
6.4	The dystrophin-glycoprotein complex in melanocytes and melanoma cell lines.....	93
7	SUMMARY.....	96
8	REFERENCES.....	98
9	ABBREVIATIONS	130
10	APPENDIX.....	132
11	PUBLICATION LIST.....	137
12	ACKNOWLEDGEMENT	138
13	CURRICULUM VITAE	139

1 INTRODUCTION

1.1 *Cutaneous malignant melanoma*

Melanoma is a tumor arising from melanocytes, the neural crest-derived pigment-producing cells located in the skin, hair follicles, stria vascularis of the inner ear, and the uveal tract of the eye. Cutaneous malignant melanoma (CMM) represents roughly 5% of skin cancers and 1% of all malignant tumors. Its incidence has increased markedly over the past 40 years in white skinned populations (Micheli et al., 2002). Melanoma responds poorly to chemical and radiation therapy and the most effective treatment is surgical excision before the tumor is well advanced (for review see (Thompson et al., 2005)).

Five major steps of tumor progression have been described for cutaneous melanoma (Hsu et al., 2002) (Figure 1). The common acquired nevus is postulated as earliest benign hyperplastic melanocytic lesion, whereas the candidate precursor for cutaneous melanoma is the dysplastic nevus, which shows an increased level of cytological and architectural atypia (Kraemer and Greene, 1985). The radial growth phase (RGP) primary melanoma is the first recognizable malignant stage, where tumor cells are either confined to the epidermis or locally invasive but do not show the capacity for rapid growth or metastasis. In vertical growth phase (VGP) primary melanoma lesions, melanoma cells infiltrate as an expanding mass into the dermis and the subcutaneous tissue with the associated risk of systemic dissemination. Finally, metastasis represents the most advanced step of tumor progression.

It is important to recognize, that initial disruptions in the normal molecular dialogue between basal keratinocytes and melanocytes may indirectly incite phenotypic as well as genomic changes as is already evident in benign melanocytic lesions. Nevocytes comprising common acquired nevi differ already from normal melanocytes by their polygonal or epithelioid morphology and aberrant growth, leading to nest formation initially confined to the dermal-epidermal junction (junctional nevus) but eventually expanding to the underlying dermis (compound and dermal nevi) (Hsu et al., 2002). Interestingly, forced physical proximity of dermal nevocytes with undifferentiated keratinocytes renders a normal melanocytic phenotype (Shih et

al., 1994). This phenotypic plasticity suggests, that at least at the very early stage melanocytic transformation does not involve major genetic events but is rather a consequence of losing normal regulatory control exerted by basal keratinocytes. Nevertheless, once malignant transformation has occurred, melanoma cells become autonomous and no longer respond to keratinocytes.

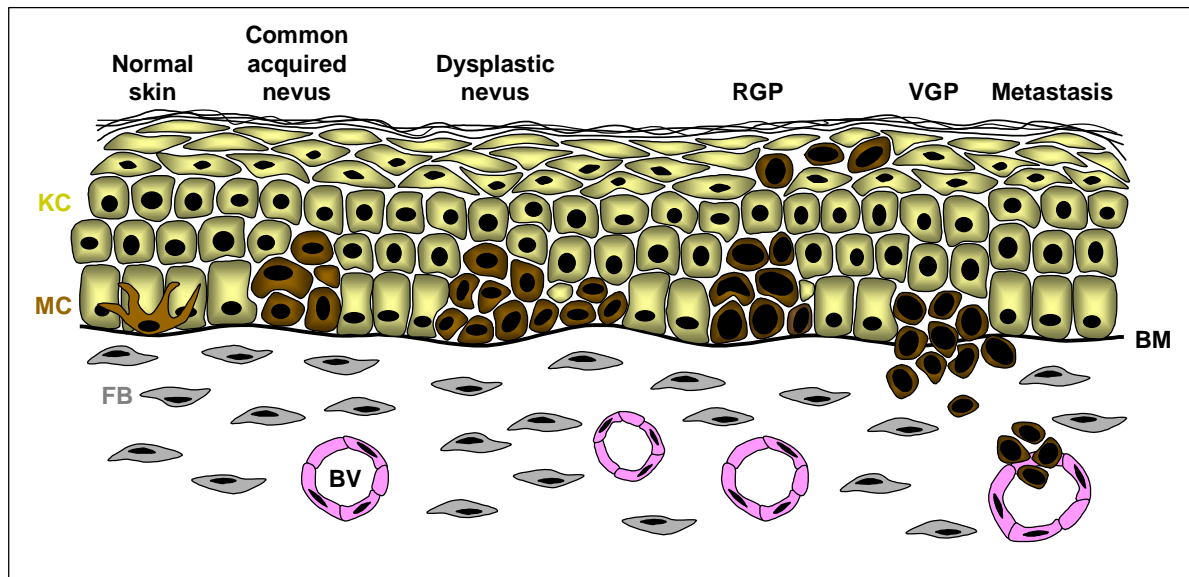


Figure 1 The five major stages of tumor progression postulated for cutaneous malignant melanoma. Normal dermal melanocytes (MC, colored in brown) reside at the basement membrane (BM), which separates the dermis from the epidermis, and are controlled in their proliferation by cell-cell interactions with the surrounding keratinocytes (KC, colored in beige). Nevi are characterized by aberrant cell growth, consisting of enlarged, coalescent nests of nevocytes, which display different degrees of cytologic dysplasia. Further progression results in malignant cells, which grow only within or in close proximity to the epidermis (RGP, radial growth phase). Eventually, cells acquire the ability to invade deeply into dermis (VGP, vertical growth phase) and then into lymphatic and blood vessels (BV), leading to systemic dissemination (metastatic melanoma). FB; fibroblast (colored in gray). Modified from (Hsu et al., 2002).

During melanoma progression, down-regulation of E-cadherin with upregulation of N-cadherin leads to a switch of communication partners from the surrounding keratinocytes to dermal fibroblasts and endothelial cells (Hsu et al., 1996). Expression of melanoma-associated antigens (MAAs), such as MelCAM and its ligand, further favor physical association of melanocytic cells with vascular endothelial (St Croix et al., 2000), smooth muscle (Shih et al., 1994), and activated T cells (Pickl et al., 1997). Thereby, the normal cells recruited to the melanoma microenvironment are integral parts of the tumorigenic process by producing a multitude of factors that affect the biological functions of melanoma cells in terms of

growth stimulation, motility, expression of adhesion molecules, and synthesis of proteolytic enzymes (Li and Herlyn, 2000).

Apart from the microenvironment controlling melanocyte proliferation, several environmental factors can influence melanoma incidence such as geographical parameters (Armstrong and Krickler, 2001) and early exposure to ultraviolet light (Armstrong and Krickler, 1993). Other genetically determined host factors – fair complexion, red hair, and multiple benign or dysplastic nevi - have also been associated with increased melanoma risk (Bataille et al., 1996; Grange et al., 1995).

In addition, several genes have been identified that play a substantial role in the development of cutaneous melanoma, such as those that confer a highly significant predisposition to melanoma if mutated in the germ line, or contribute to the development of melanoma if mutated somatically. Familial melanomas, which represent approximately 8-12% of all melanoma cases (Fountain et al., 1990), have shed light on the genetic lesions that govern the genesis of both familial and sporadic forms of the disease. Through linkage analysis studies and candidate gene searches in melanoma prone families, two melanoma susceptibility genes have been identified, namely *CDKN2A* (Hussussian et al., 1994) and *CDK4* (Zuo et al., 1996).

1.1.1 Germ line mutations in melanoma

1.1.1.1 CDKN2A

CDKN2A (*cyclin-dependent kinase inhibitor 2A*) is located on chromosome 9p21 and encodes two unrelated proteins, p16INK4A (*inhibitor of cyclin-dependent kinase*) and p14ARF (*alternative reading frame*) by using different first exons (1 α and 1 β) spliced to a common set of exons. Both proteins are tumor suppressors involved in cell cycle regulation. p16INK4A negatively regulates cell division by inhibition of CDK4 and CDK6, which phosphorylate proteins of the retinoblastoma family (pRb, p130, p107) (Schulze et al., 1994). Hypophosphorylated retinoblastoma family proteins act as repressors of E2F-mediated gene transcription and thereby prevent progression through the cell cycle. p14ARF on the other hand binds to HDM2, inhibiting its function of targeting p53 for degradation (Zhang et al., 1998). p53,

among many other targets, can upregulate p21, an inhibitor of CDK2, which also acts on cell cycle regulation.

Overall, *CDKN2A* mutations have been found in 20-40% of melanoma prone families compared to only 0.2-2% of sporadic melanoma patients (Aitken et al., 1999; Tsao et al., 2000). Mutations in *CDKN2A* in melanoma frequently eliminate both p16^{INK4A} and p14^{ARF} (Ruas and Peters, 1998), with the majority of cases being missense mutations scattered throughout the coding sequences of exons 1 α and 2. Recently, melanomas have also been associated with polymorphisms in the 5' and 3' untranslated regions of *CDKN2A*, expanding the range of 9p21-associated familial melanoma alleles to those that alter translation or possibly regulate mRNA stability of p16^{INK4A} (Kumar et al., 2001; Liu et al., 1999). Although *CDKN2A* is a definitive melanoma-susceptibility gene, a significant proportion of familial cases segregating with 9p21 markers do not possess germ line mutations targeting p16^{INK4A}. Therefore, p14^{ARF} has emerged as an additional candidate. Indeed, somatic mutations that exclusively affect the p14^{ARF}-coding sequence in the shared exon 2 have been described in human melanomas (Piccinin et al., 1997), and a p14^{ARF}-specific exon 1 β deletion has been identified in two metastatic melanoma cell lines (Kumar et al., 1998).

To further study the role of the *CDKN2A* locus in the development and progression of malignant melanoma, several mouse models were established. The first reported *Cdkn2a* knockout mice, with inactivation of both *Ink4a* and *Arf* transcripts, did not develop melanoma, although they were susceptible to the development of fibrosarcomas and lymphomas (Serrano et al., 1996). When these mice were crossed with *Tyr-Hras* transgenic mice, which harbored an activated *Hras* mutation in their melanocytes, the resulting progeny spontaneously developed cutaneous malignant melanoma with short latency (Chin et al., 1997). However, the melanomas were only locally invasive and did not metastasize. These data indicate, that inactivation of *Cdkn2a* is insufficient for the development of melanoma and further genetic changes are necessary for late stage melanoma progression in mice.

Recently, the contribution of *Ink4a* versus *Arf* to melanoma suppression has been compared more directly using specific knockout mice for the two proteins. Animals that are specifically deficient for *Ink4a* show a low frequency of melanoma spontaneously or after carcinogen treatment (Krimpenfort et al., 2001; Sharpless et

al., 2002). However, melanoma susceptibility imparted by *Ink4a* deficiency could be significantly enhanced when the mice were crossed with *Arf* hemizygotes (Krimpenfort et al., 2001), suggesting a cooperation between the *Ink4a* and *Arf* pathways in melanoma development. When crossed onto the melanoma-prone *Tyr-Hras* transgenic allele, either *Ink4a* or *Arf* loss facilitated melanoma formation (Sharpless et al., 2003). Interestingly, in melanomas from *Tyr-Hras/Arf*^{-/-} mice Rb-pathway lesions were encountered, whereas in *Tyr-Hras/Ink4a*^{-/-} mice p53-pathway lesions were detected. These results provide direct evidence, that both products of the *Cdkn2a* locus have prominent roles in melanoma suppression *in vivo*.

1.1.1.2 CDK4

CDK4 (*cyclin-dependent kinase 4*) is located on chromosome 12q14 and mutations in this gene have been found in seven families worldwide (Soufir et al., 1998; Zuo et al., 1996). These mutations affect a single site in the *CDK4* coding sequence that renders the molecule resistant to p16INK4A binding and inhibition. The identical lesion has also been observed as a somatic mutation in a sporadic melanoma case (Wolfel et al., 1995). By abrogating the interaction between p16INK4A and CDK4, phosphorylation of retinoblastoma family proteins is not inhibited, thereby driving the cell through the cell cycle. The *CDK4* mutations are epistatic to p16INK4A inactivation in melanoma, further supporting the view that the important function of p16INK4A in melanoma suppression is the regulation of CDK4/6 activity. This hypothesis is in accordance with the indistinguishable clinical impact of germ line *CDKN2A* (*p16INK4A*) and *CDK4* mutations, manifesting with a similar mean age of melanoma diagnosis, mean number of melanomas and number of nevi (Goldstein et al., 2000).

1.1.2 Pigmentary traits

Pigmentary traits such as red hair, a fair complexion, the inability to tan and a tendency to freckle (“red hair color” or RHC phenotype) have been shown to act as independent risk factors for all skin cancers, including melanoma (Valverde et al., 1995). Therefore, it is logical to suspect that allelic variants of genes encoding proteins involved in melanin synthesis or transport play a role in melanoma susceptibility. Key determinants of the pigmentary process are MC1R (melanocortin 1 receptor) and α -MSH (melanocyte-stimulating hormone), which is produced by the intermediate lobe of the pituitary gland. The human MC1R is a G-protein coupled receptor that is expressed on epidermal melanocytes. Upon stimulation of MC1R with its ligand α -MSH, the cyclic AMP (cAMP) pathway is upregulated (Busca and Ballotti, 2000). This in turn leads to activation of MITF (Microphthalmia-associated transcription factor), a critical basic helix-loop-helix (bHLH) transcription factor of the melanocyte lineage, which potently transactivates pigmentary genes such as *TRP-1* (*tyrosinase-related protein-1*) and *DCT* (*dopachrome tautomerase*) (Widlund and Fisher, 2003). Recently, two groups reported that MITF can transcriptionally activate key regulators of the cell cycle, but the results are contradictory. Du et al. showed that CDK2 is regulated in a tissue specific manner by MITF leading to melanoma growth and proliferation (Du et al., 2004). On the other hand, Carreira et al. reported that MITF can act as anti-proliferative transcription factor by activating *p21^{CIP1}* and thereby inducing a G1 cell cycle arrest (Carreira et al., 2005). This ability to activate transcription can be potentiated by cooperation between MITF and Rb1.

MC1R is highly polymorphic in human populations and three common variants of *MC1R* have been associated with the RHC phenotype (Box et al., 2001; Palmer et al., 2000). Carrying a single RHC *MC1R* variant has been shown to significantly diminish the ability of the epidermis to respond to damage by UV light, presumably leading to increased melanoma risk (Healy et al., 2000; Palmer et al., 2000). However, several studies have shown that the impact of *MC1R* variants on melanoma risk can not be entirely attributed to its effect on skin type alone and that *MC1R* variants markedly modify the penetrance of mutations at the *CDKN2A* locus (Box et al., 2001; van der Velden et al., 2001).

1.1.3 Somatic mutations in melanoma

1.1.3.1 Mitogen-activated protein kinase signaling pathway

The MAPK (mitogen-activated protein kinase) signaling cascade is activated via sequential phosphorylation of a number of kinases to rapidly alter cellular behavior, for example gene expression, mitosis, movement, metabolism, and programmed cell death in response to diverse environmental stimuli like growth factors or UV light (Johnson and Lapadat, 2002). Such stimuli activate the RAS family of proto-oncoproteins (NRAS, HRAS, and KRAS), which in turn activate the RAF family of serine/threonine kinases (c-RAF1, BRAF, and ARAF). RAF then phosphorylates the MAPK kinase MEK, which subsequently phosphorylates and activates ERK1 and ERK2 (Busca et al., 2000). Activated ERKs translocate to the nucleus, where they phosphorylate specific substrates that are involved in the regulation of various cellular responses.

In sporadic melanoma, activating mutations of *RAS* have been identified with an incidence of 10-15%. For example, activating *NRAS* point mutations have been correlated with nodular lesions and sun exposure (Jafari et al., 1995; van Elsas et al., 1996) and occur in as many as 33% of primary melanomas and 26% of metastatic melanoma samples (Demunter et al., 2001). On the other hand, *NRAS* mutations are rarely found in dysplastic nevi (Albino et al., 1989; Papp et al., 2003). Also, *HRAS* is occasionally involved in melanoma and has been shown to be amplified in acral melanoma (Bastian et al., 2000).

Activating *BRAF* mutations have been identified in up to 60% of human melanoma samples and cell lines (Davies et al., 2002). Importantly, these point mutations are clustered in specific regions of biochemical importance, and 80% of them resulted in a single amino acid substitution (V600E) in the kinase-activating domain, which is known to constitutively activate BRAF (Wellbrock et al., 2004). *BRAF* mutations have also been shown to be common in benign and dysplastic nevi (Pollock et al., 2003), supporting the hypothesis that activation of ERKs is an early event in melanoma progression (Cohen et al., 2002). In addition, recent findings show, that oncogenic BRAF signaling initially stimulates moderate melanocyte

proliferation but subsequently leads to a growth-inhibitory response, which is associated with classical hallmarks of senescence (Michaloglou et al., 2005). These findings point to a potential initiating role of BRAF in transformation and to the need for additional cooperating genetic events to achieve full malignancy. It is interesting to note, that activating mutations in *BRAF* and *NRAS* are mutually exclusive on the genetic level, suggesting that these mutants are functionally equivalent in transformation.

1.1.3.2 HGF/SF-MET signaling pathway

HGF/SF (hepatocyte growth factor/scatter factor) acts as ligand for its tyrosine-kinase receptor c-MET, which is present on epithelial cells and melanocytes (Bottaro et al., 1991). Although HGF normally acts in a paracrine manner, autocrine activation of HGF/SF-MET has been shown in various transformed cells and tumors, including melanoma (Li et al., 2001). HGF/SF can stimulate proliferation and motility of human melanocytes in culture (Halaban et al., 1992) and disrupts adhesion between melanocytes and keratinocytes via down-regulation of E-cadherin and desmoglein-1 (Li et al., 2001). The resultant decoupling of melanocytes from keratinocytes is thought to be permissive for deregulated proliferation and scattering (Li et al., 2001). In addition, HGF/SF-MET activation has also been implicated in melanoma progression. Increased c-MET expression has been observed in metastatic melanoma (Natali et al., 1993), and gain of 7q33-qter, where *c-MET* resides, seems to be a late event in melanoma progression (Bastian et al., 1998).

1.1.3.3 PTEN-AKT signaling pathway

PTEN (*phosphatase and tensin homolog*) is located on chromosome 10q23.3 and the protein functions as a dual-specificity phosphatase with lipid and protein phosphatase activity (Simpson and Parsons, 2001). As lipid phosphatase PTEN negatively regulates the phosphatidylinositol 3-kinase (PI3K)-AKT pathway, which plays an important role in cell survival, protecting cells from apoptosis (Stambolic et al., 1998). On the other hand, PTEN also inhibits MAPK signaling through its protein

phosphatase activity (Wu et al., 2003). In melanoma, allelic loss or mutations of PTEN have been described in 5-15% of uncultured melanoma specimens and metastases, as well as in 30-40% of established melanoma cell lines (Guldborg et al., 1997; Teng et al., 1997). In addition, ectopic expression of PTEN in PTEN-deficient melanoma cell lines was able to suppress growth, tumorigenicity and metastasis (Hwang et al., 2001; Robertson et al., 1998). Although *PTEN* is a *bona fide* tumor suppressor of 10q23.3, the existence of additional melanoma suppressors has been inferred by the fact, that in the 30-50% of human melanomas with LOH (loss of heterozygosity) of the 10q region reintroduction of PTEN seems to have no growth-suppressive effect (Robertson et al., 1998). A strong candidate for another melanoma suppressor gene on 10q is the MYC antagonist MXI1, although its role in melanoma genesis has not been rigorously evaluated (Schreiber-Agus et al., 1998).

1.2 Methods for cytogenetic and whole-genome analyses

Carcinogenesis requires several genetic alterations that convey a selective growth advantage. Most cancers accumulate numerous genetic changes at the level of the nucleotide, gene and chromosome (Lengauer et al., 1998). Many cancers also acquire epigenetic changes, which can alter gene expression (Jones and Baylin, 2002). These findings have led to the suggestion, that the acquisition of some form of inherent genomic instability is a hallmark of tumorigenesis (Hanahan and Weinberg, 2000).

The most important genetic changes involve alterations in oncogenes, tumor-suppressor genes, and stability genes. Oncogenes are mutated in ways that render the gene constitutively active or active under conditions in which the wild-type gene is not. This activation can result from chromosomal translocations, gene amplifications, or subtle intragenic mutations. Tumor-suppressor genes on the other hand are targeted through inactivation of the gene product. Such inactivations arise from missense mutations, mutations that truncate the resulting protein, deletions or insertions, or from epigenetic silencing. Mutations in oncogenes and tumor-suppressor genes drive the neoplastic process by increasing tumor cell number through the stimulation of cell division or the inhibition of apoptosis or cell-cycle arrest.

Stability genes or caretakers promote tumorigenesis in a different way when mutated (Hoeijmakers, 2001; Markowitz, 2000). These genes are responsible for repairing mistakes made during normal DNA replication or upon exposure to mutagens and control mitotic recombination and chromosomal segregation. Stability genes keep genetic alterations to a minimum, and thus when they are inactivated, mutations in other genes occur at a higher rate (Friedberg, 2003).

To detect chromosomal aberrations in tumors, numerous cytogenetic and molecular methods have been developed. Some of these methods, namely M-FISH, CGH, and digital karyotyping, have been used in this work to analyze malignant melanoma cell lines and are described in detail in the following sections.

1.2.1 Fluorescence *in situ* hybridization

For several decades chromosomes were analyzed by traditional karyotyping, which depends on the analysis of characteristic banding patterns along the length of each chromosome (Caspersson et al., 1968; Caspersson et al., 1970). However, the major disadvantage of conventional cytogenetic banding methods is their limited resolution, which depends on the number of chromosomal bands that can be visualized after staining with a certain dye. This drawback was overcome by the development of the fluorescence *in situ* hybridization (FISH) technique, allowing the direct visualization and localization of selected DNA regions within a genome (Cremer et al., 1988; Lichter et al., 1988; Pinkel et al., 1988). Thereby, a small DNA fragment of known origin (a painting probe) is fluorescently labeled and hybridized to metaphase chromosome spreads or interphase nuclei. The probe binds to homologous sequences within the chromosomes, which can be visualized by fluorescence microscopy.

Initially, painting probes were often used to verify a chromosomal rearrangement, which was obvious or suspected in banding analysis. However, the deciphering of complex rearrangements with involvement of unidentifiable chromosomal material is inefficient if only one or two chromosome paints per hybridization are used. Therefore, technologies were developed which allow the simultaneous hybridization of multiple chromosome painting probes in different colors. With the introduction of 24-color FISH, namely M-FISH and SKY, all 22

autosomes and the two sex chromosomes can be visualized simultaneously. Multiplex fluorescence *in situ* hybridization (M-FISH) uses combinatorial labeling with a total of seven fluors to uniquely identify each of the 24 chromosomes based on different optical filters (Speicher et al., 1996). Spectral karyotyping (SKY) on the other hand is a technique, that also employs the combinatorial labeling strategy for probe discrimination (Schrock et al., 1996) but the detection is interferometer-based.

The 24-color karyotyping technologies have proven to be useful tools in clinical diagnostics (Uhrig et al., 1999) and in deciphering complexly rearranged tumor karyotypes (Veldman et al., 1997). For example, it is possible to rapidly identify numerical and structural aberrations, as well as translocations, duplications and deletions. However, these technologies also have some limitations, which for example are difficulties in the determination of the exact band of origin of a marker or the evaluation of breakpoints of intrachromosomal rearrangements. Furthermore, the detection sensitivity for small (< 3 Mbp) intrachromosomal rearrangements, deletions or duplications is poor. Nevertheless, these problems have already been addressed and solutions have been proposed by increasing the number of fluorochromes for probe labeling (Azofeifa et al., 2000), by replacing painting probes with region-specific probes (Fauth et al., 2001), or by developing so called “bar coding” strategies (Lengauer et al., 1993).

1.2.2 Comparative genomic hybridization

Comparative genomic hybridization (CGH) was developed for genome-wide analysis of DNA sequence copy number in a single experiment (du Manoir et al., 1993; Kallioniemi et al., 1992). Thereby, total genomic DNA from a “test” (tumor) and a “reference” (normal) cell population are differentially labeled with green and red fluorochromes and co-hybridized to normal metaphase chromosomes, where the green and red labeled DNA fragments compete for hybridization to their locus of origin. The resulting ratio of the fluorescence intensities is measured along the chromosome axis and is approximately proportional to the ratio of the copy numbers of the corresponding DNA sequences in the test and reference genomes at that specific location on the chromosomes.

CGH has been widely applied in cancer research including the screening of tumors for genetic aberrations (Monni et al., 1998; Riopel et al., 1998), the search for genes involved in the carcinogenesis of particular subsets of cancers (Simon et al., 1998), the analysis of tumors in experimental models to obtain an insight into tumor progression (Tienari et al., 1998), diagnostic classification (Simon et al., 1998), and prognosis assessment (Isola et al., 1995).

Although useful in cancer research, CGH has also some drawbacks, for example it cannot detect structural chromosomal aberrations without copy number changes, such as balanced chromosomal translocations, inversions, or ring chromosomes, and it does not yield information in the context of tissue architecture. The sensitivity of CGH can be hampered by contamination of tumor material with normal cells and also depends on the level and size of the copy number changes. The use of metaphase chromosomes limits the detection of events involving small regions of the genome, the resolution of closely spaced aberrations and hampers the linking of ratio changes to genomic/genetic markers. Based on CGH experiments, the resolution was estimated to be in the range of 10-20 Mbp (Bentz et al., 1995; Bentz et al., 1998). Much higher resolutions can be achieved with newly developed techniques such as array-CGH (Pinkel et al., 1998) or matrix-CGH (Solinas-Toldo et al., 1997). For example, whole genome arrays or single chromosome tiling path arrays achieve resolutions of ~10 Mbp or ~100 kbp, respectively.

1.2.3 Digital karyotyping

The digital karyotyping (DK) technique has been developed to examine genome-wide DNA copy number changes with so far unprecedented resolution (Wang et al., 2002). Digital karyotyping quantitatively analyses short sequence fragments of 21 bp (tags), which are obtained from specific locations in the genome and which contain sufficient information to uniquely identify the genomic loci from which they were derived (Figure 2).

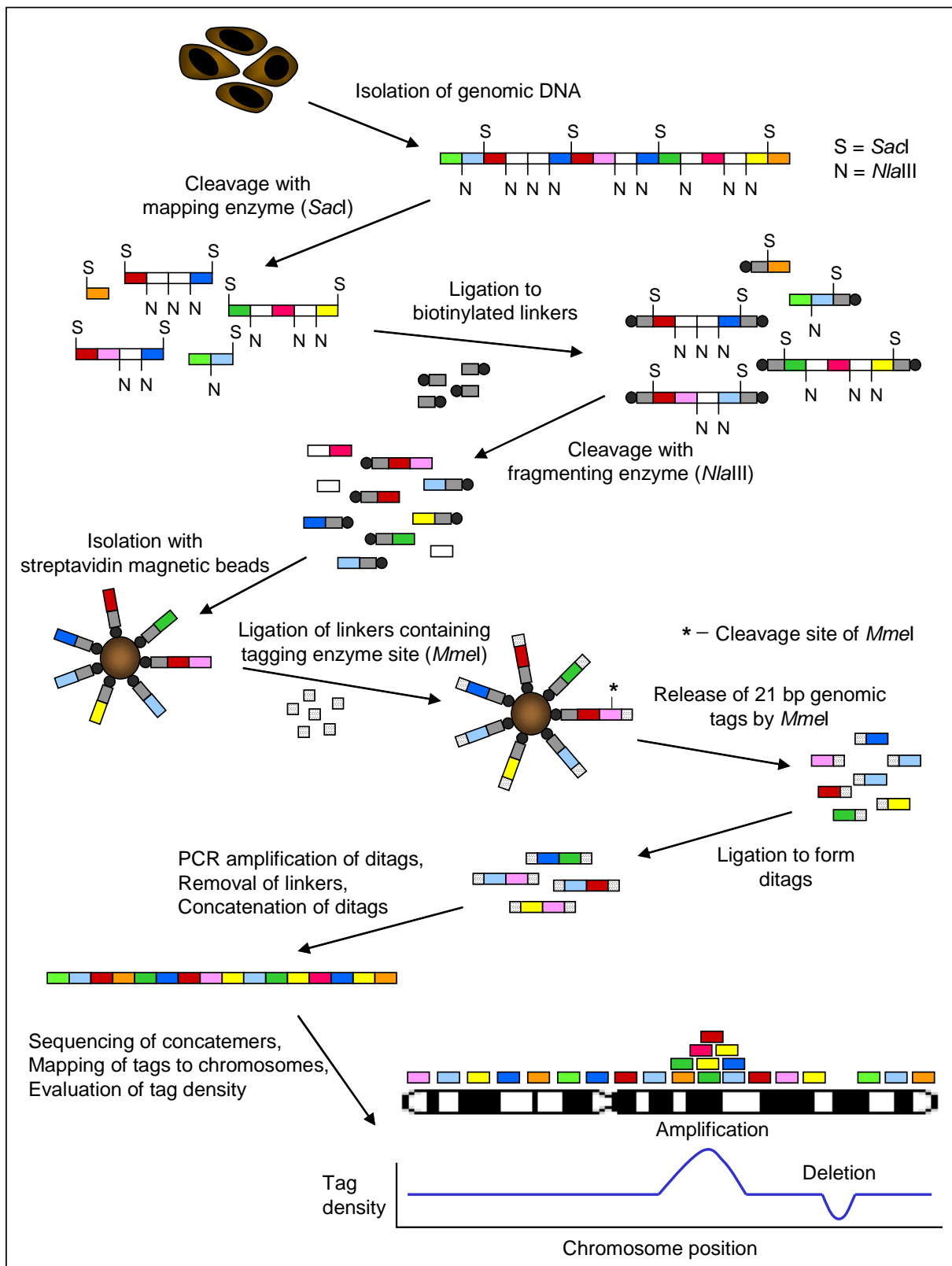


Figure 2 Scheme of the digital karyotyping approach. Colored boxes represent genomic tags, gray and dotted boxes represent linkers. Small black circles denote biotin modifications and large brown circles denote streptavidin magnetic beads. Cleavage sites of restriction enzymes are labeled with S (for *SacI*), N (for *NlaIII*), or * (for *MmeI*). Modified from (Parrett and Yan, 2005; Wang et al., 2002)

To obtain these tags, genomic DNA of a cell population, for example a tumor cell line, is fragmented by a mapping restriction endonuclease into representative fragments of a certain size. For example, fragments of approximately 4 kbp can be obtained after cleavage with *SacI*. After ligation of biotinylated linkers, the DNA molecules are isolated with streptavidin magnetic beads and further digested with a second fragmenting restriction endonuclease, cutting on average 16 times inside the already obtained fragments (for example *NotI*). Linkers containing a recognition site for a type IIS restriction endonuclease (for example *MmeI*) are ligated to the DNA molecules, which are still captured by the streptavidin magnetic beads. Subsequently, the DNA fragments are cleaved by *MmeI*, releasing 21 bp genomic tags. Isolated tags are self-ligated to form ditags, which are PCR amplified, concatenated, cloned, and sequenced. After sequencing, tags can be extracted with the SAGE2000 software, which identifies the fragmenting enzyme site between ditags and are then matched to a virtual tag library extracted from the human genome sequence, which contains only tags obtained from unique loci. Experimental tags with the same sequence as virtual tags are used for subsequent analysis with the digital karyotyping software. Thereby, tags are matched to their genomic position along each chromosome and tag densities are calculated. Regions with over- or underrepresentation of tags contain possible sites of copy number changes in the analyzed genome.

Digital karyotyping is assumed to be highly reliable from the standpoint of comparing genetic dosage signals from different areas of the genome, as tag counts are directly proportional to the amount of genetic material present and do not depend upon quantitating and comparing a non-linear hybridization signal across heterogeneous nucleotide probes. The theoretical resolution of digital karyotyping is also the highest of the current high-resolution whole-genome screens (for review see (Parrett and Yan, 2005; Shih le and Wang, 2005)). At present, however, the resolution for the detection of gene dosage alterations is limited by the number of experimentally derived tags that can be sequenced economically, which is approximately 100,000-200,000. For example, the analysis of 100,000 tags is expected to reliably detect a 10-fold amplification ≥ 100 kbp, homozygous deletions ≥ 600 kbp, or a single gain or loss of regions ≥ 4 Mbp in a diploid genome (Wang et al., 2002).

1.3 *Dystrophin*

1.3.1 *DMD* gene and isoforms

Dystrophin (*DMD*) is the second largest gene in humans and located on chromosome Xp21.2. It spans about 2.5 Mbp of genomic sequence with a full-length messenger RNA of 14 kbp (for review see (Blake et al., 2002; Muntoni et al., 2003)). Three independently regulated promoters (for brain, muscle and Purkinje cells) control expression of the full-length *DMD* transcript with a unique first exon spliced to a common set of 78 exons (Figure 3 and Table 1). The brain promoter drives expression primarily in cortical neurons and the hippocampus of the brain (Gorecki et al., 1992; Nudel et al., 1989). The transcript from the Purkinje promoter is expressed in the cerebellar Purkinje cells and at a very low level in skeletal muscle (Bies et al., 1992; Bies et al., 1992). The muscle transcript is mainly expressed in skeletal muscle and cardiomyocytes in addition to the expression at a low level in some glial cells in the brain (Yaffe et al., 1992). An additional full-length lymphocyte isoform has been described (Nishio et al., 1994), although recent findings suggest that it might represent an artifact, making its functional role uncertain (Wheway and Roberts, 2003).

The *DMD* gene has at least four internal promoters that give rise to shorter dystrophin transcripts that encode truncated COOH-terminal isoforms (Figure 3 and Table 1). Each of these internal promoters uses a unique first exon that is spliced to exons 30, 45, 56, and 63 to generate proteins of 260 kD (Dp260) (Pillers et al., 1993), 140 kD (Dp140) (Lidov et al., 1995), 116 kD (Dp116) (Byers et al., 1993), and 71 kD (Dp71) (Bar et al., 1990). Dp71 is detected in most non-muscle tissues including brain, kidney, liver, and lung (Hugnot et al., 1992; Lederfein et al., 1992), while the remaining short isoforms are primarily expressed in the central and peripheral nervous system (Byers et al., 1993; D'Souza et al., 1995; Lidov et al., 1995; Schofield et al., 1994). In addition, Dp140 has also been implicated in the development of the kidney (Durbeej et al., 1997). The COOH-terminal isoforms contain the necessary binding sites for a number of dystrophin-associated proteins (see chapter 1.3.5), and although the molecular and cellular function of these

isoforms has not been elucidated, they are thought to be involved in the stabilization and function of non-muscle dystrophin-like protein complexes.

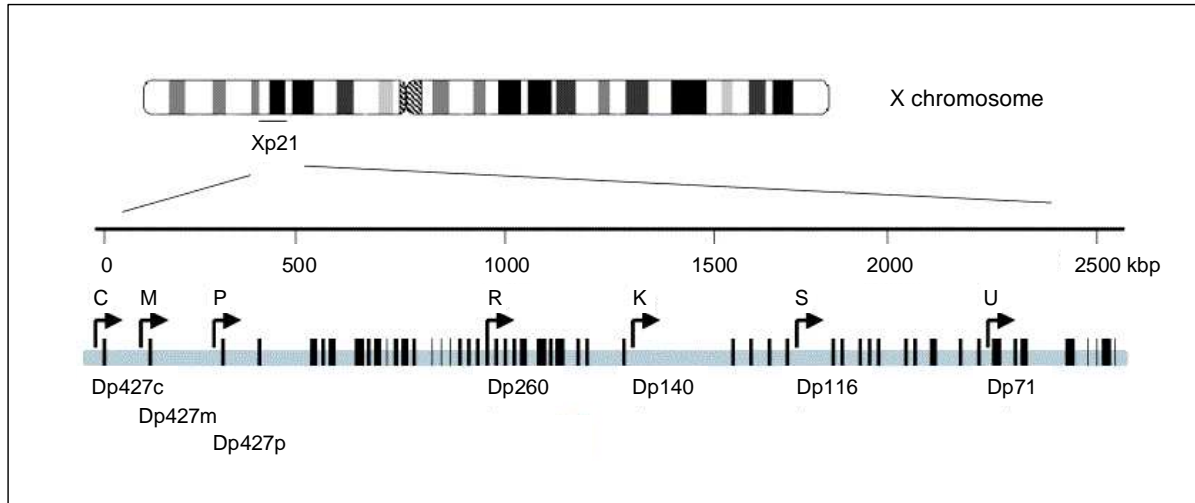


Figure 3 Structure of the *dystrophin (DMD)* gene. *DMD* is located on Xp21 and spans about 2.5 Mbp of genomic sequence as indicated underneath the chromosome ideogram. The vertical black lines represent the 79 exons of the *DMD* gene. The arrows indicate the different promoters, which correspond to the different protein isoforms; namely the cortical (C; Dp427c), the muscle (M; Dp427m), the Purkinje (P; Dp427p), the retinal (R; Dp260), the kidney (K; Dp140), the Schwann cell (S; Dp116), and the ubiquitously (U; Dp71) expressed transcript. Modified from (Muntoni et al., 2003).

In addition to these shorter isoforms, the dystrophin gene produces many isoforms generated through alternative splicing events in a tissue-specific way (Bies et al., 1992; Feener et al., 1989). These splice variants not only affect full-length dystrophin but are also found in the shorter isoforms such as Dp71. They are formed both through the exclusion of some exons from the primary transcript (exon skipping) and by subversion of the reciprocal order of exons (exon scrambling) (Sadoulet-Puccio and Kunkel, 1996; Suroño et al., 1999). It has been suggested, that this differential splicing may regulate the binding of dystrophin to dystrophin-associated proteins at the membrane (Crawford et al., 2000).

Table 1 Expression pattern and position of the transcription start site of the different dystrophin isoforms.

Name	Isoform	Promoter and first exon	Pattern of protein expression
Dp427c	cortical (brain)	5' of the muscle promoter	cortical neurons, skeletal and cardiac muscle
Dp427m	muscle	between the cortical promoter and intron 1	skeletal and cardiac muscle, glial cells
Dp427p	Purkinje	between intron 1 and 2	Purkinje cerebellar neurons
Dp260	retinal	intron 29	retina
Dp140	kidney	intron 44	CNS, kidney
Dp116	S-dystrophin	intron 55	Schwann cells
Dp71	G-dystrophin	intron 62	ubiquitously expressed in most tissues except for skeletal muscle

Modified from (Muntoni et al., 2003). Abbreviations: CNS; central nervous system.

1.3.2 Dystrophin protein

Dystrophin is a 427 kD cytoskeletal protein that is a member of the β -spectrin/ α -actinin protein family (Koenig et al., 1988). Dystrophin can be organized into four separate domains based on sequence homologies and protein-binding capabilities – the actin-binding domain at the NH₂ terminus, the central rod domain, the cysteine-rich domain, and the COOH-terminal domain (Figure 4). The NH₂ terminus is homologous to α -actinin and binds directly to but does not cross-link cytoskeletal actin (F-actin) (Rybakova et al., 1996). The central rod domain is formed by 24 spectrin-like triple-helical elements. These repeats are interrupted by four proline-rich non-repeat segments, the so-called hinge regions. The central domain accounts for the majority of the dystrophin protein and is thought to give the molecule a flexible rod-like structure (Koenig and Kunkel, 1990). The central rod domain is followed by a WW domain, which is a protein-binding module found in several signaling and regulatory molecules. The WW domain binds to proline-rich substrates and mediates interaction with the cytoplasmic domain of β -dystroglycan (Rosa et al., 1996). The cysteine-rich domain shows similarity to α -actinin and contains a ZZ domain and two potential EF-hand motifs that could bind intracellular Ca²⁺ (Koenig et al., 1988). The ZZ domain comprises a number of conserved cysteine residues and

is similar to many types of zinc fingers. In addition, it can bind to calmodulin in a Ca^{2+} -dependent manner (Anderson et al., 1996). The COOH terminus of dystrophin contains two polypeptide stretches that are predicted to form coiled coils and therefore has been named the CC domain. The CC region forms the binding site for dystrobrevin and can modulate the interaction between syntrophin and other dystrophin-associated proteins (Blake et al., 1995).

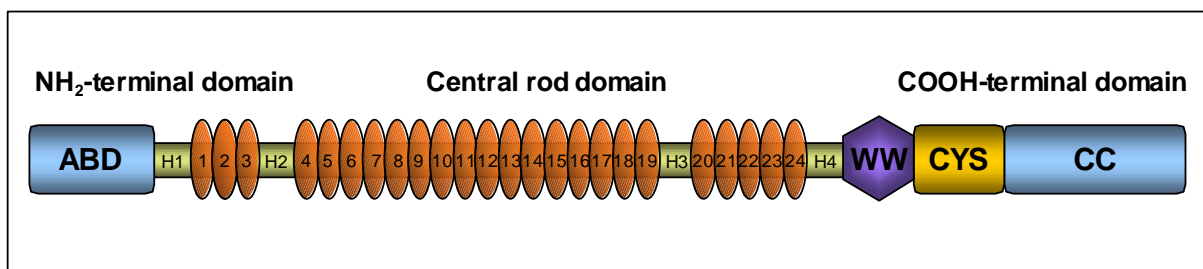


Figure 4 Structure of the dystrophin protein. The NH_2 -terminus of dystrophin contains the actin-binding domain (ABD), which is followed by the central rod domain consisting of 24 spectrin-like repeats (1-24) that are interrupted by four proline-rich hinge regions (H1-H4). Adjacent to the rod domain follows the WW domain and the cysteine-rich domain (CYS). The COOH-terminus forms a coiled coil structure (CC).

1.3.3 Duchenne and Becker Muscular Dystrophies

Duchenne and Becker muscular dystrophies (DMD/BMD) are X-linked recessive disorders that are caused by defects in the *DMD* gene (Emery, 1993). These gene mutations lead to a deficiency of the dystrophin protein in skeletal muscle as well as in other tissues in which isoforms of dystrophin are normally expressed, such as brain, retina, and smooth muscle (see chapter 1.3.1). Typically, DMD patients are clinically normal at birth with 1 in 3500 males being affected. The first symptoms of DMD are generally observed between the ages of 2 and 5 years with a delay in the achievement of motor milestones, including a delay in walking, unsteadiness, and difficulty in running (Jennekens et al., 1991). Eventually, decreased lower-limb muscle strength and joint contractures result in wheel-chair dependence, usually by the age of 12. Most patients die in their early twenties as a result of respiratory complications. Death can also be the result of cardiac dysfunction caused by cardiomyopathy (Emery, 1993).

In individuals affected by BMD, the clinical course is similar to that of DMD, although the onset of symptoms and the rate of progression are delayed. More than 90% of patients are still alive in their twenties (Comi et al., 1994). There is a continuous clinical spectrum between a mildly affected BMD patient and a severely affected DMD patient. In addition, some BMD and DMD patients are affected by mild cognitive impairment, indicating that nerve cell function is also abnormal in these disorders (Mehler, 2000).

1.3.4 Mutations in *DMD*

The most common changes in *DMD* are intragenic deletions, which account for 65% of *DMD* mutations (Koenig et al., 1989; Monaco et al., 1985). The frequency of duplications may range from 5% to 15%, whereas the remaining cases are caused by small mutations, pure intronic deletions, or exonic insertions of repetitive sequences (Roberts et al., 1994). The vast majority of large deletions detected in BMD and DMD cluster around two mutation “hot spots” (Koenig et al., 1989). The first region is located at the 3′-end of *DMD* and involves exons 45-53 (Beggs et al., 1990), whereas the other hotspot includes exons 2-20 at the 5′-end of *DMD* (Liechti-Gallati et al., 1989). One-third of DMD cases are caused by very small deletions and point mutations, most of which introduce premature stop codons and appear to be evenly distributed throughout the gene (Gardner et al., 1995; Prior et al., 1995). Mutations that maintain the reading frame (in-frame) generally result in abnormal but partially functional dystrophin and are associated with BMD (Monaco et al., 1988). In patients with DMD, deletions, duplications or mutations disrupt the reading frame (frame-shift), resulting in unstable RNA that eventually leads to the production of nearly undetectable concentrations of truncated proteins (Kerr et al., 2001). Exceptions to this reading-frame hypothesis do exist and these include patients with BMD who carry frame-shift deletions or duplications and patients with DMD with in-frame deletions or duplications (Love et al., 1990; Nevo et al., 2003).

1.3.5 Dystrophin-glycoprotein complex

The identification of the dystrophin protein and its localization to the muscle cell membrane led to the biochemical co-purification of a group of sarcolemmal and sub-sarcolemmal proteins, that form the dystrophin-glycoprotein complex (DGC) (Campbell and Kahl, 1989; Yoshida and Ozawa, 1990) (Figure 5). In skeletal muscle, the NH₂ terminus of dystrophin binds to cytoskeletal actin (Rybakova et al., 1996), whereas the COOH terminus binds the intracellular domain of β -dystroglycan (Jung et al., 1995). β -dystroglycan is a transmembrane protein with its extracellular domain binding to α -dystroglycan (Ibraghimov-Beskrovnaya et al., 1993). α -dystroglycan acts as a receptor for a number of extracellular matrix components, including laminin (Ibraghimov-Beskrovnaya et al., 1992), agrin (Gee et al., 1994), and perlecan in muscle, and neurexin in brain (Sugita et al., 2001). Thus, the dystrophin-dystroglycan complex serves as a transmembrane link between the extracellular matrix and the cytoskeleton, and this structural role may protect the muscle from the shearing forces of contraction (Petrof et al., 1993).

In skeletal muscle several other proteins are associated with dystrophin and dystroglycan, namely the dystrobrevins and syntrophins, and the sarcoglycan-sarcospan complex. In non-muscle tissues intracellular binding partners for β -dystroglycan include the Dp260, Dp140, Dp116 and Dp71 isoforms of dystrophin (Jung et al., 1995; Saito et al., 1999) and utrophin, the autosomal homolog of dystrophin (Chung and Campanelli, 1999). Other proteins that bind to the DGC are calmodulin (Madhavan et al., 1992), Grb2 (Yang et al., 1995), and NOS1 (Brenman et al., 1996) suggesting a role for the DGC in cellular signaling.

Many of the dystrophin/dystroglycan-associated proteins found in skeletal and cardiac muscle are also expressed in other tissues. Thus, different dystroglycan complexes may form in different tissues playing roles in epithelial cell development (Durbeej et al., 1995), basement membrane formation (Henry and Campbell, 1998; Williamson et al., 1997), and synaptogenesis (Montanaro et al., 1998).

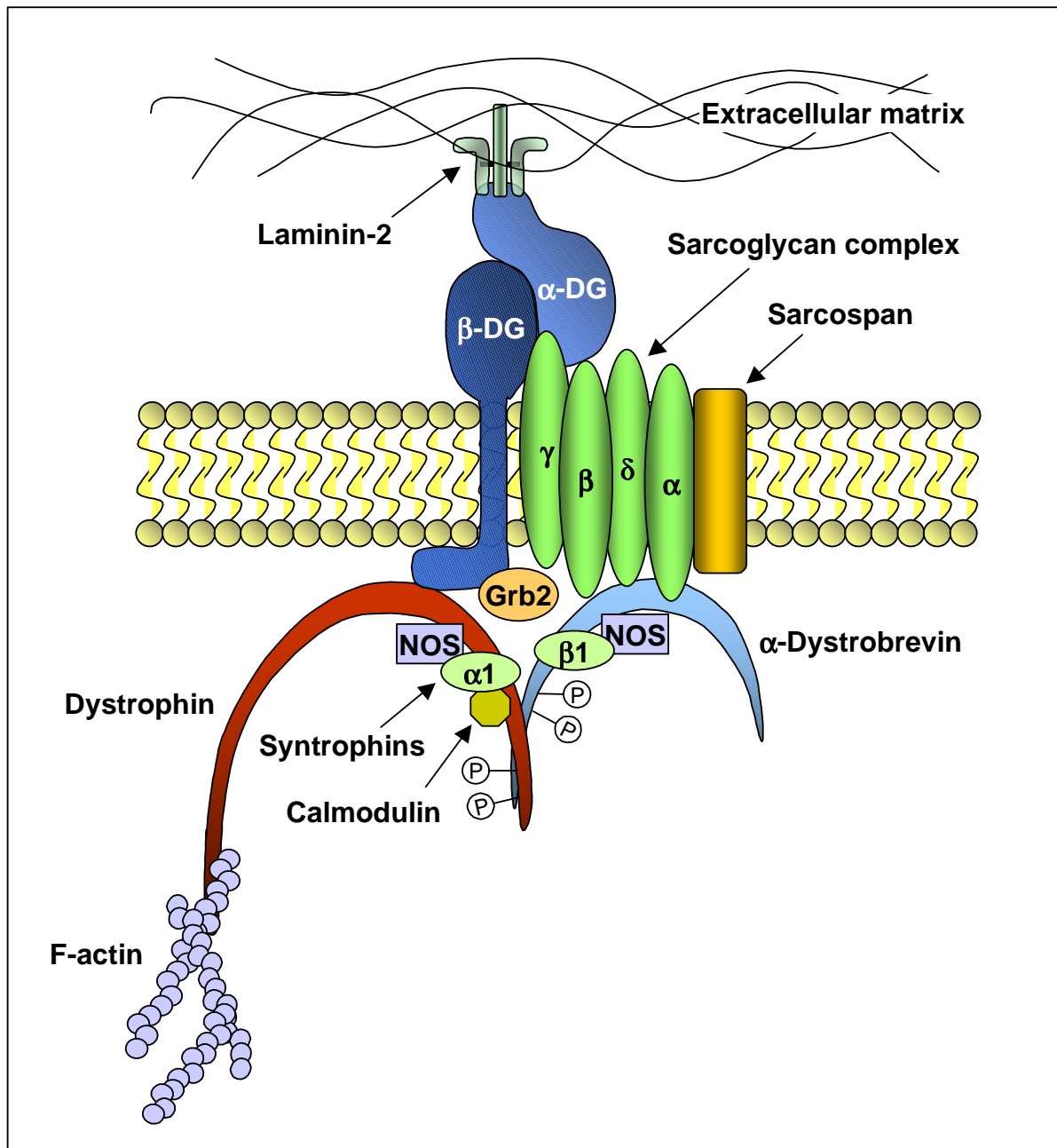


Figure 5 The dystrophin-glycoprotein complex (DGC) at the muscle cell membrane. The dystroglycans (α -DG and β -DG) anchor the DGC at the muscle cell membrane. α -DG can bind to several ligands (e.g. laminin-2) present in the extracellular matrix, whereas β -DG binds to dystrophin, which is linked to F-actin facilitating a connection with the intracellular cytoskeleton. Associated with the dystroglycans is the sarcoglycan complex, which also binds to sarcospan. Intracellular binding partner for the sarcoglycan complex is α -dystrobrevin, which at the same time can bind to dystrophin. Several signaling molecules are associated intracellularly with the DGC, namely Grb2, NOS1, the syntrophins α 1 and β 1 as well as calmodulin. In addition, both dystrophin and α -dystrobrevin can be modified by multiple phosphorylations.

2 AIM OF THE STUDY

The present study had the following aims:

- I. Characterization of chromosomal aberrations in a panel of newly established melanoma cell lines by M-FISH and CGH analysis

- II. Detection of genome-wide genetic alterations employing the digital karyotyping technique in malignant melanoma cell lines in order to identify single gene copy number changes, which might indicate the presence of tumor-suppressor genes or oncogenes

- III. Functional analysis of candidate tumor-suppressor genes or oncogenes

3 MATERIALS

3.1 Chemicals

Chemical	Supplier
1,4-diazabicyclo(2,2,2)octane (DAPCO)	<i>Sigma, Taufkirchen, Germany</i>
3-(N-morpholine)propanesulphonic acid (MOPS)	<i>ICN Biomedicals, Shelton, USA</i>
4,6-diamidino-2-phenylindole (DAPI)	<i>Sigma, Taufkirchen, Germany</i>
5-bromo-4-chloro-3-indolyl β -D-galactopyranoside (X-gal)	<i>Sigma, Taufkirchen, Germany</i>
Acrylamide	<i>Serva, Heidelberg, Germany</i>
Agarose	<i>Peqlab, Erlangen, Germany</i>
Ammonium peroxodisulfate (APS)	<i>Bio-Rad, München, Germany</i>
Ampicillin	<i>Sigma, Taufkirchen, Germany</i>
β -mercaptoethanol	<i>Merck, Darmstadt, Germany</i>
Biotin-16-dUTP	<i>Boehringer, Ingelheim, Germany</i>
Bisacrylamide	<i>Roth, Karlsruhe, Germany</i>
Bovine serum albumin (BSA)	<i>NEB, Frankfurt/Main, Germany</i>
Bromphenol blue	<i>Sigma, Taufkirchen, Germany</i>
Coomassie G250	<i>Serva, Heidelberg, Germany</i>
Cot-1 DNA	<i>Roche, Mannheim, Germany</i>
Cy3 (cyanine-dye)	<i>Amersham, Piscataway, USA</i>
Cy5.5 (cyanine-dye)	<i>Amersham, Piscataway, USA</i>
Cy7 (cyanine-dye)	<i>Amersham, Piscataway, USA</i>
Deionized formamide pH 7.0	<i>Sigma, Taufkirchen, Germany</i>
Demecolcine (colcemid)	<i>Sigma, Taufkirchen, Germany</i>
Deoxynucleotides (dATP/dCTP/dGTP/dTTP)	<i>ABgene, Hamburg, Germany</i>
Dextran sulfate	<i>Sigma, Taufkirchen, Germany</i>
Diethylaminocoumarine (DEAC)	<i>Amersham, Piscataway, USA</i>
Digoxigenin-11-dUTP	<i>Boehringer, Ingelheim, Germany</i>
Dimethyl sulfoxide (DMSO)	<i>Sigma, Taufkirchen, Germany</i>
Dithiothreitol (DTT)	<i>Sigma, Taufkirchen, Germany</i>
Ethidium bromide	<i>Sigma, Taufkirchen, Germany</i>
Ficoll [®] 400	<i>Sigma, Taufkirchen, Germany</i>
Fluorescein isothiocyanate (FITC)	<i>Amersham, Piscataway, USA</i>
Geneticin [®] (G418, neomycin)	<i>Invitrogen, Karlsruhe, Germany</i>
Glutaraldehyde	<i>Serva, Heidelberg, Germany</i>
Isopropyl β -D-1-thiogalactopyranoside (IPTG)	<i>Roth, Karlsruhe, Germany</i>
Kanamycin	<i>Sigma, Taufkirchen, Germany</i>
Matrigel basement membrane matrix	<i>Becton Dickinson, Heidelberg Germany</i>
Mitomycin C	<i>Sigma, Taufkirchen, Germany</i>
N,N,N',N'-tetramethylethylenediamine (TEMED)	<i>Serva, Heidelberg, Germany</i>
Paraformaldehyde	<i>Sigma, Taufkirchen, Germany</i>
Phenol/chloroform/isoamylalcohol (25:24:1)	<i>Roth, Karlsruhe, Germany</i>

Chemical	Supplier
Phenylmethylsulfonylfluoride (PMSF)	<i>Sigma, Taufkirchen, Germany</i>
Propidium iodide	<i>Sigma, Taufkirchen, Germany</i>
Protease inhibitor cocktail complete mini	<i>Roche, Mannheim, Germany</i>
Puromycin dihydrochloride	<i>Sigma, Taufkirchen, Germany</i>
Salmon-sperm DNA	<i>Sigma, Taufkirchen, Germany</i>
Sodium fluoride	<i>Sigma, Taufkirchen, Germany</i>
Sodium orthovanadate	<i>Aldrich, Steinheim, Germany</i>
TexasRed	<i>Invitrogen, Karlsruhe, Germany</i>
Triton X-100	<i>Roth, Karlsruhe, Germany</i>
Tween [®] 20	<i>Sigma, Taufkirchen, Germany</i>

3.2 Enzymes

Enzyme	Supplier
Alkaline phosphatase calf intestine (CIP)	<i>NEB, Frankfurt/Main, Germany</i>
DNA polymerase I	<i>Boehringer, Ingelheim, Germany</i>
DNase I	<i>Sigma, Taufkirchen, Germany</i>
FIREPol [®] DNA polymerase	<i>Solis BioDyne, Tartu, Estonia</i>
Pepsin	<i>Sigma, Taufkirchen, Germany</i>
Platinum [®] Taq DNA polymerase	<i>Invitrogen, Karlsruhe, Germany</i>
Proteinase K	<i>Sigma, Taufkirchen, Germany</i>
Restriction endonucleases	<i>NEB, Frankfurt/Main, Germany</i>
	<i>MBI Fermentas, St. Leon-Rot, Germany</i>
T4-DNA ligase	<i>Roche, Mannheim, Germany</i>
Trypsin	<i>Invitrogen, Karlsruhe, Germany</i>

3.3 Commercial kits and other materials

Product	Supplier
3MM Whatman [®] filter paper	<i>Whatman, Dassel, Germany</i>
BigDye [®] Terminator v3.1 Sequencing Kit	<i>Applied Biosystems, Darmstadt, Germany</i>
Cell culture plastics	<i>Corning, Schiphol, Netherlands</i>
	<i>Nunc, Wiesbaden, Germany</i>
	<i>BD Falcon, Bedford, USA</i>
DNA ladder, 1 kbp	<i>Invitrogen, Karlsruhe, Germany</i>
DNA ladder, 100 bp	<i>Roth, Karlsruhe, Germany</i>
Dynabeads [®] M-280 Streptavidin	<i>Dynal Biotech, Swestad, Norway</i>
FastStart-DNA Master SYBR Green 1	<i>Roche, Mannheim, Germany</i>
FuGENE6 [™]	<i>Roche, Mannheim, Germany</i>
Immobilon-P PVDF membrane	<i>Millipore, Schwalbach, Germany</i>
Oligonucleotides	<i>Metabion, Martinsried, Germany</i>
PageRuler [™] Prestained Protein Ladder	<i>MBI Fermentas, St. Leon-Rot, Germany</i>
	<i>Germany</i>
QIAGEN Plasmid Maxi Kit	<i>Qiagen, Hilden, Germany</i>

Product	Supplier
QIAprep Miniprep Kit	<i>Qiagen, Hilden, Germany</i>
QIAquick Gel Extraction Kit	<i>Qiagen, Hilden, Germany</i>
RNAagents total RNA isolation system	<i>Promega, Mannheim, Germany</i>
Siliconized microcentrifuge tubes	<i>Fisher Scientific, Schwerte, Germany</i>
Spin-X tubes	<i>Costar, Schiphol, Netherlands</i>
SuperScript TM III first-strand synthesis system	<i>Invitrogen, Karlsruhe, Germany</i>
SuperSignal [®] West Dura	<i>Pierce, Rockford, USA</i>
Western Lightning Chemiluminescence Reagent Plus	<i>Perkin Elmer, Boston, USA</i>

3.4 Buffers and stock solutions

All buffers and solutions were prepared with bidistilled water unless stated otherwise.

Solution	Recipe
Bradford solution (5x)	50% (w/v) Coomassie G250 23.75% (v/v) ethanol 42.5% (v/v) phosphoric acid
Coomassie G250 staining solution	0.25% (w/v) Coomassie G250 45% (v/v) methanol 10% (v/v) acetic acid
Crystal violet solution	5 mg/ml crystal violet 20% (v/v) methanol
DAPCO antifade	23.3 mg/ml DAPCO 20 mM Tris/HCl pH 8.0 90% (v/v) glycerol
Destaining solution	50% (v/v) methanol 15% (v/v) acetic acid
DNA loading buffer (10x)	20% (w/v) Ficoll [®] 400 1 mM EDTA pH 8.0 0.05% (w/v) bromphenol blue
Gel drying solution	2% (v/v) glycerol 20% (v/v) ethanol

Solution	Recipe
Laemmli buffer (2x)	100 mM Tris/HCl pH 6.8 10% (w/v) SDS 50% (v/v) glycerol 0.05% (w/v) bromphenol blue 10% (v/v) β -mercaptoethanol
LB agar	1.5% (w/v) agar in LB medium
LB medium	1% (w/v) tryptone 0.5% (w/v) yeast extract 1% (w/v) NaCl pH 7.2
Low TBST	20 mM Tris/HCl pH 7.5 100 mM NaCl 0.05% (v/v) Tween [®] 20
Lower Tris buffer (4x)	1.5 M Tris base 0.4% (w/v) SDS pH 8.8 (HCl)
MOPS buffer (10x)	200 mM MOPS 50 mM sodium acetate 10 mM EDTA pH 7.0 (NaOH)
PBS	13.7 mM NaCl 2.7 mM KCl 80.9 mM Na ₂ HPO ₄ 1.5 mM KH ₂ PO ₄ pH 7.4 (HCl)
PCR buffer (10x)	166 mM (NH ₄) ₂ SO ₄ 670 mM Tris/HCl pH 8.8 67 mM MgCl ₂ 100 mM β -mercaptoethanol
Proteinase K buffer	10 mM Tris/HCl pH 8.0 100 mM NaCl 25 mM EDTA pH 8.0

Solution	Recipe
RIPA lysis buffer	50 mM Tris/HCl pH 7.5 150 mM NaCl 1 mM EDTA 1% (v/v) NP-40 0.1% (w/v) SDS 0.25% (w/v) sodium deoxycholate 1 mM PMSF 1 mM NaF 1 mM Na ₃ VO ₄
RNA loading buffer (4x)	6.47% (v/v) formaldehyde 50% (v/v) formamide 10% (v/v) glycerol 1.5 µg/ml ethidium bromide 0.2% (w/v) bromphenol blue 0.2% (w/v) xylene cyanol in MOPS buffer
SDS/proteinase K solution	0.1 mg/ml proteinase K 0.1% (w/v) SDS in proteinase K buffer
SSC buffer (20x)	3 M NaCl 342 mM sodium citrate pH 7.0 (HCl)
TAE buffer (10x)	400 mM Tris/acetate 10 mM EDTA pH 8.0 (acetic acid)
TBS	100 mM Tris/HCl pH 7.5 150 mM NaCl
TBST	100 mM Tris/HCl pH 7.5 150 mM NaCl 0.05% (v/v) Tween [®] 20
TE	10 mM Tris/HCl pH 8.0 0.1 mM EDTA pH 8.0
LoTE	3 mM Tris/HCl pH 7.5 0.2 mM EDTA pH 7.5
Transfer buffer (25x)	300 mM Tris base 2.4 M glycine

Solution	Recipe
Tris-Glycine-SDS buffer (10x)	248 mM Tris/HCl pH 7.5 1918 mM glycine 1% (w/v) SDS
Triton X-100 lysis buffer	50 mM HEPES pH 7.5 150 mM NaCl 1 mM EGTA 10% (v/v) glycerol 1% (v/v) Triton X-100 100 mM NaF 10 mM Na ₄ P ₂ O ₇ * 10 H ₂ O 1 mM PMSF 1 mM Na ₃ VO ₄
Upper Tris buffer (4x)	500 mM Tris base 0.4% (w/v) SDS pH 6.8 (HCl)
X-gal stain (pH 6.0)	3 mM K ₃ Fe(CN) ₆ 3 mM K ₄ Fe(CN) ₆ 1 mM MgCl ₂ 1 mg/ml X-gal in PBS pH 6.0

3.5 Antibodies

3.5.1 Primary antibodies

Antibody	Supplier/Reference
mouse monoclonal anti-dystrophin Ab-1 (clone 1808)	<i>Dunn Labortechnik, Asbach, Germany</i>
mouse monoclonal anti-dystrophin NCL-Dys1	<i>Novocastra, Newcastle, UK</i>
mouse monoclonal anti-dystrophin NCL-Dys2	<i>Novocastra, Newcastle, UK</i>
mouse monoclonal anti-VSV (clone p5d4)	<i>Department of Molecular Biology, MPI of Biochemistry</i>
mouse monoclonal anti- α -dystroglycan IIH6	gift from Dr. K. P. Campbell (Ervasti and Campbell, 1991)
rabbit polyclonal anti- β -actin	<i>Sigma, Taufkirchen, Germany</i>

3.5.2 Secondary antibodies

Antibody	Supplier/Reference
avidin-Cy3.5-conjugate	<i>Amersham, Piscataway, USA</i>
donkey anti-mouse IgG Cy3-conjugate	<i>Jackson ImmunoResearch, West Grove, USA</i>
goat anti-mouse IgG HRP-conjugate	<i>Promega, Mannheim, Germany</i>
goat anti-rabbit IgG HRP-conjugate	<i>Sigma, Taufkirchen, Germany</i>
sheep anti-Dig FITC-conjugate	<i>Roche, Mannheim, Germany</i>

3.6 DNA constructs

Table 2 Description of DNA constructs.

Vector	Description	Origin
attb-pDysE	pCR3.1 backbone with CMV promoter, attb site and expression of dystrophin N-terminally tagged with EGFP	gift from Dr. J. P. Tremblay (Chapdelaine et al., 2000)
attb-pEGFP	EGFP from pEGFP-C1 cloned into the backbone of attb-pDysE	this work
pCMV-DAG1-VSV	pEGFP-C1 backbone with expression of dystroglycan (cloned from pDAG1) C-terminally tagged with VSV	this work
pDAG1	pcDNA3.1 backbone with expression of dystroglycan	gift from Dr. C. Herzog (Herzog et al., 2004)
pEGFP-C1	mammalian expression plasmid with CMV promoter and enhanced cyan fluorescent protein (ECFP)	<i>BD Clontech, Heidelberg, Germany</i>
pEGFP-C1	mammalian expression plasmid with CMV promoter and enhanced green fluorescent protein (EGFP)	<i>BD Clontech, Heidelberg, Germany</i>
pRetroSuper	self-inactivating retroviral vector for short hairpin RNA expression	Dr. T. R. Brummelkamp (Brummelkamp et al., 2002)
pRetroSuper shDMD	pRetroSuper backbone with expression of short hairpin RNA targeting <i>DMD</i>	this work

3.7 Oligonucleotides

Table 3 Sequence and description of oligonucleotides.

Name	Sequence 5'-3'	Product length	Reference
DMD LC Fw	CCCATTTCTTCACAGCATTT	187 bp	Alex Epanchintsev
DMD LC Rv	GTCTTTCACCACTTCCACATCA		
Dp427c Fw	CGTATCAGATAGTCAGAGTGGTTAC	561 bp	NM_000109
Dp427m Fw	CCTGGCATCAGTTACTGTGTTGAC	548 bp	NM_004006
Dp427p Fw	CCTATGAAGGTGTGTAGCCAGCC	331 bp	NM_004009
Dp427 Rv	CCATCTACGATGTCAGTACTTCC		NM_004006
Dp260 Fw	AGGAACATTTCGACCTGAGAAAG	214 bp	NM_004011
Dp260 Rv	TCCACCTTGTCTGCAATATAAGC		
Dp140 Fw	ATTGCTGGCTGCTCTGAACTAA	161 bp	NM_004013
Dp140 Rv	CATCTGTTTTTGAGGATTGCTG		
Dp116 Fw	GGGTTTTCTCAGGATTGCTATG	364 bp	NM_004014
Dp116 Rv	CCGGCTTAATTCATCATCTTTC		
Dp71 Fw	GAAGCTCACTCTCCACTCGTA	393 bp	NM_004015
Dp71 Rv	AGCCAGTTCAGACACATATCCAC		
shDMD	TTAACTGGCTGGAGTATCA	-	Alex Epanchintsev
DMD1b	CTCTCCATCAATAGAAGCTGCC	-	(Roberts et al., 1991)
UTRN Fo1	GCTCACCACATACCTGACTGAC	180 bp	NM_007124
UTRN Re1	ACATCCATCTGACTTCCCTCCTCT		
DAG1 Fo1	TGCCGCTGATACCTTGATGATAT	60 bp	(Arning et al., 2004)
DAG1 Re1	TGACCATTCCAACAGATTTGATTG		
SNTB2 Fo1	GCTGGCAGAACAGGCAAAC	65 bp	(Arning et al., 2004)
SNTB2 Re1	TCACAGCCATGAGGACAGGTC		
SGCB Fo1	CAGCAAAGTTCCAATGGTCCTG	67 bp	(Arning et al., 2004)
SGCB Re1	TGACACTCCTTCTCTCAACAGCCT		
SGCE Fo1	GCGCCTGAACGCCATAAAC	95 bp	(Arning et al., 2004)
SGCE Re1	CCATGACATAAACGCCCTCCT		
LAMA2 Fo1	CTGTTGCTGATAACCTCCTCTTT	185 bp	NM_000426
LAMA2 Re1	CCCAGTTCTTGATGCTACGATAC		
SSPN Fo1	GGCTTGTTTATGCTTTGTGTCTC	157 bp	NM_005086
SSPN Re1	ACTGTGTGAGCTGCGAATAGTG		
NOS1 Fo1	GTGATGTCTTCTGTGTGGGAGAT	211 bp	NM_000620
NOS1 Re1	GTTGACCGACTGGATTTAGGG		
DTNA Fo1	CCAAGGACAGTGAAGTAGAGCAG	137 bp	NM_001390
DTNA Re1	GACATACAACCCGATGAGAACAT		
LAMA2 Fo2	ACACTCTGCTGGTCTCCTCTTTA	547 bp	NC_000006
LAMA2 Re2	GTGCTCTTATGCTTTGGCTTGTA		
16q22/+6000 Fo	CTACTCACTTATCCATCCAGGCTAC	209 bp	NC_000016
16q22/+6000 Re	ATTCACACACTCAGACATCACAG		
C-MYC Int2 Fo	CTTCTCAGCCTATTTTGAACACTG	164 bp	NC_000008
C-MYC Int2 Re	TGGTATGACTTTAGCAACTCCCTAT		
AKT3 Fo	CTGCTACTTCACTGTCATCTTCAAT	162 bp	NC_000001
AKT3 Re	TGCGTGTATGTGTGTTTTCA		
RaTERT Fo	TCCGAGGTGTCCCTGAGTATGG	193 bp	Dr. Dmitri Lodygin
RaTERT Re	AGGTGCGCTCACCTGGAGTAGT		
ACTB Fo2	TGACATTAAGGAGAAGCTGTGCTAC	213 bp	NM_001101
ACTB Re2	GAGTTGAAGGTAGTTTCGTGGATG		
p16Int1 Fo	CTTTCTGTGTTTGGCTTATTTTATT	312 bp	NC_000009
p16Int1 Re	TTCTCTCTGACTGTGACCCTCTAAT		

Table 3 continued.

Name	Sequence 5'-3'	Product length	Reference
LEZ500_9a Fo7	GCACAATCACAGAAATGGAAAC	449 bp	NC_000009
LEZ500_9a Re7	CAGTATGGAGGGGAGTAAAAAGAGT		21.546 Mbp
LEZ500_9a Fo4	TGATGAGACTGAATAACTGAAGGAG	272 bp	NC_000009
LEZ500_9a Re4	AAAATGGGACTTGGAGGTAGTGA		21.615 Mbp
LEZ500_9a Fo1	CTCCATTTCTTCCTCCTCCTCATA	493 bp	NC_000009
LEZ500_9a Re1	CTCAAAGTCAAAGTCTCCAATCTG		21.843 Mbp
LEZ500_9a Fo2	GCCCCTTCTGTCTTTTCCTTAG	499 bp	NC_000009
LEZ500_9a Re2	CACTTCCCTGCTGTCTTTCTTT		22.105 Mbp
LEZ500_9a Fo3	TACTTGCCTTAGTCTTTGGTTGTG	452 bp	NC_000009
LEZ500_9a Re3	CTGCCTTTTTTCATCTGGAGTCT		22.996 Mbp
LEZ500_9a Fo5	TGAGTGTATGGTTGTTAGAGGAC	282 bp	NC_000009
LEZ500_9a Re5	CTATGGAGGATGAAGCAGGAGA		23.312 Mbp
LEZ500_9a Fo8	AGAGATGTAGAAAGAACTGGAGCAA	241 bp	NC_000009
LEZ500_9a Re8	GAGACCTGAAACTGGGTGTAAATAA		23.463 Mbp
LEZ500_9a Fo9	TTTAGTTACAGGTCTCTGGGTCATC	200 bp	NC_000009
LEZ500_9a Re9	CTATTTGTTCTCTCTGCTTTCTCT		23.473 Mbp
LEZ300_1b Fo1	GGTCTTTCTTTCTTTGTGCTTAG	240 bp	1p22.1
LEZ300_1b Re1	GTTCCAGTTCACCAGTATCTATCA		
LEZ300_10c Fo1	CCCATCTTCCTATTTGAGTCCTTT	475 bp	10q25
LEZ300_10c Re1	CTAAGTTTGAGCATCCCTCCATT		
SU7100_1b Fo	GAGATGAGGACAGGATGAAGAAA	300 bp	1p36.2
SU7100_1b Re	ACAGACCAACAAGCAAATGAAC		
SU7200_4b Fo	GTAGACCAGCAAGACTCGGAAAA	294 bp	4q31-q32
SU7200_4b Re	GAAGGAAGGTGAAGGCAAATC		
SU7200_6c Fo	CCACCCAGGTTATTAGGATTA	288 bp	6q25
SU7200_6c Re	AAGGAAACGAGTGAGGAAGAAA		
SacI linker A	biotin-TTTGCAGAGGTTTCGTAATCGAGTTGGGTGAGCT		(Wang et al., 2002)
SacI linker B	phosphate-CACCCAACCTCGATTACGAACCTCTGC		
LS linker 1A	TTTGGATTTGCTGGTGACAGTACAACCTAGGCTTAATATC		(Wang et al., 2002)
	CGACATG		
LS linker 1B	phosphate-TCGGATATTAAGCCTAGTTGTACTGCACCA		
	GCAAATCC-amino-modified C7		
LS linker 2A	TTTCTGCTCGAATTCAAGCTTCTAACGATGTACGTCC		(Wang et al., 2002)
	GACATG		
LS linker 2B	phosphate-TCGGACGTACATCGTTAGAAGCTTGAATTC		
	GAGCAG-amino-modified C7		
LS primer 1	biotin-TTTTTTTTTGGATTTGCTGGTGCAGTACA		(Wang et al., 2002)
LS primer 2	biotin-TTTTTTTTTCTGCTCGAATTCAAGCTTCT		
M13F	GTAAAACGACGGCCAGT	-	(Wang et al., 2002)
M13R	GGAAACAGCTATGACCATG		

3.8 Bacteria strains

Table 4 Description of bacteria strains.

Strain	Description	Origin
XL1-Blue	<i>recA1 endA1 gyrA96 thi-1 hsdR17 supE44 relA1 lac</i> [F' <i>proAB lacI^fΔM15 Tn10(Tet^r)</i>]	Stratagene, La Jolla, USA
XL10-Gold	Tet ^r $\Delta(mcrA)183 \Delta(mcrCB-hsdSMR-mrr)173$ <i>endA1</i> <i>supE44 thi-1 recA1 gyrA96 relA1 lac Hte</i> [F' <i>proAB</i> <i>lacI^fΔM15 Tn10(Tet^r) Amy Cam^r</i>]	Stratagene, La Jolla, USA

3.9 Cell lines and cell culture media

All cell lines, their origin and culturing conditions are listed in Supplementary Table 1. The following media and supplements were obtained from Invitrogen (Karlsruhe, Germany): Hanks' Balanced Salt Solutions (HBSS), Dulbecco's Modified Eagle Medium (DMEM) with high or low glucose, McCoy's 5A medium, RPMI 1640 medium, Minimal Essential Medium (MEM), Leibovitz's L15 medium, penicillin-streptomycin solution, non-essential amino acid solution, and sodium pyruvate solution. MCDB 153 medium powder and bovine insulin were from Sigma (Taufkirchen, Germany), and fetal bovine serum (FBS) from Perbio Science (Bonn, Germany).

3.10 Equipment

Equipment	Supplier
Axioplan II Imaging epifluorescence microscope	<i>Karl Zeiss, Oberkochen, Germany</i>
Axiovert 200M fluorescence microscope with a CoolSNAP-HQ CCD camera and Metamorph software	<i>Karl Zeiss, Oberkochen, Germany Photometrics, Tucson, USA Universal Imaging, Downingtown, USA</i>
Axiovert 25 microscope with a HyperHad CCD camera and ImageBase software	<i>Karl Zeiss, Oberkochen, Germany Sony, Köln, Germany Kappa Optoelectronics, Gleichen, Germany</i>
Capillary sequencer 3700	<i>Applera, Norwalk, USA</i>
Digital karyotyping software	gift from Dr. K. Kinzler
DMRXA-RF8 epifluorescence microscope	<i>Leica Microsystems, Wetzlar, Germany</i>
DryEase [®] Mini-Gel Drying System	<i>Invitrogen, Karlsruhe, Germany</i>
FACScan unit	<i>BD Biosciences, Mountain View, USA</i>
Kodak Imager (440CF imaging system)	<i>Kodak, Stuttgart, Germany</i>
Leica QFISH software	<i>Leica Microsystems, Wetzlar, Germany</i>
LightCycler [™] real-time PCR system	<i>Roche, Mannheim, Germany</i>
Metafer/Isis software	<i>MetaSystems, Altlußheim, Germany</i>
Mini Trans-Blot [®] Cell system	<i>Bio-Rad, Hercules, USA</i>
Mini-PROTEAN [®] 3 Electrophoresis System	<i>Bio-Rad, Hercules, USA</i>
PCR thermocycler Perkin Elmer 9700	<i>Applied Biosystems, Foster City, USA</i>
SAGE2000 software	gift from Dr. V. Velculescu
Ultra Evolution 384-well plate reader	<i>Tecan, Crailsheim, Germany</i>

4 METHODS

4.1 *Chromosome metaphase spreads*

Cells were treated with 0.1 µg/ml colcemid at 37°C for 3 hours, trypsinized and pelleted. The cell pellet was resuspended in 10 ml of 0.8% sodium citrate and incubated for 25-40 minutes at 37°C. Cells were pelleted again, fixed with ice-cold methanol/glacial acetic acid (3:1) and incubated on ice for 5 minutes. Afterwards, cells were washed four times in fixative, resuspended in 1-2 ml of fixative and stored at -20°C. For chromosome metaphase spreads fixed cells were dropped onto glass slides and air-dried.

4.2 *Comparative genomic hybridization*

All CGH experiments were performed in the laboratory of Dr. M. R. Speicher. 1 µg of genomic DNA from melanoma cell lines and normal placenta was nick-translated with 1x NT-buffer (0.5 M Tris/HCl pH 8.0; 50 mM MgCl₂; 0.5 mg/ml BSA), 10 mM β-mercaptoethanol, 0.05 mM ACG-mix (dATP; dCTP; dGTP), 1 mM labeled dUTP (digoxigenin-11-dUTP for normal DNA and biotin-16-dUTP for tumor DNA), 4.5 ng DNase I and 5 U DNA polymerase I in a total of 50 µl for 2 hours at 15°C. The labeled fragments of tumor and normal DNA were combined and ethanol precipitated together with 70 µg Cot-1 DNA and 182 µg salmon-sperm DNA. The pellet was resuspended in 4 µl of deionized formamide for 10 minutes at 42°C and mixed with 4 µl of 30% dextran sulfate. Chromosome metaphase spreads from normal males on glass slides were used for hybridization. First, metaphase chromosomes were incubated in a pepsin solution (0.03 mg/ml in 0.01N HCl, pH 2.3) for 1-3 minutes at 37°C. Then, slides were washed briefly in PBS and dehydrated in 70%, 90%, and 100% ethanol for 3 minutes each. The chromosomes on the slides were denatured in 70% formamide/SSC for 1 minute and 45 seconds at 72°C. Afterwards, the slides were dehydrated in a cold (-20°C) ethanol series (70%, 90%, 100%) for 5 minutes each. At the same time, the hybridization mixture was denatured for 7 minutes at

78°C and pre-hybridized for 20 minutes at 42°C. The hybridization mixture was then applied onto the slides with the denatured chromosomes, covered with a coverslip, sealed and hybridized in a water bath for 72 hours. After hybridization, slides were washed three times 5 minutes in 4x SSC/0.2% Tween[®] 20 at 42°C, three times 5 minutes in 1x SSC at 60°C and blocked with 3% BSA/4 xSSC/0.2% Tween[®] 20 for 30 minutes at 37°C. The slides were washed briefly in 4xSSC/0.2% Tween[®] 20 and incubated with the primary antibodies sheep anti-Dig-FITC (dilution 1:100) and avidin-Cy3.5 (dilution 1:300) in 1% BSA/4xSSC/0.2% Tween[®] 20 for 45 minutes at 37°C. Finally, slides were washed three times 5 minutes in 4xSSC/0.2% Tween[®] 20 at 42°C, briefly incubated in DAPI solution (0.2 µg/ml) and covered with a coverslip. CGH analysis was done as described previously (du Manoir et al., 1993; Kallioniemi et al., 1992).

4.3 7-Fluor M-FISH

All M-FISH experiments were performed in the laboratory of Dr. M. R. Speicher. For FISH analysis, labeling of DNA with seven fluorochromes (24-color FISH) was done as described (Azofeifa et al., 2000). The labeling pattern of chromosomes with the seven different fluorophores is shown in Table 5.

Table 5 Labeling of single chromosomes with seven different fluorophores.

Chromosome	1	2	3	4	5	6	7	8	9	10	11	12	13	14	15	16	17	18	19	20	21	22	X	Y	ps
DEAC	X					X				X			X			X							X		X
FITC	X			X	X		X											X	X		X				
Cy3			X			X	X			X					X			X		X					
TexasRed			X	X					X	X							X					X		X	X
Cy5		X										X	X		X		X				X				
Cy5.5					X			X				X		X								X	X		X
Cy7		X					X	X		X				X		X									

Treatment of chromosomes and hybridization of labeled probes was done as described in section 4.2.

4.4 Digital karyotyping

Digital karyotyping was performed according to the protocol provided by Wang et al. (Wang et al., 2002). Genomic DNA from the melanoma cell lines M2 and M3 was extracted as described in section 4.5. First, 4 µg of genomic DNA were incubated with 120 U of the mapping enzyme *SacI* for 1.5 hours at 37°C. The digested DNA was extracted with phenol/chloroform, ethanol precipitated and resuspended in 5 µl LoTE. For ligation of biotinylated linkers both primers (*SacI* Linker A and *SacI* Linker B) were first annealed to form linkers. Therefore, 1.8 µg of both primers were mixed, heated to 95°C for 2 minutes, placed at 65°C and 37°C for 10 minutes each, and cooled down at room temperature for 20 minutes. Then, 56 ng of annealed *SacI* linker were mixed with 1 µg of digested DNA in ligation buffer, heated to 50°C for 2 minutes and cooled down at room temperature for 10 minutes. Afterwards, 5 U of T4 DNA ligase were added and the ligation reaction was carried out at 16°C for 3 hours. DNA fragments were extracted with phenol/chloroform, ethanol precipitated, and resuspended in 20 µl LoTE.

Cleavage with the fragmenting enzyme was carried out with 80 U of *NlaIII* at 37°C for 1 hour. The DNA was extracted with phenol/chloroform, ethanol precipitated, and resuspended in 10 µl LoTE. DNA fragments ligated to biotinylated linkers were isolated with streptavidin-linked magnetic beads. First, 200 µl Dynabead M-280 streptavidin slurry were washed with 400 µl washing buffer D (5 mM Tris/HCl pH 7.5, 0.5 mM EDTA, 1 M NaCl, 200 µg/µl BSA), mixed with 300 µl washing buffer D containing the 10 µl DNA solution, and incubated for 20 minutes at room temperature with intermittent shaking. The beads were washed three times with 400 µl washing buffer D, once with 300 µl 1x ligation buffer, and resuspended in 300 µl of 1x ligation buffer. The beads were divided equally into two tubes and LS linkers were ligated to the bound genomic DNA. Annealing of LS primer 1A/1B and LS primer 2A/2B to form linkers was carried out as described for *SacI* linkers. The 1x ligation buffer was removed from both tubes containing the DNA fragments bound to Dynabeads[®] and 23.5 µl LoTE and 7 µl 5x ligation buffer were added. In addition, 2 µl annealed LS linker 1A/B were added to tube 1 and 2 µl annealed LS linker 2A/B were added to tube 2. Both tubes were heated for 2 minutes at 50°C and cooled down at room temperature for 10 minutes. 12.5 U T4 ligase were added to each tube

and the ligation was carried out for 2 hours at 16°C with gentle mixing every 15 minutes. After ligation, each tube was washed four times with 600 µl washing buffer D. The beads were transferred to two new tubes, washed once with washing buffer D and twice with 200 µl 1x buffer 4 (NEB), and resuspended in 200 µl 1x buffer 4.

For the release of genomic tags, buffer 4 was removed from both tubes and 118 µl LoTE, 15 µl 10x buffer 4, 15 µl 10x S-adenosylmethionine, and 70 U *MmeI* were added to each tube and incubated for 1 hour at 37°C with intermittent mixing. Afterwards, 100 µl supernatant were collected from each tube and combined for subsequent use as ligation reaction (tube 1) and 50 µl supernatant from each tube were combined as no ligation control reaction (tube 2). The DNA in both tubes was extracted with phenol/chloroform, ethanol precipitated, and resuspended in 1.5 µl LoTE.

In the following reaction blunt-ended tags were ligated to form ditags. A 2x ligase mix (5 µl 3 mM Tris/HCl pH 7.5, 6 µl 5x ligase buffer, 4 µl T4 ligase (5 U/µl)) and a 2x no ligase mix (9 µl 3 mM Tris/HCl pH 7.5, 6 µl 5x ligase buffer) were prepared. 1.5 µl of the ligase mix were added to tube 1 and 1.5 µl of the no ligase mix were added to tube 2 which served as negative control in the following PCR reaction. The ligation reaction was carried out overnight at 16°C. Afterwards, 14 µl LoTE were added to tube 1 containing the ligase mixture.

In the next step, ditags were amplified by PCR in a volume of 50 µl containing 1x PCR buffer, 3 µl DMSO, 75 mmol dNTPs, 175 ng LS PCR primer 1, 175 ng LS PCR primer 2, 2.5 U Platinum[®] *Taq* DNA polymerase, and 1 µl ligation product. PCR was carried out at 94°C for 1 minute, then 26-30 cycles at 94°C for 30 seconds, 55°C for 1 minute, and 70°C for 1 minute, with a final extension of 5 minutes at 70°C. First, PCR conditions were optimized by testing different dilutions of the template of 1/20, 1/40, and 1/80. Likewise, the PCR reaction was carried out for 26, 28, and 30 cycles. The starting amount of template and cycle number is critical for isolating an adequate amount of DNA for subsequent steps. The aim was to obtain a high yield of ditags with only minor amounts of incorrect byproducts. For the amplification of ditags from the cell line M2 a dilution of 1/20 with 26 cycles and for the cell line M3 a dilution of 1/40 with 28 cycles were chosen. Template from the no ligase control reaction was not diluted and amplified with 35 cycles. It did not contain any product of the size of the ditags. After optimization of the PCR conditions, large-scale amplification of

ditags was performed with 250 reactions (50 μ l each) aliquoted into three 96-well plates. Afterwards, PCR products were pooled, ethanol precipitated, resuspended in 144 μ l LoTE, and heated at 37°C for 5 minutes. After addition of 36 μ l 5x loading buffer, ditags were loaded onto two 16% polyacrylamide gels and run at 40 V overnight. Amplified ditags of 134 bp were excised and the gel pieces were placed into 0.5 ml tubes pierced at the bottom with a 21-gauge needle. The 0.5 ml tubes were placed in 2.0 ml siliconized microcentrifuge tubes and centrifuged at 13,000 rpm for 2 minutes. Thereby, the gel pieces were broken up into smaller fragments, which remained at the bottom of the 2.0 ml tube. The 0.5 ml tubes were discarded and 250 μ l LoTE and 50 μ l 7.5 M ammonium acetate were added to the gel fragments in each tube in order to extract the ditags. The tubes were vortexed and placed at 65°C for 15 minutes with intermittent mixing. Afterwards, the supernatant from each tube was transferred to a SpinX microcentrifuge tube and centrifuged at 13,000 rpm for 5 minutes. This procedure separated the supernatant from any remaining gel pieces. The cleared eluates were extracted with phenol/chloroform, ethanol precipitated, and resuspended in 80 μ l LoTE.

Before concatenation of the isolated ditags, biotinylated linkers were removed by cleavage with the restriction endonuclease *Nla*III. Therefore, the 80 μ l of ditags were divided equally into two tubes and incubated each with 200 U of *Nla*III in a total volume of 200 μ l for 1 hour at 37°C. Afterwards, biotinylated linker fragments were removed from ditags by incubation with streptavidin-linked magnetic beads. First, 1600 μ l of beads were prewashed three times with the same volume of washing buffer D and divided equally into eight tubes. Then, 400 μ l 2x B&W buffer (10 mM Tris/HCl pH 7.5, 1 mM EDTA, 2 M NaCl) and 4 μ l 100x BSA were added to a total volume of 400 μ l of restriction digest solution, mixed and divided into the first two tubes containing magnetic beads. Both tubes were mixed end over end for 15 minutes at room temperature. The supernatant was removed and applied to the next set of tubes with beads and mixed end over end for 15 minutes at room temperature. At the same time, the first set of tubes with beads was washed with 200 μ l of 1x B&W buffer and 1x BSA and mixed end over end for 15 minutes at room temperature. This procedure was continued; the supernatant from the second set of tubes was collected and applied to the third and fourth set. Likewise, the B&W solution from the first set was applied sequentially to the remaining sets of tubes. After washing of the

last set of tubes all supernatants were consolidated and in order to prevent disassembly of the ditags all subsequent steps were performed on ice. First, the ditags were extracted with phenol/chloroform, ethanol precipitated, and resuspended in 7 μ l TE. After addition of sample buffer, ditags were loaded onto a 16% polyacrylamide gel and run at 40 V overnight. A 36 bp band corresponding to the ditags was excised and the gel pieces were placed into 0.5 ml tubes pierced at the bottom with a 21-gauge needle. The 0.5 ml tubes were placed in 2.0 ml siliconized microcentrifuge tubes and centrifuged at 13,000 rpm for 2 minutes. The 0.5 ml tubes were discarded and 250 μ l TE and 50 μ l 7.5 M ammonium acetate were added to the gel fragments in each tube in order to extract the ditags. The tubes were vortexed and placed at 37°C for 20 minutes with intermittent mixing. Afterwards, the supernatant from each tube was transferred to a SpinX microcentrifuge tube and centrifuged at 13,000 rpm for 5 minutes. The cleared eluates were ethanol precipitated and resuspended in 10.5 μ l cold LoTE.

After purification, ditags were ligated to form concatemers, which were then cloned and sequenced. For the ligation reaction, 5x ligation buffer and 7.5 U T4 DNA ligase were added to the purified ditags and incubated for 2 hours at 16°C. Afterwards, sample buffer was added and the sample was heated at 65°C for 5 minutes. The concatemers were applied to a 1.5% agarose gel, which was run at 60V for 2.5 hours. The concatemers formed a smear on the gel, which ranged from 100 bp to about 8 kbp. Concatemers in the range of 600 – 1100 bp were excised, purified with the QIAquick gel extraction kit, extracted with phenol/chloroform, ethanol precipitated, and resuspended in 10 μ l LoTE.

For cloning of concatemers, 1 μ g of the pZERO vector was cleaved with the restriction endonuclease *Sph*I, phenol/chloroform extracted, ethanol precipitated and resuspended in LoTE. The ligation was performed with 3 μ l purified concatemers, 25 ng linearized pZERO vector, and 1 U T4 DNA ligase at 16°C overnight. Afterwards, the ligation reaction was extracted with phenol/chloroform, ethanol precipitated, and resuspended in 30 μ l LoTE. 1 μ l of the ligated concatemers was transfected into ElectroMAX DH10B electrocompetent bacteria by electroporation. 1/10 of the transfected bacteria was then plated onto 10 agar plates containing zeocin for selection of positive transformants. Between 200 – 300 colonies were counted on each plate and at least 60 colonies were subsequently analyzed by PCR

to assess the size of the inserted fragment. PCR was carried out in a total volume of 25 µl containing 1x PCR buffer, 1.25 µl DMSO, 12.5 mmol dNTPs, 175 ng M13F primer, 175 ng M13R primer, 1 U FIREPol[®] DNA polymerase, and a small amount of bacteria from a single colony. PCR was performed with an initial denaturation of 94°C for 5 minutes, then 30 cycles with 94°C for 45 seconds, 54°C for 30 seconds, 72°C for 1 minute, and a final elongation at 72°C for 5 minutes. PCR products were evaluated on 1% agarose gels and usually more than 95% of colonies contained inserts between 800 bp and 1100 bp in size. After verification of sufficient amounts of positive transformants and the correct size of the inserted concatemers, the purified ligation reaction was sent to the Agencourt Biosciences company (Beverly, USA) for contract sequencing.

About 7000 clones corresponding to approximately 200,000 tags were sequenced for each library. Afterwards, extraction of 21 bp tags was carried out with the SAGE2000 software. Repetitive sequences were removed by aligning tags to a virtual tag library generated from the June 28, 2002 human genome assembly containing only tags obtained from unique loci. Tag densities were calculated by matching tags to their genomic position along each chromosome. Sites with over- or underrepresentation of genomic tags, representing potential sites of genomic amplifications and deletions, were visualized with the map viewer of the digital karyotyping software using a sliding window size of 100 to 1000, which corresponds to a resolution of 200 kbp to 4 Mbp. The position and size of potential genomic alterations was determined by blasting the 21 bp tags located at the borders of the alteration against the human genome assembly. Then, primers were designed to confirm potential sites of deletion or amplification by conventional PCR or qPCR, respectively. SAGE 2000 and digital karyotyping software were a kind gift from Dr. V. Velculescu and Dr. K. Kinzler.

4.5 Isolation of genomic DNA from cell lines and paraffin-embedded tissue sections

Tissue sections were de-paraffinized using xylol and briefly stained with hematoxylin and eosin. Tissue material was scratched off from designated areas and subjected to extraction of genomic DNA. For extraction of genomic DNA from cell lines, cells were trypsinized, washed, and pelleted. Genomic DNA was isolated by overnight incubation with 100 µg/ml proteinase K and 0.1% (w/v) SDS in proteinase K buffer at 55°C. Subsequently, a phenol/chloroform extraction was performed and genomic DNA was precipitated using isopropanol.

4.6 RNA isolation and RT reaction

RNA was isolated using the RNAagents total RNA isolation system according to the manufacturer's protocol. For RT, 2-3 µg of total RNA were reverse transcribed using an oligo(dT)₂₀ primer or the DMD-specific primer DMD1b and SuperScript™ III first-strand synthesis system. The RT reaction was performed at 50°C or 55°C for 60 min in a total volume of 20 µl.

4.7 RT-PCR analysis

For PCR analysis, all cDNAs were diluted twofold. If necessary, the amount of cDNA was normalized on a LightCycler with β-actin as standard. For analysis of expression of the full-length *DMD* isoforms (*Dp427c*, *Dp427m*, *Dp427p*, *Dp427l*), cDNA transcribed with the *DMD*-specific primer DMD1b was used, whereas for analysis of *Dp260*, *Dp140*, *Dp116*, *Dp71*, and the components of the DGC cDNA transcribed with the oligo(dT)₂₀ primer was used. The PCR reaction contained 1 µl of cDNA, 5 µl 10 x PCR buffer, 1 µl dNTP mix (10 mM dATP, 10 mM dCTP, 10 mM dGTP, 10 mM dTTP), 20 pmol of gene-specific primer (see Table 3, chapter 3.7), and 2.5 U of Platinum® *Taq* DNA polymerase in a total volume of 50 µl. PCR was carried

out for 40 cycles with an annealing temperature of 58°C to 60°C. The total reaction was analyzed by agarose gel electrophoresis.

4.8 qPCR analysis

Quantification of *DMD*, *hTERT*, *C-MYC*, and *AKT3* was performed by real-time PCR with gene-specific primers (see Table 3, chapter 3.7) using FastStart-DNA Master SYBR Green 1 on a LightCycler. The generation of specific products was confirmed by melting-curve analysis and gel electrophoresis. Each primer pair was tested with a logarithmic dilution of cDNA to generate a linear standard curve (crossing point [CP] plotted vs. log of template concentration), which was used to calculate the primer pair efficiency ($E = 10^{(-1/\text{slope})}$). cDNAs were normalized using β -actin primers, whereas genomic DNA was normalized with the 16q22/+6000 primer. For data analysis, the second-derivative maximum method was applied, and induction of a cDNA or amplification of a locus on genomic DNA (geneX) was calculated according to Pfaffl (Pfaffl, 2001) as follows:

$$\frac{\left(E_{geneX}\right)^{\Delta CP(normal\ cDNA - tumor\ cDNA)}}{\left(E_{\beta-actin}\right)^{\Delta CP(normal\ cDNA - tumor\ cDNA)}} = fold\ induction$$

4.9 PCR analysis of genomic DNA

For deletion analysis of *p16INK4A* in melanoma cell lines, primers LEZ500, LEZ300, SU7100, and p16Int1 were used (see Table 3, chapter 3.7). PCR reactions were performed in a total volume of 50 μ l containing 50 ng of genomic DNA, 5 μ l 10x PCR buffer, 2.5 μ l DMSO, 1 μ l dNTP mix (10 mM dATP, 10 mM dCTP, 10 mM dGTP, 10 mM dTTP), 20 pmol of each primer, and 1-2 U of Platinum[®] Taq DNA polymerase. PCR amplification was performed with an initial denaturation of 4 minutes at 94°C, 28 to 40 cycles of denaturation for 30 seconds at 94°C, annealing for 30 seconds at 50°C to 60°C, elongation at 72°C with 1 minute/kbp of product, and a final elongation for 2 minutes at 72°C.

4.10 DNA sequencing

300 ng of template DNA were used in each sequencing reaction together with 5 pmol primer, 1.5 μ l BigDye[®] Terminator v3.1 sequencing mix, and 1 μ l 5x BigDye[®] sequencing buffer in a total volume of 10 μ l. PCR amplification was performed with 30 cycles of denaturation for 20 seconds at 96°C, annealing for 10 seconds at 50°C, and elongation at 60°C for 4 minutes. Purification and sequencing of the PCR products was carried out by the sequencing service of the Max-Planck Institute of Biochemistry.

4.11 Western blot analysis

Exponentially growing cells were lysed in Triton X-100 or RIPA lysis buffer. Protein concentration was measured with the Bradford assay. 30-150 μ g of protein lysate were diluted in 2x Laemmli buffer, separated on 6% or 10% SDS/polyacrylamide gels, and transferred to Immobilon-P PVDF membranes. Membranes were blocked with 5% nonfat dry milk and incubated with primary antibody diluted in TBST or low TBST. Dystrophin (Dp427m isoform) was detected with the NCL-Dys1 antibody diluted 1:100, the NCL-Dys2 (Dp116 isoform) antibody 1:25, or the Dystrophin Ab-1 (Dp71 isoform) antibody 1:200. α -dystroglycan was detected with the IIH6 antibody (1:200) diluted in low TBST. Signals were visualized in combination with HRP-conjugated secondary antibody diluted 1:10,000. Equal loading was confirmed using β -actin antibody (dilution 1:1000). For the description of antibodies see chapter 3.5.

4.12 Generation of stable cell lines

For the expression of short hairpin RNAs mediating down-regulation of *DMD* mRNA, three different 19 bp sequences (shDMD) targeting the full-length *Dp427* isoforms were cloned into pSUPER based constructs (Brummelkamp et al., 2002) by Alex Epanchintsev and were tested by transient transfection in HEK293T cells. The ability to down-regulate expression of ectopic dystrophin was assessed by Western

blot analysis and the most efficient construct was chosen for further experiments. The entire H1-promoter-shDMD cassette was released from pSUPER after restriction digest with *EcoRI* and *BamHI* and inserted into the same sites of the self-inactivating retroviral vector pRetroSuper. The resulting construct or empty vector as control were transfected into the Phoenix A packaging cell line, which produced the respective retroviruses. Afterwards, the melanoma cell lines C-32 and M7 were infected with the retrovirus containing pRetroSuper empty vector or pRetroSuper shDMD. Resistant pools were selected with puromycin for seven days and single cell clones were generated by limiting dilution.

For ectopic expression of dystrophin, the attb-pDysE vector expressing full-length dystrophin N-terminally fused to eGFP was used. The melanoma cell lines WM-793 and RPMI-7951 were transfected with attb-pDysE or attb-pEGFP control vector. Resistant pools were obtained by selection for two weeks in the presence of neomycin (G418).

4.13 Cell growth in matrigel

Matrigel basement membrane matrix was diluted with growth medium (without FBS) to a concentration of 3 mg/ml and stored at -20°C . For each assay an aliquot of matrigel was thawed on ice overnight and mixed carefully. 60 μl of matrigel were transferred to a Costar 96-well plate and allowed to gel for three hours or overnight at 37°C . For the analysis of branching morphology, cells were trypsinized and resuspended in normal growth medium. 1×10^4 cells were seeded in each well on top of the matrigel layer. Cells were incubated at 37°C and morphology was assessed over a period of ten days. Every seven days the growth medium was carefully exchanged without disturbing the cells in the matrigel matrix. Pictures of three different areas in each well were taken every day with an Axiovert 25 microscope equipped with a HyperHAD CCD camera and ImageBase software.

4.14 Cell migration assays

To assess cell migration in the scratch assay, confluent monolayers of cells were treated with 10 $\mu\text{g/ml}$ mitomycin C for 2 hours to inhibit cell proliferation. Subsequently, the cell monolayer was scratched with the sealed tip of a Pasteur pipette. Cells were washed and fresh medium was added. Cell migration was monitored for 24-31 hours using an Axiovert 200M microscope integrated into a $\text{CO}_2/37^\circ\text{C}$ incubator, equipped with a CCD camera. Pictures of at least four different areas in each well were taken at different time points using a motorized XY precision stage. Metamorph software was used to quantitate migration by measuring the cell-free area in each picture.

Migration was also studied using transwell chambers containing membranes with 8 μm pores. Cells were trypsinized and resuspended in normal growth medium with 0.5% FBS. 1×10^5 cells in medium supplemented with 0.5% FBS were added to the upper compartment of the transwell chamber, the lower compartment was filled with growth medium containing 10% FBS. Cells were incubated at 37°C and allowed to migrate to the underside of the membrane for 18-24 hours. Subsequently, cells were fixed with 70% ethanol for 20 minutes and stained with crystal violet for 30 minutes. Cells on top of the filter were removed with a cotton swab and membranes were rinsed with tap water to remove excess dye. Pictures of representative areas of the membranes were taken with an Axiovert 25 microscope. Finally, the dye was released from the cells on the membranes and the cell number was quantitated by measuring absorbance at 570 nm with an Ultra Evolution 384-well plate reader.

4.15 Cell proliferation assay

Cells were trypsinized and resuspended in normal growth medium without phenol red. 3×10^3 cells were seeded per well in 24-well plates in triplicates. For each time point 3-(4,5-dimethylthiazol-2-yl)-2,5-diphenyl tetrazolium bromide was added to the respective wells for 4 hours at 37°C to stain living cells. Then, triplex solution (10% (v/v) SDS, 5% (v/v) isobutanol, 0.012 M HCl) was added and plates were incubated at 37°C in the dark to release the dye from the cells. Cell number was

analyzed 20 hours later by measuring absorbance at 570 nm with an Ultra Evolution 384-well plate reader.

4.16 Analysis of apoptosis by flow cytometry

For analysis of apoptosis by flow cytometry the supernatant with floating cells as well as the adherent cells were collected and washed once with PBS. Cells were fixed with ice-cold 70% ethanol for more than 2 hours or overnight at 4°C. Afterwards, cells were pelleted, washed with PBS and incubated in staining solution containing 50 µg/ml propidium iodide, 0.2 mg/ml RNase A, and 0.1% (v/v) Triton X-100 for 30 minutes at room temperature. For each sample 1×10^4 cells were analyzed with a FACScan unit. The amount of apoptotic cells was determined by comparing the percentage of cells in the sub-G1 fraction between samples.

4.17 Senescence-associated β -galactosidase staining

Cells were washed once with PBS (pH 7.5) and fixed by incubation with 0.5% (v/v) glutaraldehyde in PBS for 5 minutes at room temperature. Cells were washed three times with PBS (pH 6.0) containing 1 mM $MgCl_2$ and stained with X-gal solution (pH 6.0) at 37°C for 5 hours or overnight protected from light. Afterwards, cells expressing senescence-associated β -galactosidase (SA- β -gal) were distinguished by their blue color (Dimri et al., 1995). Pictures of different areas were taken with an Axiovert 25 microscope equipped with a HyperHAD CCD camera and ImageBase software, and the percentage of senescent cells was evaluated by determining the amount of blue cells compared to the amount of total cells.

4.18 Immunofluorescence staining and confocal microscopy

For localization of dystrophin and β -dystroglycan, cells were grown on glass coverslips. Cells were transfected with either attb-pDysE or pCMV-DAG1-VSV vectors for ectopic expression of both proteins, because it was not possible to detect endogenous protein in immunofluorescence. As control, vectors containing only eGFP (attb-pEGFP) or a VSV-tag (pCMV-VSV) were transfected. 24 hours after transfection cells were washed once with PBS and fixed with 4% paraformaldehyde for 20 minutes at room temperature. Cells were washed three times with PBS and coverslips with cells transfected with attb-pDysE or attb-pEGFP were mounted onto glass slides with DAPCO antifade. Cells transfected with pCMV-DAG1-VSV or pCMV-VSV were permeabilized with 0.2% (v/v) Triton X-100 in PBS for 15 minutes at room temperature. After washing with PBS unspecific binding sites were blocked with 100% FBS for 30 minutes at room temperature. Cells were washed again with washing buffer (PBS containing 10% FBS and 0.05% (v/v) Tween[®] 20) and incubated for 1.5 hours at room temperature with the mouse anti-VSV antibody diluted 1:100 in washing buffer. After washing, cells were incubated with donkey anti-mouse Cy3 antibody diluted 1:400 in washing buffer for 45 minutes at room temperature. Finally, cells were washed with PBS/0.05% (v/v) Tween[®] 20, then PBS, briefly rinsed in water and mounted on glass slides with DAPCO antifade. Pictures of single cells were taken with a Leica TCS SP2 confocal laser scanning microscope.

4.19 Statistical analysis

Statistical significance was determined either with the chi square test or the student's t-test. The chi square test is a non-parametric test for bivariate tabular analysis and was used for independent and mutually exclusive variables that were generated as raw frequencies. First, a four square table was generated as drawn below (Table 6), with M1 and M2 describing independent biological variables, each of them occurring in two different states (denoted as + and -).

Table 6 Four square table showing the setup of variables for a chi square test. Two independent biological variables M1 and M2, each occurring in two different states (+ and -), were measured.

	M2	-	+	Σ
M1				
-		a	b	$a+b=n_1$
+		c	d	$c+d=n_2$
Σ		$a+c$	$b+d$	$a+b+c+d=n$

Using the four square table the chi square value (X^2) was calculated with the following equation.

$$X^2 = \frac{(n-1)(ad-bc)^2}{(a+b)(c+d)(a+c)(b+d)}$$

For each X^2 -value a corresponding P-value was derived, and $P < 0.05$ was considered statistically significant.

The student's t-test was applied to two normally distributed populations. Each of the two data sets was characterized by a number of data points. t was calculated for an unpaired t-test assuming equal variances as shown below with μ_1, μ_2 as the averages, δ_1^2, δ_2^2 as the variances, and n_1, n_2 as the number of trials of the first and second experiment, respectively. The equation represents a one-tailed comparison of t and a level of significance of $\alpha = n_1 + n_2 - 2$ degrees of freedom. t (or P) < 0.05 was considered statistically significant.

$$t = \frac{\mu_1 - \mu_2}{\sqrt{\frac{(n_1 - 1)\delta_1^2 + (n_2 - 1)\delta_2^2}{n_1 + n_2 - 2}}} \sqrt{\frac{n_1 + n_2}{n_1 n_2}}$$

5 RESULTS

5.1 Characterization of malignant melanoma cell lines

5.1.1 General characteristics

An initial panel of nine melanoma cell lines (M1-M9) was derived from metastases of malignant melanoma with cells being cultured for a few passages only. The cell lines were established in the Department of Dermatology at the University Hospital of Erlangen and were a kind gift from Dr. Beatrice Schuler-Thurner. The clinicopathologic characteristics are listed in Table 7. In addition, CRL-1974 was obtained from ATCC and has been described previously (Trevor et al., 2004).

Table 7 Clinicopathologic characteristics of nine melanoma cases.

Cell line/ patient	Age/sex	Primary tumor / Breslow thickness	Clark level	Site of metastasis
M1	68/f	SSM, 9 mm	IV	lymph node, groin
M2	47/f	n. c. melanoma, 0.5 mm	III	abdomen
M3	49/m	SSM, 1.4 mm	n. a.	adrenal gland
M4	43/m	SSM, 2 mm	IV	thorax
M5	31/f	NM, 4.5 mm	n. a.	lymph node, groin
M6	74/f	NM, 1.9 mm	n. a.	upper arm
M7	n. a./f	n. a.	n. a.	lymph node, groin
M8	65/f	SSM, n. a.	IV	labium majus
M9	60/f	SSM, 3.5 mm	IV	gluteal

Abbreviations: f, female; m, male; SSM, superficial spreading melanoma; NM, nodular melanoma; n. c., not classifiable; n. a., not available.

Chromosome metaphase spreads were prepared of eight melanoma cell lines and chromosome number and ploidy level were determined (Table 8). For the cell lines M8 and M9 it was not possible to establish suitable conditions to obtain chromosome metaphase spreads.

Table 8 Chromosome number and ploidy level of eight melanoma cell lines.

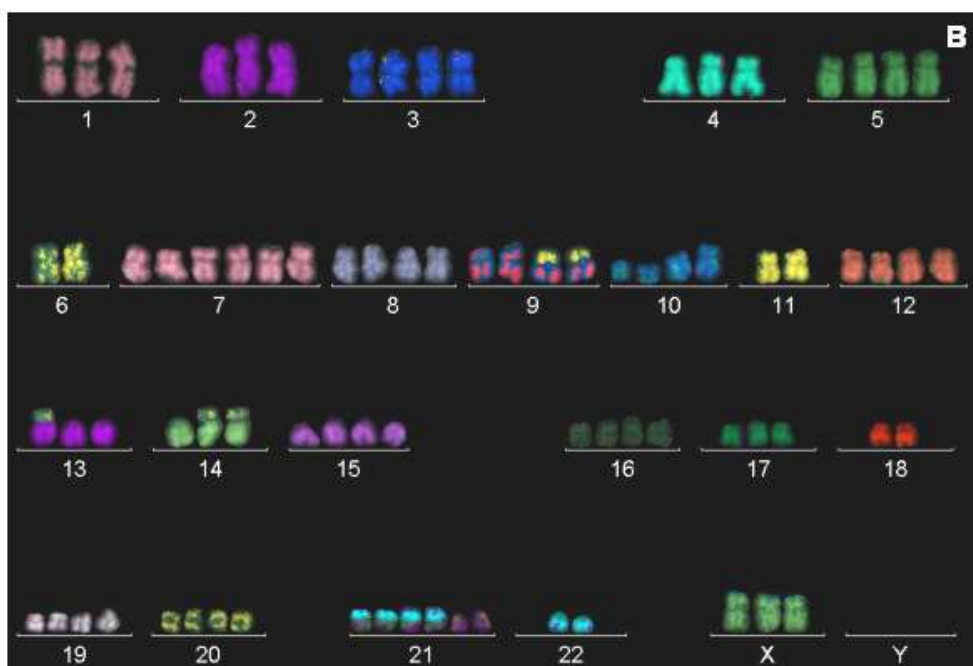
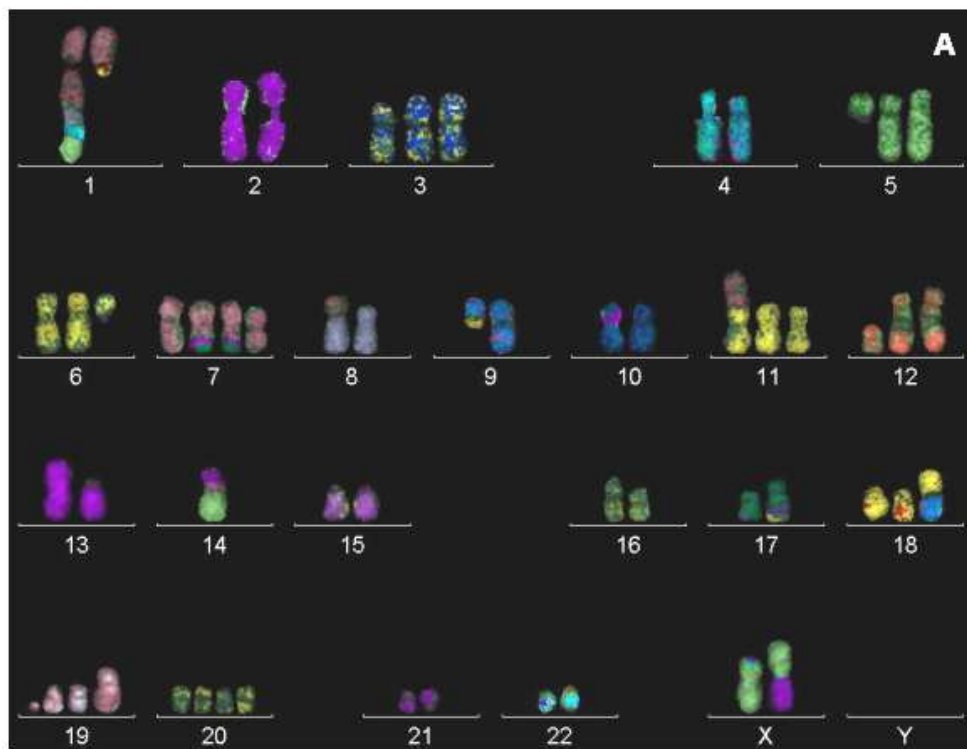
Cell line	Mean chromosome number	Ploidy level ^a
M1	57	hyperdiploid
M2	80	hypertriploid
M3	65	hypotriploid
M4	75	hypertriploid
M5	51	hyperdiploid
M6	42	hypodiploid
M7	70	hypertriploid
CRL-1974	62	hypotriploid

^aThe ploidy level was determined according to the ISCN 1995 guidelines.

5.1.2 M-FISH analysis of malignant melanoma cell lines

The melanoma cell lines M1, M2, M3, and M7 were analyzed by 7-Fluor M-FISH (Speicher et al., 1996) in the laboratory of Dr. M. R. Speicher. Chromosome metaphase spreads were prepared and hybridized with painting probes for all 24 human chromosomes. The hybridization mixture contained pools that were differentially labeled with DEAC, FITC, Cy3, Texas Red, Cy5, Cy5.5, and Cy7. All chromosomes were counterstained with DAPI. The chromosomes were identified by their specific and unique color combination and visualized by false color images (Figure 6).

For each tumor cell line at least 9 metaphases were analyzed for chromosomal aberrations. Thereby, the melanoma cell line M1 displayed a hyperdiploid karyotype with 56-59 chromosomes in each cell. Although this cell line possessed the lowest mean chromosomes number of the four cell lines analyzed the karyotype proved to be the most complex (Table 9). 52 chromosomes with translocations were found with only nine of these chromosomes (A5, A12, A14, A16, A19, A22, A25, A27, A29) present in at least 70% of the cells. Underrepresentation was observed for chromosomes 14 and 18 and overrepresentation for chromosomes 6, 7, and 20.



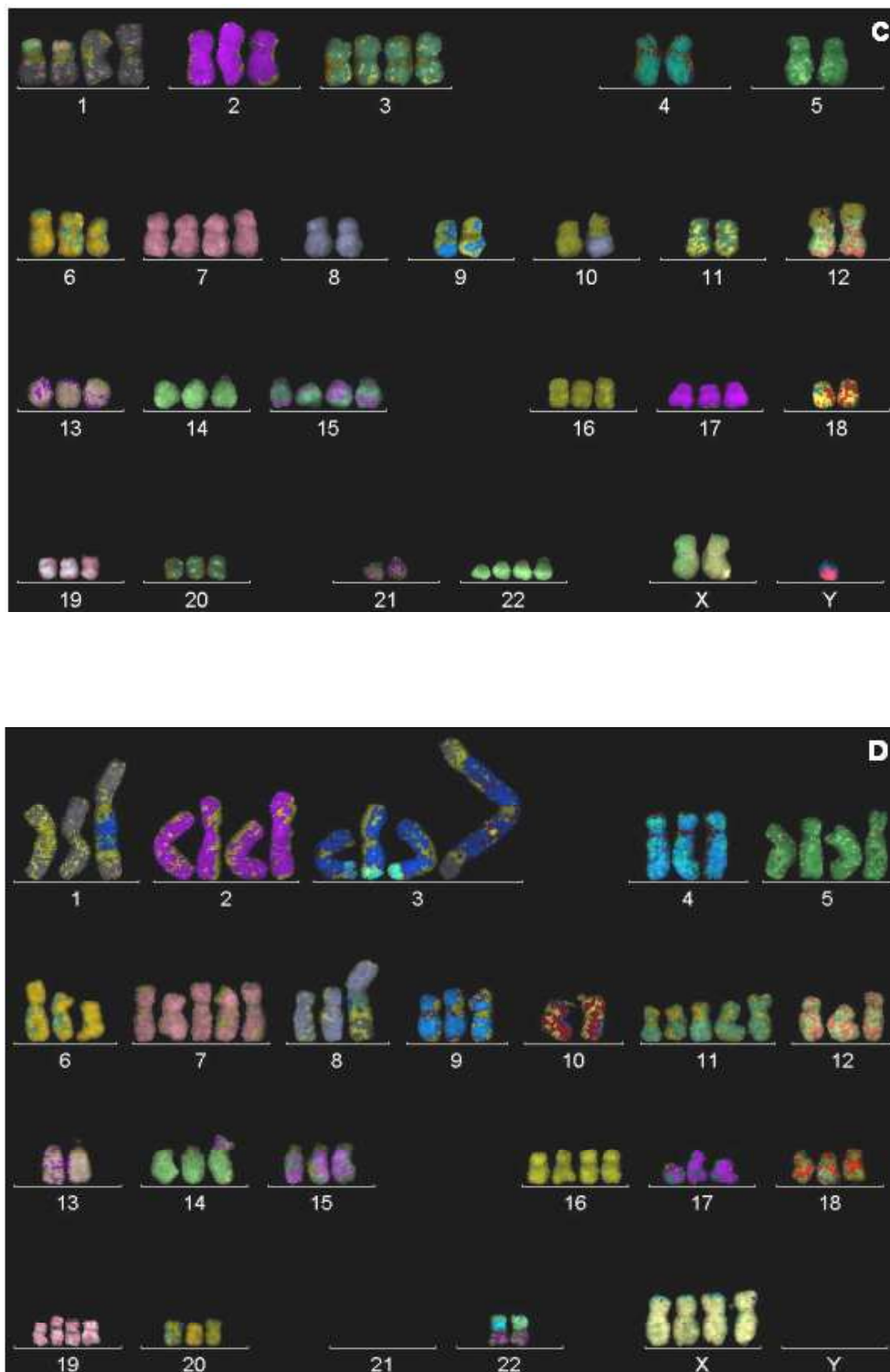


Figure 6 7-Fluor M-FISH analysis of four melanoma cell lines. Representative examples of single metaphases from the melanoma cell lines M1 (A), M2 (B), M3 (C), and M7 (D) hybridized with the 7-Fluor M-FISH painting probe mix are shown. Depicted are false color images for each chromosome, which is indicated by the respective number. Translocated fragments were assigned by the color corresponding to their chromosomal origin.

The melanoma cell line M2 showed a hypertriploid karyotype with the chromosome number varying between 75 and 84. A more homogeneous karyotype was observed in M2 with eight chromosomes containing translocations with six of them (A1, A2, A5 - A8) present in at least 70% of cells (Table 10). Chromosome 6 showed underrepresentation, whereas chromosomes 7, 15, 19, 21, and 22 were overrepresented.

In the melanoma cell line M3 a hypotriploid karyotype with 64-68 chromosomes was observed. M3 presented the least number of structural aberrations with only five chromosomes showing translocations, three of them (A1, A3, A4) present in 100% of cells (Table 11). Underrepresentation was detected for chromosomes 4 and 18 and overrepresentation for chromosomes 1, 3, 7, 15, and 22.

The melanoma cell line M7 displayed a hypertriploid karyotype with 64-75 chromosomes per cell. This cell line showed the second most complex karyotype of the four melanomas with translocations observed in 21 chromosomes with only seven of them (A5 - A7, A13, A15, A16, A20) present in at least 70% of cells (Table 12). Chromosomes 10, 13, 15, 21, and 22 displayed underrepresentation and chromosome 3 overrepresentation.

Taken together, the karyotypes of M1 and M7 showed a higher percentage of cells with non-clonal structural rearrangements. However, no distinct subpopulations of cells were detected in any of the four melanoma cell lines analyzed. Chromosome 18 was underrepresented and chromosomes 3 and 7 were overrepresented in at least two of four cell lines. In addition, chromosomes 1 and 8 were affected by translocations in three of four cell lines.

Table 9 Numerical and structural aberrations observed with M-FISH in the cell line M1. In the upper part of the table the number of the individual chromosomes per metaphase is listed, whereas the lower part describes the different translocations observed in each metaphase.

Numerical abnormalities		Metaphases 1-9								
1		2	2	3	2	2	2	2	2	2
2		2	2	2	2	3	2	3	3	2
3		3	3	2	3	3	3	3	3	3
5		3	3	3	3	3	3	3	3	3
6		4	4	3	3	4	4	3	3	4
7		4	4	4	5	3	5	4	5	4
9		2	3	3	2	3	3	2	2	2
10		2	2	3	2	2	2	2	2	3
11		3	3	3	3	3	3	3	3	3
12		3	2	2	3	3	2	3	3	3
13		3	3	3	2	3	3	3	2	3
14		1	2	2	1	2	2	2	2	1
15		2	2	2	2	1	1	1	3	2
18		2	1	1	3	1	1	1	2	2
19		3	2	3	3	3	3	4	3	4
20		4	4	3	4	3	4	5	3	3
21		3	3	3	2	1	3	2	2	3
22		2	1	3	2	3	3	3	2	2
X		2	2	2	2	2	2	2	1	1
Structural rearrangements										
A1	der(1)t(1;8;14)				1x					
A2	der(1)t(1;12)									1x
A3	der(1)t(1;20)			1x		1x		1x		
A4	der(1)t(2;1)					1x				
A5	der(1)t(2;6)							1x	1x	
A5	del(1)	1x	1x	1x	1x	1x	1x	1x	1x	1x
A7	der(2)t(2;12;17)		1x							
A8	der(3)t(3;12)			1x						
A9	del(3)					1x				
A10	der(4)t(4;12)						1x			
A11	der(5)t(5;12;22)	1x								
A12	del(5)		1x	1x	1x	1x	1x	1x	1x	1x
A13	der(6)t(6;2)	1x	1x	1x		1x	1x			1x
A14	del(6)	1x	1x		1x	1x	1x	1x	1x	1x
A15	der(7)t(7;13)								1x	
A16	der(7)t(7;17)	2x	2x	2x	2x	1x	2x	2x	2x	2x

Table 9 continued.

Structural rearrangements		Metaphases 1-9								
A17	dic(7)t(7;18)									1x
A18	del(7)									1x
A19	der(8)t(8;1)	1x	1x		1x	1x	1x	1x	1x	1x
A20	der(8)t(8;3)				1x					
A21	der(9)t(9;10)	1x								
A22	der(9)t(9;18)		1x	1x		1x	1x	1x	1x	1x
A23	del(9)	1x	1x	1x	1x	1x	1x			
A24	del(10)									1x
A25	der(11)t(11;1)	1x	1x	1x	1x	1x		1x	1x	1x
A26	der(11)t(11;1;15)						1x			
A27	der(12)t(12;1)	2x	2x	2x	2x	2x	2x	2x	2x	2x
A28	del(12)	1x			1x	1x		1x	1x	1x
A29	der(13)t(13;13)	1x	1x	1x	1x	1x	1x		1x	1x
A30	der(13)t(13;14)									1x
A31	der(13)t(13;15)							1x		
A32	der(13)t(13;21)					1x				
A33	der(13)t(13;22)				1x					
A34	der(14)t(14;8)		1x	1x				1x	1x	
A35	der(14)t(14;8;X)	1x								
A36	der(14)t(14;9)							1x		
A37	der(14)t(14;18)						1x			
A38	der(14)t(14;21)				1x					
A39	der(14)t(14;22)									1x
A40	der(15)t(15;9)									1x
A41	der(15)t(15;14)	1x								
A42	der(15)t(15;15)									1x
A43	der(15)t(15;19;22)		1x							
A44	der(17)t(17;11)						1x	1x		1x
A45	der(17)t(17;20)	1x	1x	1x	1x	1x				
A46	der(17)t(17;21)	1x				1x			1x	
A47	der(18)t(18;9)	1x			1x					
A48	der(19)t(19;7)			1x	1x	1x		1x		1x
A49	der(19)t(19;16)	1x								
A50	der(X)t(X;7)		1x							
A51	der(X)t(X;13)				1x					
A52	der(X)t(X;15)					1x				

Table 10 Numerical and structural aberrations observed with M-FISH in the cell line M2. In the upper part of the table the number of the individual chromosomes per metaphase is listed, whereas the lower part describes the different translocations observed in each metaphase.

Numerical abnormalities	Metaphases 1-10										
1	3	3	2	3	3	3	3	3	3	3	
2	4	4	4	3	3	3	3	3	4	3	
3	4	4	4	4	4	4	4	4	3	4	
4	2	3	3	3	2	3	3	2	3	3	
5	4	4	4	4	4	4	4	3	4	4	
7	6	6	6	6	6	6	6	5	6	6	
8	4	4	4	4	4	4	4	3	4	4	
9	2	2	4	4	4	4	4	5	4	4	
10	2	4	3	4	4	4	4	4	4	4	
11	4	4	2	2	2	2	2	2	1	2	
12	4	4	3	4	4	4	4	4	4	4	
13	3	3	3	3	3	3	3	3	3	3	
14	2	3	3	3	3	3	3	3	3	3	
15	3	4	4	4	4	4	4	3	2	4	
16	4	4	4	4	4	4	4	4	4	4	
17	3	3	3	3	3	3	3	3	3	3	
18	4	3	3	2	4	3	3	3	3	3	
19	4	4	3	4	4	4	4	3	4	4	
20	3	4	4	4	4	4	4	4	4	4	
21	4	5	4	6	4	4	2	5	3	4	
22	4	3	4	2	4	4	6	2	4	4	
X	3	4	3	3	3	3	3	2	2	3	
Structural rearrangements											
A1	der(9)t(9;11)			2x	2x	2x	2x	2x	3x	2x	2x
A2	del(10)		2x	2x	2x	2x	2x	2x	2x	2x	2x
A3	der(11)t(11;9)		1x	2x							
A4	del(12)								1x		
A5	der(13)t(13;6)	1x	1x	1x	1x	1x	1x	1x	2x	1x	1x
A6	der(14)t(14;6)	1x	2x	2x	2x	2x	2x	2x	1x	2x	2x
A7	der(21)t(21;22)	2x	3x	2x	4x	2x	2x		3x	2x	2x
A8	der(22)t(22;21)	2x	1x	2x		2x	2x	4x	1x	2x	2x

Table 11 Numerical and structural aberrations observed with M-FISH in the cell line M3. In the upper part of the table the number of the individual chromosomes per metaphase is listed, whereas the lower part describes the different translocations observed in each metaphase.

Numerical abnormalities		Metaphases 1-10									
1		4	4	4	4	4	3	4	4	4	4
2		3	3	4	3	4	3	3	3	4	4
3		4	4	3	4	4	4	4	4	4	4
4		2	2	2	1	2	2	2	2	2	2
6		3	3	3	3	3	3	3	3	3	3
7		4	4	4	3	4	4	4	4	4	3
10		2	2	1	2	2	2	2	2	2	2
11		2	2	3	2	2	2	2	2	2	2
13		3	3	4	4	4	3	3	3	3	4
14		3	3	2	3	3	3	3	3	3	3
15		4	4	3	4	4	4	4	4	4	4
16		3	3	3	3	3	3	3	3	3	3
17		3	3	3	3	3	3	3	3	3	3
18		2	2	2	2	2	2	2	2	2	1
19		3	3	3	3	3	3	3	3	3	3
20		3	3	3	3	3	3	3	3	3	3
21		3	2	3	3	3	2	2	2	2	3
22		2	4	4	4	4	4	4	4	4	4
X		2	2	2	2	2	2	2	2	2	2
Structural rearrangements											
A1	der(1)t(1;12)	2x	2x	2x	2x	2x	1x	2x	2x	2x	2x
A2	der(1)t(1;16)			1x							
A3	der(10)t(10;8)	1x	1x	1x	1x	1x	1x	1x	1x	1x	1x
A4	der(12)t(12;10)	2x	2x	2x	2x	2x	2x	2x	2x	2x	2x
A5	der(22)t(22;21)						1x				

Table 12 Numerical and structural aberrations observed with M-FISH in the cell line M7. In the upper part of the table the number of the individual chromosomes per metaphase is listed, whereas the lower part describes the different translocations observed in each metaphase.

Numerical abnormalities		Metaphases 1-10									
1		4	3	3	4	4	3	4	3	3	3
2		4	4	3	3	4	4	4	3	3	4
3		5	4	5	5	4	5	5	3	5	4
4		4	3	4	3	4	4	4	3	4	4
5		4	4	5	2	3	3	5	3	3	4
6		3	4	3	2	4	3	3	3	3	4
7		4	5	4	4	5	4	3	3	4	3
8		3	3	3	3	3	3	3	3	3	3
9		3	3	3	3	3	3	2	3	3	3
11		2	5	5	3	3	3	3	2	2	5
12		4	3	4	4	3	4	4	3	4	3
13		2	2	1	2	2	2	2	2	2	2
14		3	3	3	3	3	3	3	3	3	3
15		2	3	2	2	2	2	2	2	2	2
16		3	4	3	3	4	3	3	3	3	3
17		3	3	3	2	3	3	2	3	3	3
18		3	3	3	3	3	3	3	3	3	2
19		4	4	4	4	4	4	4	4	4	4
20		4	4	2	3	4	4	4	4	5	3
21		0	0	0	0	0	0	0	1	0	0
22		2	2	2	2	2	2	2	0	2	3
X		3	4	3	3	5	3	2	5	3	5
Structural rearrangements											
A1	der(1)t(1;3)			1x		1x	1x			1x	1x
A2	der(1)t(1;5)							1x		1x	
A3	der(1)t(1;11)	1x									
A4	der(1)t(1;15)				1x						
A5	der(3)t(3;1)	1x	1x	1x		1x	1x	1x	1x		1x
A6	der(3)t(3;17)	2x		2x	2x		2x	2x		2x	
A7	der(3)t(3;22)	2x	3x	2x	2x	3x	2x	2x	2x	2x	3x
A8	der(3)t(3;1;8)				1x						
A9	der(3)t(3;1;2)									1x	
A10	del(4)							1x			
A11	der(5)t(5;3)	1x						1x			
A12	del(6)	1x						1x			
A13	der(8)t(8;1;3)	1x	1x	1x	1x	1x	1x	1x	1x	1x	1x

Table 12 continued.

Structural rearrangements		Metaphases 1-10									
A14	del(11)		2x	2x		2x					
A15	der(14)t(14;21)	1x	1x	1x	1x	1x	1x	1x	1x	1x	1x
A16	del(17)		1x	1x		1x	1x		1x	1x	1x
A17	der(20)t(20;6)							1x			
A18	der(20)t(20;11)	1x									
A19	der(21)t(21;22)							1x			
A20	der(22)t(22;21)	2x	2x			2x	2x	2x		2x	3x
A21	del(X)					1x					

5.1.3 CGH analysis of malignant melanoma cell lines

The melanoma cell lines M1-M7, M9, and CRL-1974 were analyzed by conventional metaphase CGH for regions with over- or underrepresentation of genomic material. The experiments were performed in the laboratory of Dr. M. R. Speicher. Genomic DNA of all nine cell lines was prepared and labeled, and together with normal placental DNA hybridized to normal metaphase chromosomes (46, XY). Thereby, several genomic aberrations were detected, which are listed in Table 13. In addition, Figure 7 shows a graphical summary of the CGH results of all melanoma cell lines. Taken together, the most frequently overrepresented chromosomal regions were 1q, 6p, 7p/q, 20p/q, 22p/q, and Xp/q, whereas the most frequently underrepresented chromosomal regions were 6q, 9p, and 10q. In total, more chromosomal gains (8.6 gains per tumor) than losses (4.7 losses per tumor) were observed.

In some of the melanoma cell lines high level gains or losses of specific chromosomal regions were detected (examples are shown in Figure 8). For example, in the cell line M4 the distal end of chromosomes 1q, 5p, and 8q were locally amplified, and in the cell line M7 two regions on chromosome 3 (3p13-p14 and 3q21-q25) showed distinct amplicons (Figure 8). On chromosomes 5p15.33 and 8q24 two genes frequently amplified in tumors are located, namely *hTERT* (Pirker et al., 2003) and *C-MYC* (Morrison et al., 2005). In addition, frequent losses were observed at the distal end of chromosome 9, especially in the cell line M2. This region harbors the tumor-suppressor gene *p16INK4A* (9p21) (Castellano et al., 1997).

Table 13 Chromosomal alterations detected by CGH in nine melanoma cell line. For each cell line the gains and losses of genomic material are listed.

Cell line	Gains	Losses
M1	1p31-33, 6p21, 13q13-q14, 13q31-q34, 17q21-q23, 20p, 20q	6q14-q21, 9p23-p24
M2	21q, 22q, Xp11.22-22.2, Xq12-q21, Xq22-q28	1p, 1q21.2-q32, 2p, 2q22-q37, 4p, 4q, 6q, 9p13-p24, 10q21-q26, 11q12.3-q25, 13q21-q34, 14q11.1-q32
M3	1q, 2p, 2q, 3p, 3q, 6p, 7p, 7q, 10q23-q25, 12p, 13q, 15q, 17q11-q21, 22q, Xp, Xq	
M4	1q21.2-q32, 1q41-q44, 5p14-15.3, 6p21.1-p22, 6p23-p25, 8q22-q24.3, 17q, 22q11.2-q13	4p13-p16, 10p12-p14, 10q21-q26, 11p11.2-p15, 11q13-q24
M5	1q31-q41, 2q23-qter, 6p21.3-pter, 7p, 7q, 8q, 12p, 12q12-q21, 17p, 20p, 20q, Xp, Xq	
M6	3p25-p26, 5q34-q35, 17q24-q25, 22q13	6q22-q24
M7	1q24-q32.1, 3p13-p14, 3q21-q25, Xp, Xq	1q41-q42, 3p21-p26, 6q, 8p21-p23, 8q23-q24.3, 9p21-p24, 10p, 10q, 11p12-p14, 11q14-q25, 13q, 17p, 18p
M9	1p13.1-p21, 1q, 2q22-q33, 6p21.3-p25, 7p, 7q, 13q, 20p, 20q, 22q	6q14-q27, 9p21-p23
CRL-1974	1q21-q44, 4q12-q28, 4q32-q35, 6p, 7p, 7q, 20p, 20q, 22q	1p13-p22, 5p12-p15.3, 5q12-q35, 9p21-p24, 10q21-q26, 15q13-q24, 16q11.2-q24

At this time, no specific candidate genes had been described in melanoma for the regions amplified on chromosomes 1, 3, and 12. Nevertheless, for the amplicon on chromosome 1 in the cell line M4 a region containing the *AKT3* gene (1q43-q44) was chosen for further analysis. As AKT activity can be negatively regulated by PTEN (for review see (Robertson, 2005)), which itself often displays decreased activity in melanoma, this seemed to be a likely target for amplification.

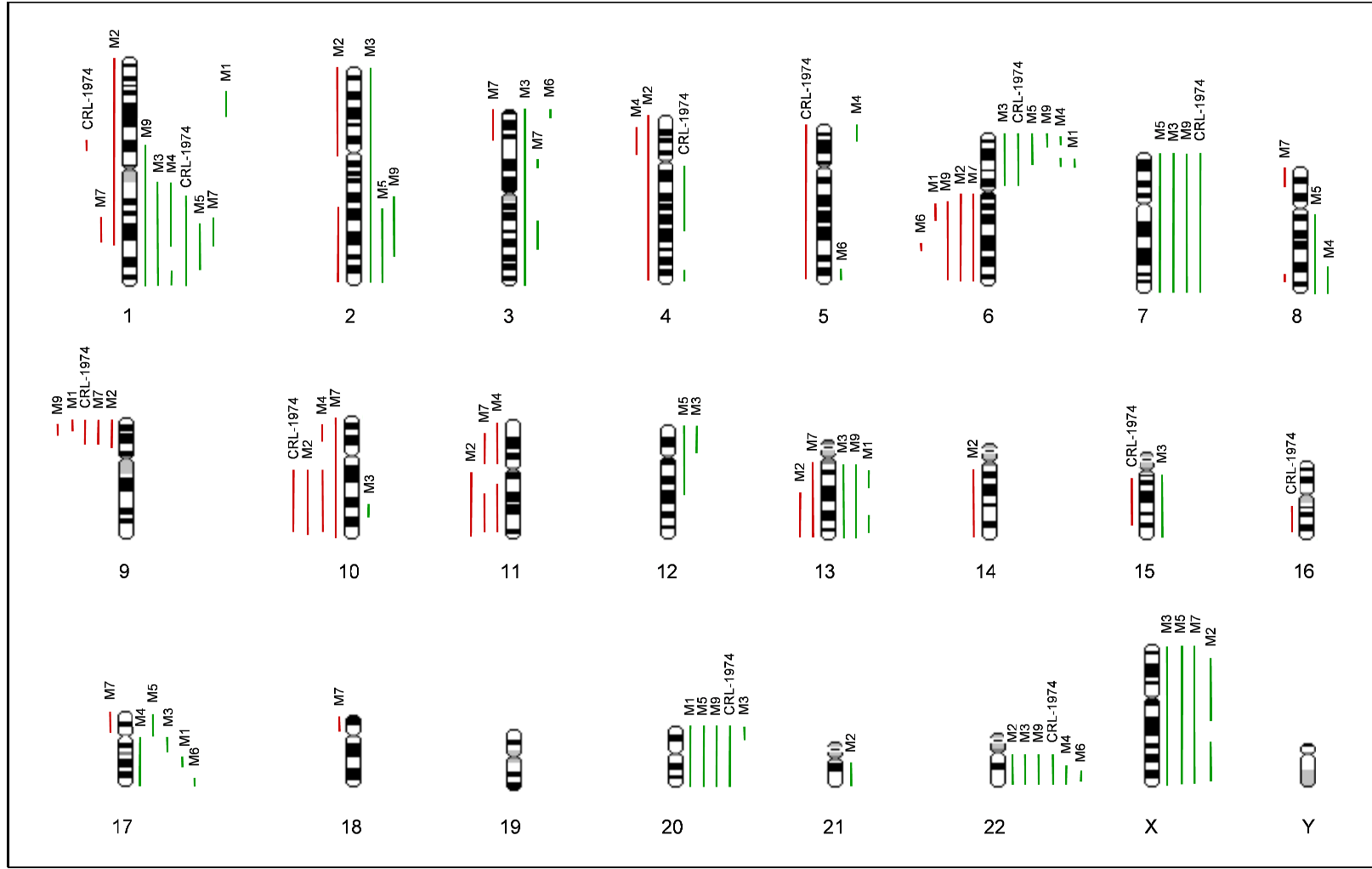


Figure 7 Summary of copy number aberrations found by CGH analysis of nine malignant melanoma cell lines. The vertical red lines on the left side of each chromosome ideogram show regions of reduced copy number, and the green lines on the right side show regions of increased copy number. Each line is labeled with the tumor in which the alteration occurred. For each tumor between 22 and 30 metaphases were evaluated.

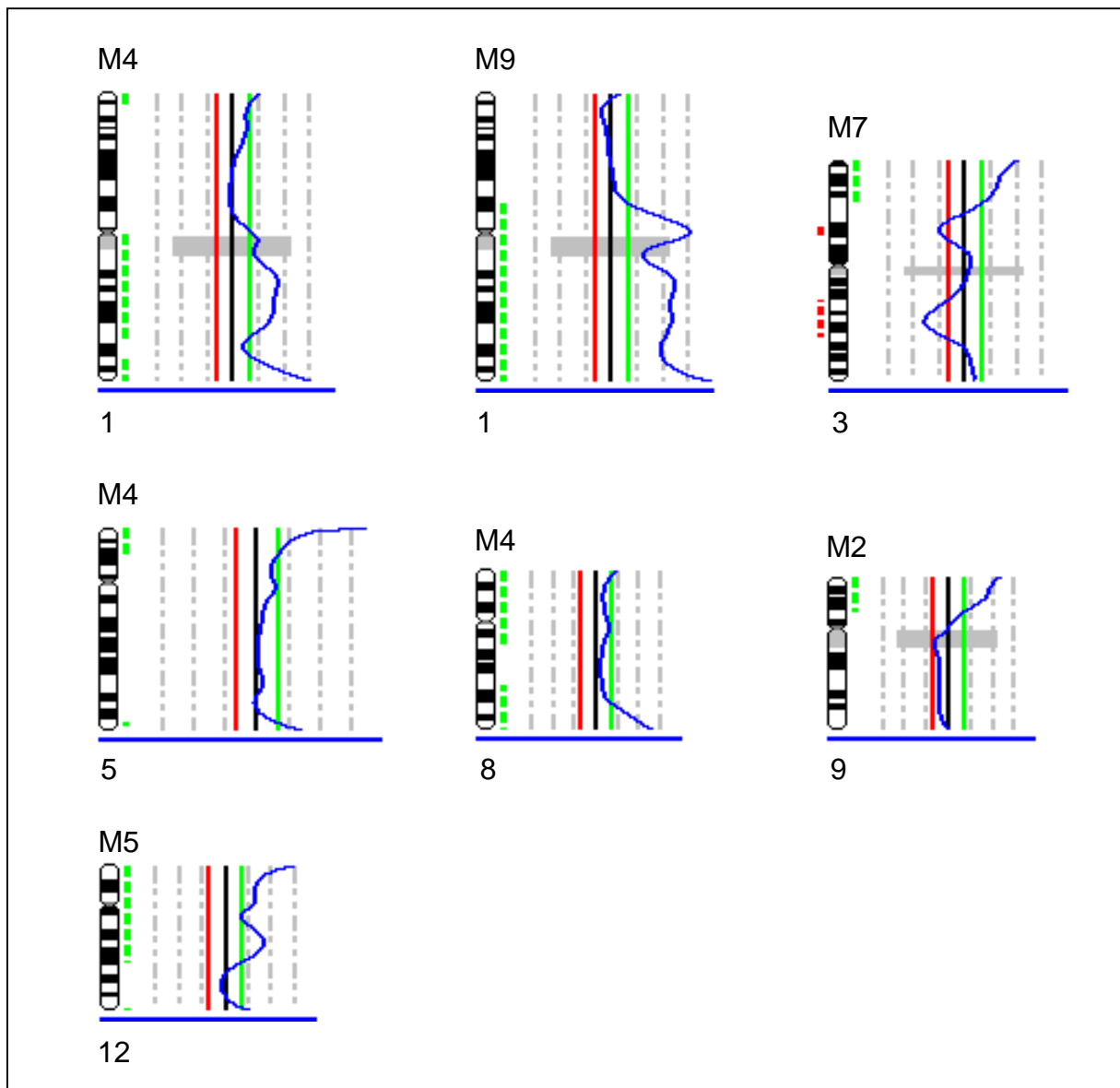


Figure 8 Examples of single chromosome CGH profiles of different malignant melanoma cell lines. The name of the cell line is indicated above each ideogram and the chromosome number is given below. For M2 and M7 gains are indicated in red on the left side of the chromosome ideogram and losses in green on the right side. For M4, M5, and M9 gains are indicated in green on the right side of the chromosome ideogram and losses in red on the left side.

To validate some of the CGH results, *C-MYC*, *hTERT*, and *AKT3* were analyzed for copy number changes by quantitative PCR (qPCR) with primers specific for each gene. Genomic DNA isolated from the melanoma cell lines M1-M7, M9, and CRL-1974 was normalized utilizing a primer in a region with low gene density on chromosome 16q22, which has not been described to be affected by chromosomal aberrations in melanoma. Copy number changes were evaluated by comparison with

genomic DNA isolated from early passage human diploid fibroblasts (HDF), and the results are listed in Table 14.

Table 14 Copy number values determined in nine malignant melanoma cell lines by qPCR analysis and deletion status of the *p16INK4A* gene. Copy number values were calculated per haploid genome. Copy numbers ≥ 2.0 are marked in bold. Abbreviations: n. d., not determined; P, present; HD, homozygous deletion.

Cell line	<i>C-MYC</i>	<i>hTERT</i>	<i>AKT3</i>	<i>p16INK4A</i>
M1	1.1	3.2	2.2	P
M2	1.1	2.4	1.7	HD
M3	1.2	1.9	1.6	HD
M4	5.9	11.2	4.3	HD
M5	1.4	1.8	1.6	HD
M6	1.4	2.9	n. d.	P
M7	1.0	2.7	2.6	P
M9	0.8	0.8	1.3	HD
CRL-1974	2.0	2.4	3.3	P

The *p16INK4A* gene was analyzed for homozygous deletion by conventional PCR. Absence of a PCR product with a primer located inside the *p16INK4A* gene together with presence of a PCR product from the primer located at 16q22 was scored as homozygous deletion. Again, genomic DNA from HDF was used as positive control. The results are listed in Table 14.

Overall, the PCR analyses showed a good correlation with the results from CGH. The analyzed genes (*C-MYC*, *hTERT*, *AKT3*) proved to be amplified in the regions with high-level gains in the respective cell lines. Also, homozygous deletion of *p16INK4A* was frequently observed in the underrepresented chromosomal region on 9p. In addition, these amplifications and homozygous deletions were also observed by PCR in other melanoma cell lines without being detected by CGH. Nevertheless, other genes located inside the regions with high level gains or losses, which are likewise affected by copy number alterations could also contribute to the pathogenesis of malignant melanoma.

5.2 Digital karyotyping analysis of malignant melanoma cell lines

With the cytogenetic characterization of melanoma cell lines by M-FISH and CGH analysis, a general overview of genomic alterations was gained. Based on these findings, a technique with higher resolution was utilized in order to search for small genomic regions with amplifications or deletions, which may indicate the presence of so far unknown oncogenes or tumor-suppressor genes. Therefore, digital karyotyping was applied, as this newly developed technique allows for a much higher resolution than conventional karyotyping techniques (Figure 2, chapter 1.2.3) (Wang et al., 2002). In total, four digital karyotyping experiments were performed with the cell lines M1, M2, M3, and CRL-1974, which were chosen because no high level gains or losses were detected in chromosomal regions containing known tumor-suppressor genes or oncogenes.

The digital karyotypings of M1 and CRL-1974 were carried out by Alex Epanchintsev. About 210,000 tags were sequenced for each library so that after the removal of repetitive sequences about 100,000 tags could be used for analysis (for details see Table 15).

Table 15 Size of the digital karyotyping libraries obtained from four malignant melanoma cell lines. The column tags describes the total number of tags sequenced, whereas filtered tags denotes tags without repetitive sequences, which can be used for analysis.

Cell line	Tags	Filtered tags
M1	210,004	101,428
M2	204,768	103,301
M3	206,465	111,245
CRL-1974	207,543	104,071

5.2.1 Validation of the digital karyotyping results

First, tag densities were dynamically analyzed along each chromosome by using sliding windows containing $\geq 1,000$ virtual tags. The term “virtual tags” refers to those tags that were computationally extracted from the human genome assembly and represent unique loci. The aforementioned resolution of $\geq 1,000$ virtual tags was

predicted to reliably detect subchromosomal changes $\geq 4\text{Mbp}$, for example gains and losses of chromosomal arms. The tag density maps for each chromosome generated by the digital karyotyping software for the cell lines M2 and M3 revealed several changes, which were compared with the CGH single chromosome profiles of these cell lines. Thereby, the overall changes detected for each chromosome were largely consistent with the CGH analysis. As example, a comparison between digital karyotyping and CGH for the chromosomes 1 and 6 in the cell line M3 is shown in Figure 9.

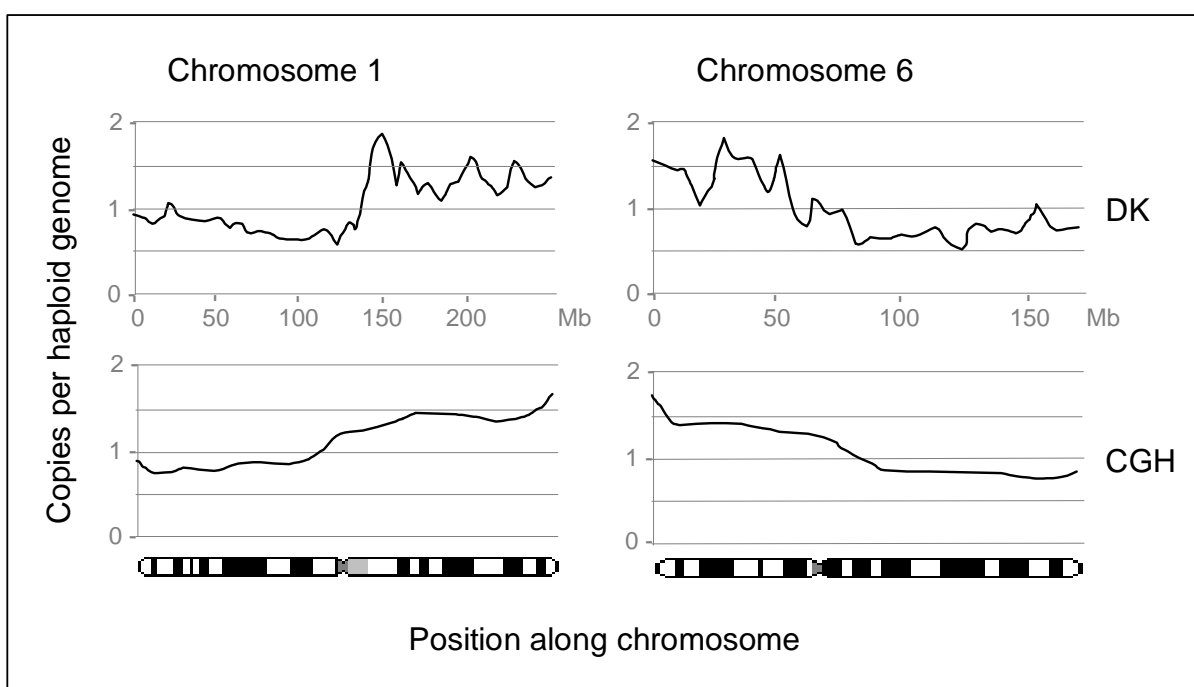


Figure 9 Examples of subchromosomal changes of chromosomes 1 and 6 in the cell line M3 revealed by low-resolution tag density maps. The upper set in each graph corresponds to the digital karyotype (DK), while the lower graph represents the CGH profile. Values on the x-axis indicate position along the chromosome and values on the y-axis represent copies per haploid genome.

For the detailed analysis of amplifications in the digital karyotyping libraries of the cell lines M2 and M3, sliding window sizes of 50 virtual tags were used. This window size was expected to reliably detect amplifications with 10-fold copy numbers of at least 200 kbp in size. With the digital karyotyping software only very few regions, which displayed amplifications of three to six fold per haploid genome, were detected in both libraries. To validate these amplifications, primers were designed for every region and qPCR was performed. Thereby, the only amplification which could be validated was located on chromosome 20q13.3 with a 2.3-fold change in the

melanoma cell line M2. Two genes were located in the amplified region – *STMN3* (*stathmin-like 3*) and *C20orf41* (now called *RTEL1*, *regulator of telomere elongation helicase 1*). *STMN3* belongs to the stathmin/oncoprotein 18 family of microtubule-destabilizing phosphoproteins (Gavet et al., 1998), whereas *RTEL1*, also a member of the stathmin family, may contribute to cell growth and tumor progression through amplification or overexpression (Bai et al., 2000; Ding et al., 2004). Both proteins are located in a gene-rich cluster on chromosome 20 with other potentially tumor-related genes. Therefore, genomic DNA from other melanoma cell lines was analyzed by qPCR and increases of 2-fold could be shown for 20q13.3 in the cell lines M1 and M8. As no high level amplifications for 20q13.3 were detected in any of the melanoma cell lines, this region was not further analyzed.

Deletions in the digital karyotyping libraries were analyzed with a sliding window size of 150 virtual tags, which corresponds to a resolution of around 600 kbp when analyzing a total of 100,000 tags. The detection of homozygous deletions was expected to be more difficult than the detection of amplifications, because the copy number difference for homozygous deletions (two copies in normal cells compared to zero copies in deleted regions) is far less than that observed for amplifications (about 10-200 copies in amplified regions). In both libraries evidence was found for several regions with apparent deletions. The most prominent region was located in the cell line M2 on chromosome 9p21 with an estimated size of 1.9 Mbp. This deletion was verified by PCR and spanned the *CDKN2A* locus, which encodes *p16INK4A* and *p14ARF* (Figure 10A). Homozygous deletion of *p16INK4A* had already been observed in the cell line M2 when validating the results from CGH analysis (Table 14).

All other deletions predicted by the digital karyotyping software in the libraries of M2 and M3 could not be confirmed by PCR. Nevertheless, in some of the regions analyzed a substantial reduction in genomic content was observed. Examples of PCR analysis of potentially deleted regions in both cell lines are shown in Figure 11. Not detected by digital karyotyping was the homozygous deletion of *p16INK4A* in the cell line M3 (Table 14). By PCR analysis this deletion was shown to span only 250 kbp (data not shown), which is below the resolution achieved by digital karyotyping when analyzing a total of 100,000 tags.

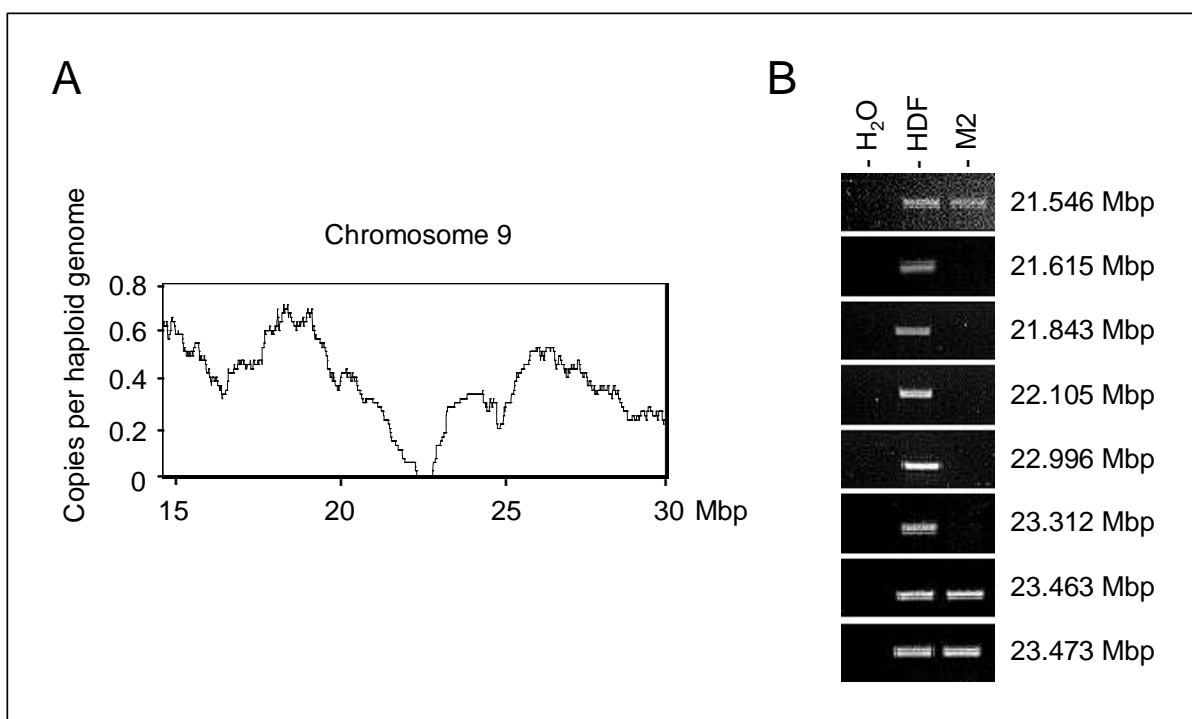


Figure 10 Homozygous deletion of the *CDKN2A* locus in the cell line M2. **(A)** Graphical representation of the homozygous deletion on chromosome 9p21 in the cell line M2 with the digital karyotyping software. Tag density values were calculated in sliding windows of 200 virtual tags. Values on the x-axis represent position along the chromosome, values on the y-axis show copies per haploid genome. **(B)** PCR analysis of the homozygous deletion of the *CDKN2A* locus detected by digital karyotyping in the cell line M2. DNA from HDF (human diploid fibroblast) was used as positive control. Numbers on the right indicate chromosome position.

Analysis of the library generated from the cell line M1, which was derived from a female patient, revealed a homozygous deletion on the X chromosome inside the *DMD* gene. The deletion was confirmed by PCR with genomic DNA by Alex Epanchintsev and spanned 570 kbp. This resulted in an in-frame removal of exons 3-29 of the *DMD* gene.

So far, deletions in *DMD* had only been associated with the muscle-wasting diseases Duchenne or Becker Muscular Dystrophy but not with cancer. Therefore, it was of interest to elucidate whether the loss of dystrophin might play a role in pathologic states such as malignant melanoma.

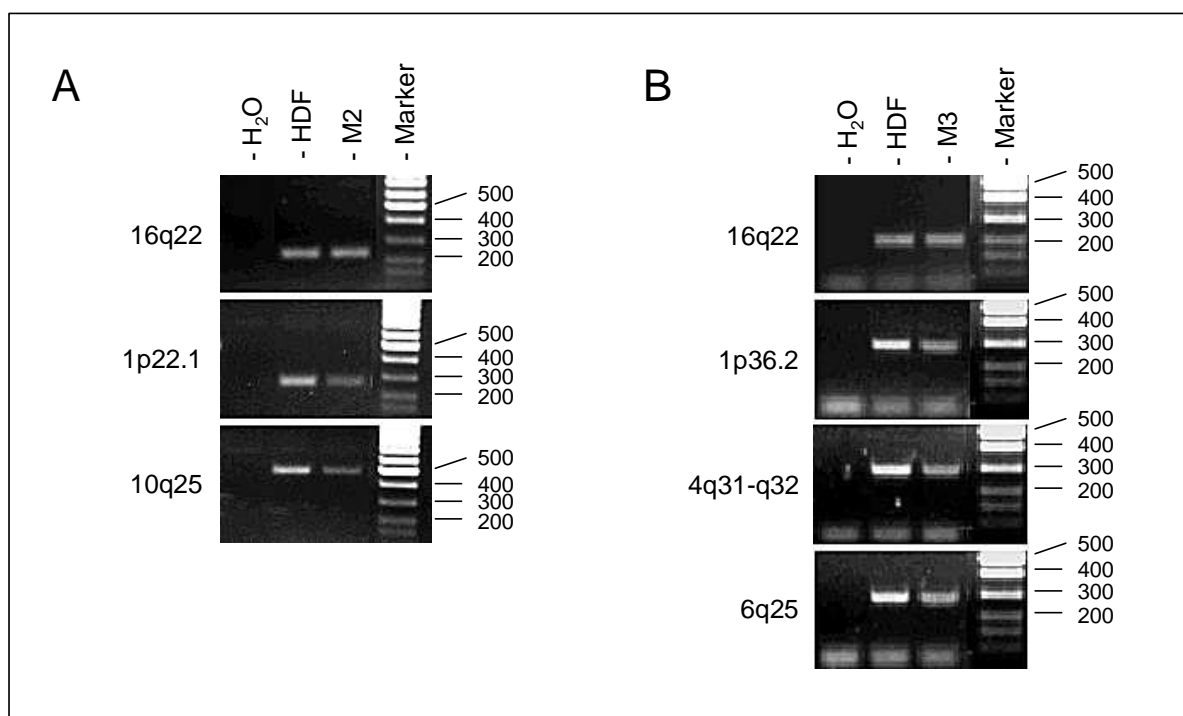


Figure 11 PCR analysis of regions potentially deleted in the melanoma cell lines M2 and M3. **(A)** PCR analysis of two regions on chromosomes 1 and 10 in the cell line M2. Expected sizes of PCR products: 16q22 (209 bp), 1p22.1 (240 bp), 10q25 (475 bp). **(B)** PCR analysis of three regions on chromosomes 1, 4, and 6 in the cell line M3. Expected sizes of PCR products: 16q22 (209 bp), 1p36.2 (300 bp), 4q31-q32 (294 bp), 6q25 (288 bp). DNA from HDFs (human diploid fibroblasts) was used as standard diploid genome. The primer 16q22 served as control for equal amounts of DNA. The PCR reaction had been optimized in order to compare the amount of product before plateau phase was reached.

5.3 Analysis of *DMD* in malignant melanoma

5.3.1 Deletion of *DMD* in malignant melanoma cell lines

All PCR reactions analyzing the deletion status of *DMD* in melanoma cell lines were performed by Alex Epanchintsev. First, to confirm whether the deletion in the *DMD* gene in the cell line M1 was a tumor specific event, genomic DNA isolated from paraffin-embedded non-tumor cells of the same patient was evaluated. By PCR analysis no deletion of exons 3-29 could be detected, demonstrating that the *DMD* deletion in M1 represents a somatic event not present in other cells of the patient. Next, different regions of the *DMD* gene using genomic DNA from a panel of 49 melanoma cell lines (including M2-M9 and CRL-1974) were examined by PCR.

Thereby, an additional homozygous deletion spanning exons 17-30 of the *DMD* gene was identified in the cell line RPMI-7951 (derived from a female patient), resulting in an in-frame truncation of the dystrophin protein. No matching non-tumor material was available for the cell line RPMI-7951 to evaluate tumor-specificity of the deletion. Another deletion of exons 42-43 resulting in the termination of the dystrophin protein in exon 44 was identified in the cell line WM-793 (derived from a male patient). This deletion was absent in genomic DNA derived from immortalized B-cells from the same patient and consequently represents a tumor-specific event.

5.3.2 Expression of *DMD* isoforms in primary melanocytes

So far, expression of the full-length 427 kD dystrophin protein had only been observed in muscle cells and nerve cells, together with a differential expression of shorter isoforms in different tissues (for details see chapter 1.3.1). In order to evaluate if deletions in *DMD* could be of functional consequence in melanoma cells, the expression of dystrophin isoforms was analyzed in primary melanocytes. Early passage cultures of primary melanocytes were kindly provided by Dr. Carola Berking (Department of Dermatology, LMU Munich). RNA was isolated from three different cultures of melanocytes and reverse transcribed with either the *DMD*-specific primer DMD1b, which binds in the 5'-end of *DMD*, or an oligo(dT)₂₀ primer.

To analyze expression of the full-length *Dp427* isoforms, cDNA from three different donors transcribed with the DMD1b primer was used for PCR with primers specific for each of the isoforms. In all cases only the muscle-specific *Dp427m* isoform could be detected, but not *Dp427c*, *Dp427p*, or *Dp427l* (Figure 12A). To complete the picture, *Dp427l* was included in the analysis, although recent findings suggest that this isoform might represent an artifact, making its functional role uncertain (Wheway and Roberts, 2003).

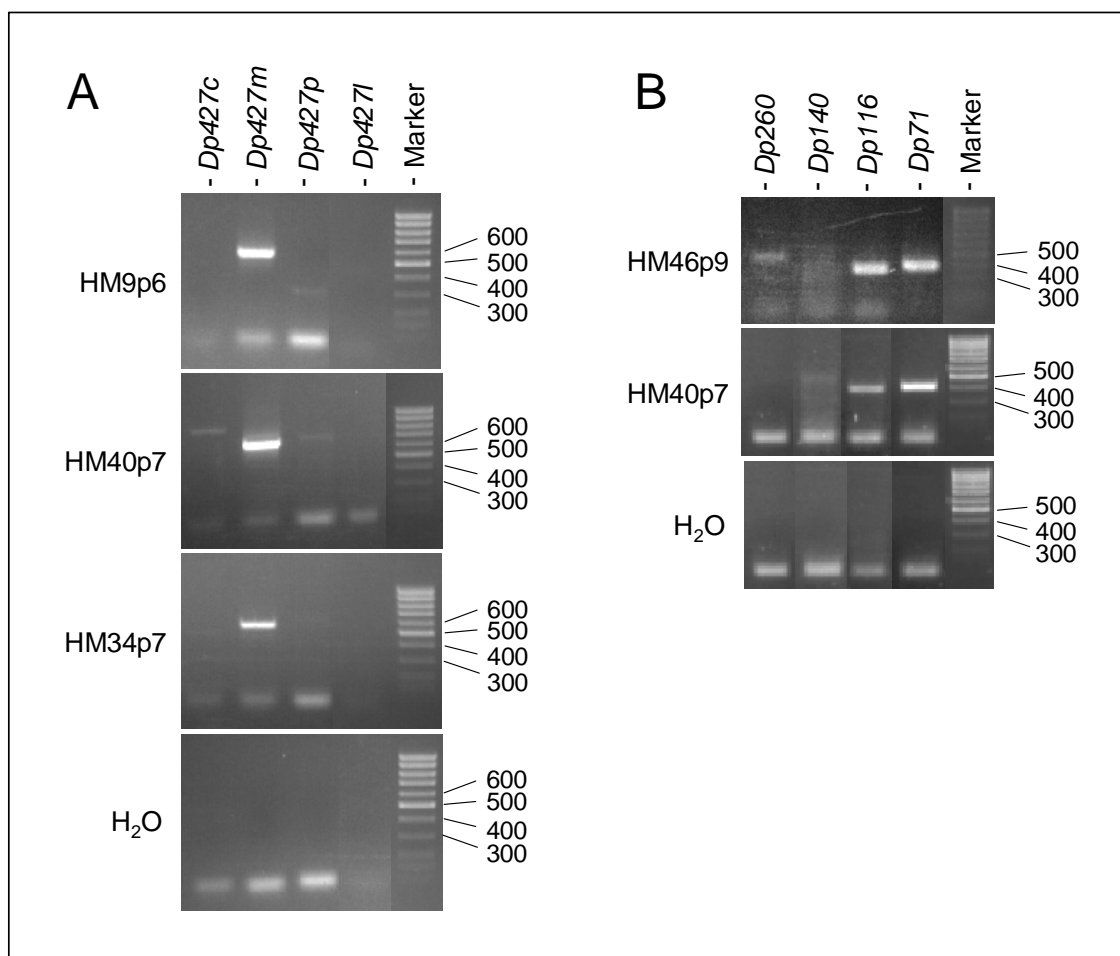


Figure 12 RT-PCR analysis of *DMD* isoforms in primary melanocytes. **(A)** Analysis of differential *Dp427* isoform expression. RT-PCR was performed with RNA from three different cultures of primary human melanocytes (HM) using primer pairs specific for the indicated *DMD* isoforms. Expected sizes of PCR products: *Dp427c* (561 bp), *Dp427m* (548 bp), *Dp427p* (331 bp), *Dp427l* (319 bp). **(B)** RT-PCR analysis of the *DMD* isoforms *Dp260*, *Dp140*, *Dp116*, and *Dp71*. Total RNA was obtained from primary human melanocytes (HM) from two donors. RT-PCR was carried out using primer pairs specific for the indicated isoforms. Expected sizes of PCR products: *Dp260* (214 bp), *Dp140* (161 bp), *Dp116* (364 bp), *Dp71* (393 bp).

cDNA from two different donors transcribed with the oligo(dT)₂₀ primer was used to examine expression of the shorter *DMD* isoforms, and PCR was carried out with primers specific for each isoform. Thereby, specific PCR products for *Dp71* and *Dp116*, but not *Dp140* and *Dp260* were detected in primary melanocytes (Figure 12B).

5.3.3 Expression of dystrophin isoforms in melanoma cell lines

Protein expression of the Dp427 full-length isoform in melanoma cell lines was assessed by Western blot analysis (Figure 13). Protein lysates from a panel of 55 melanoma cell lines and primary melanocytes were examined with the dystrophin antibody NCL-Dys1, which recognizes an epitope in the central rod domain of the protein. In untransformed primary melanocytes the expression of the Dp427m protein was high. In contrast, in 38 of 55 (69%) melanoma cell lines the dystrophin protein was absent and in 10 of 55 (18%) only present at very low levels. Only the cell line WM-115 displayed a higher amount of dystrophin than primary melanocytes.

In addition, expression of the shorter dystrophin isoforms was analyzed in melanoma cell lines (Figure 14). By Western blot analysis expression of the Dp116 and Dp71 isoforms could be detected with the dystrophin antibodies NCL-Dys2, which recognizes the C-terminus of dystrophin and Ab-1 (epitope not determined). Dp116 was present in 5 of 7 (71%) cell lines positive for the expression of the full-length dystrophin protein and in 1 of 5 (20%) that were negative for Dp427 protein (Figure 14A, upper panel). On the other hand, all of eight melanoma cell lines analyzed showed expression of Dp71 (Figure 14A, lower panel). Of those eight cell lines two showed expression of the full-length dystrophin protein, whereas in the six other cell lines the full-length dystrophin protein was absent. Therefore, expression of the Dp71 isoform seems to be retained in melanoma cell lines independent of the expression of the Dp427 isoform, whereas the Dp116 isoform seems to be preferentially expressed in a subset of melanoma cell lines, which still express full-length dystrophin.

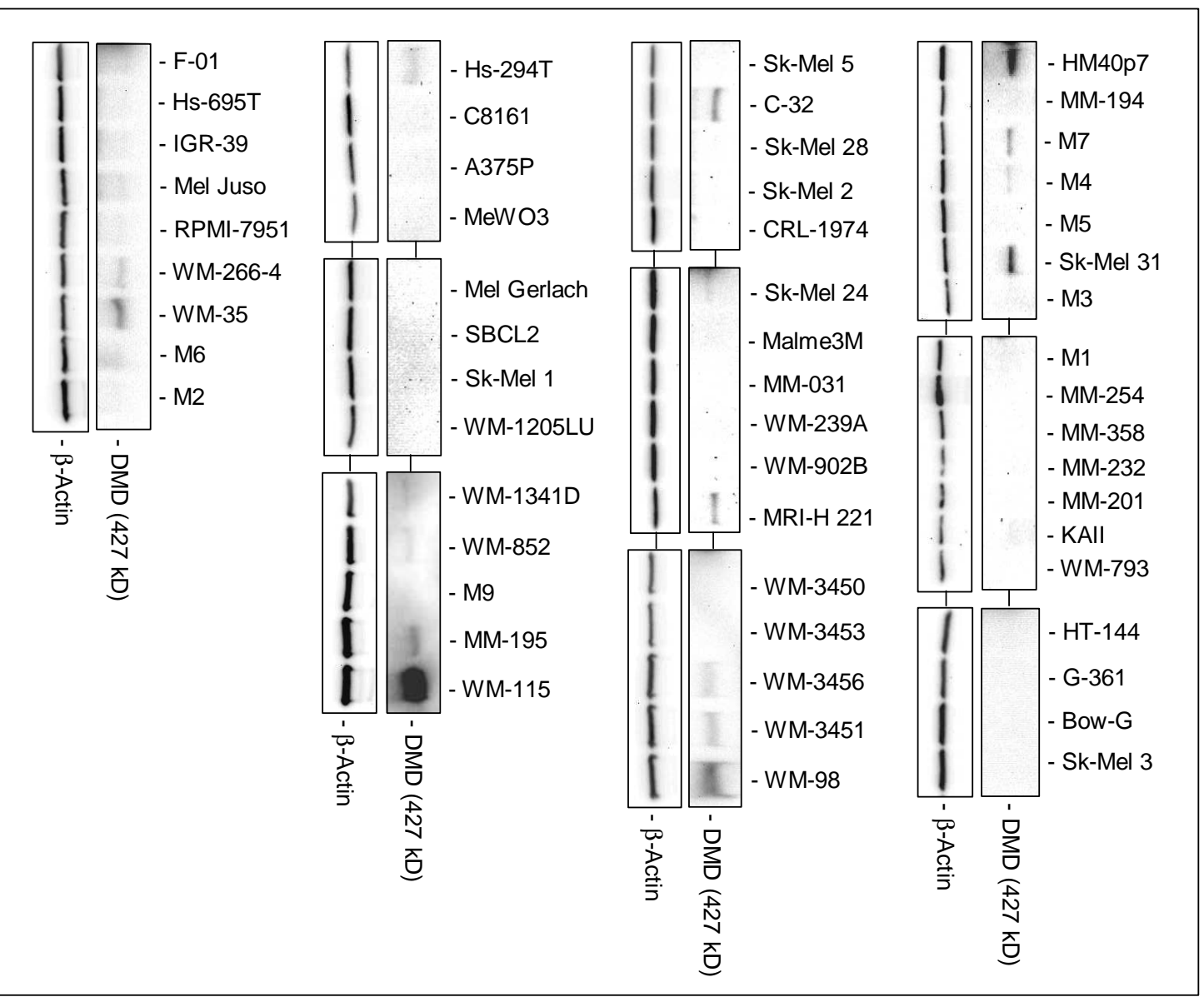


Figure 13 Detection of dystrophin protein by Western blot analysis. Dystrophin protein expression (Dp427 isoform) was analyzed in protein lysates from primary melanocytes (HM40p7) and 55 melanoma cell lines with the antibody NCL-Dys1. Expression of β -actin was used as control.

As confirmation of the Western blot analysis, RNA was prepared from the cell line WM-115, which showed expression of Dp116 and Dp71 protein and reverse transcribed with an oligo(dT)₂₀ primer. By PCR with primer pairs specific for the shorter isoforms, expression of *Dp116* and *Dp71* could be confirmed (Figure 14B).

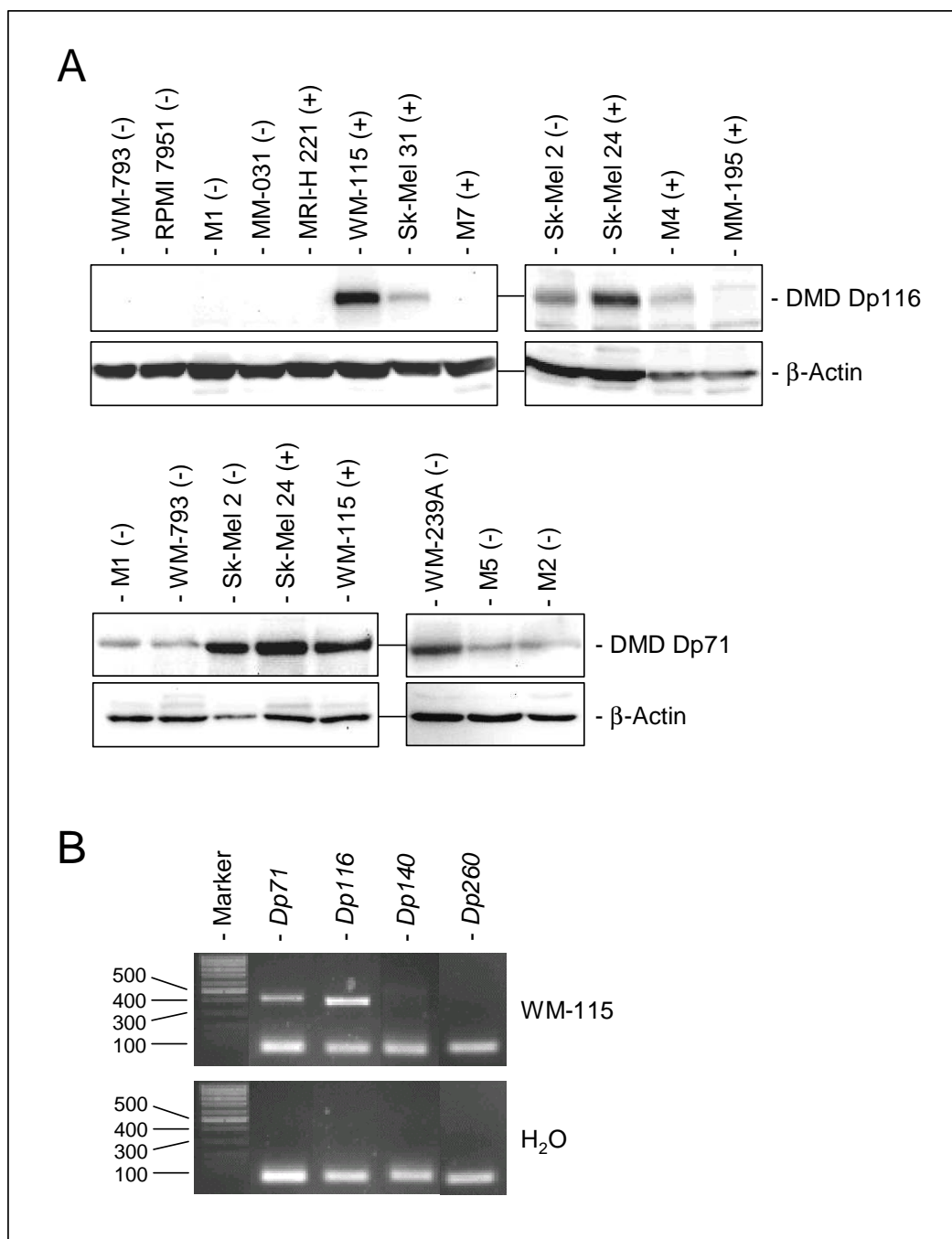


Figure 14 Expression of shorter dystrophin isoforms in melanoma cell lines. **(A)** Western blot analysis of the expression of Dp116 and Dp71 in melanoma cell lines. Dp116 was detected with the NCL-Dys2 antibody and Dp71 with the Ab-1 antibody. β-actin was used as control. (+) and (-) indicate presence or absence of full-length dystrophin protein expression. **(B)** RT-PCR analysis of the expression of the *DMD* isoforms *Dp260*, *Dp140*, *Dp116*, and *Dp71* in the melanoma cell line WM-115. Expected sizes of PCR products: *Dp260* (214 bp), *Dp140* (161 bp), *Dp116* (364 bp), *Dp71* (393 bp).

In addition to the analysis of the level of dystrophin protein in melanoma cell lines, expression of *DMD* mRNA was quantitated. RNA was prepared from a subset of 37 melanoma cell lines, including 16 cell lines with and 21 without full-length dystrophin protein expression, and reverse transcribed with an oligo(dT)₂₀ primer. mRNA expression was analyzed by quantitative real-time PCR (qPCR) with the *DMD* LC primer, which is specific for the *Dp427* isoforms. Figure 15 shows an example of an agarose gel with the products from qPCR after 40 cycles. The amount of *DMD* mRNA was calculated based on crossing point differences between the individual samples normalized to the β -actin control with the *DMD* expression in primary melanocytes set to 100% (for details see chapter 4.8). Only five melanoma cell lines (MRI-H 221, M7, Hs-294T, Sk-Mel 31, WM-98) showed expression levels of *DMD* mRNA similar to primary melanocytes, whereas in all other cell lines a diminished *DMD* expression was detected (Figure 16).

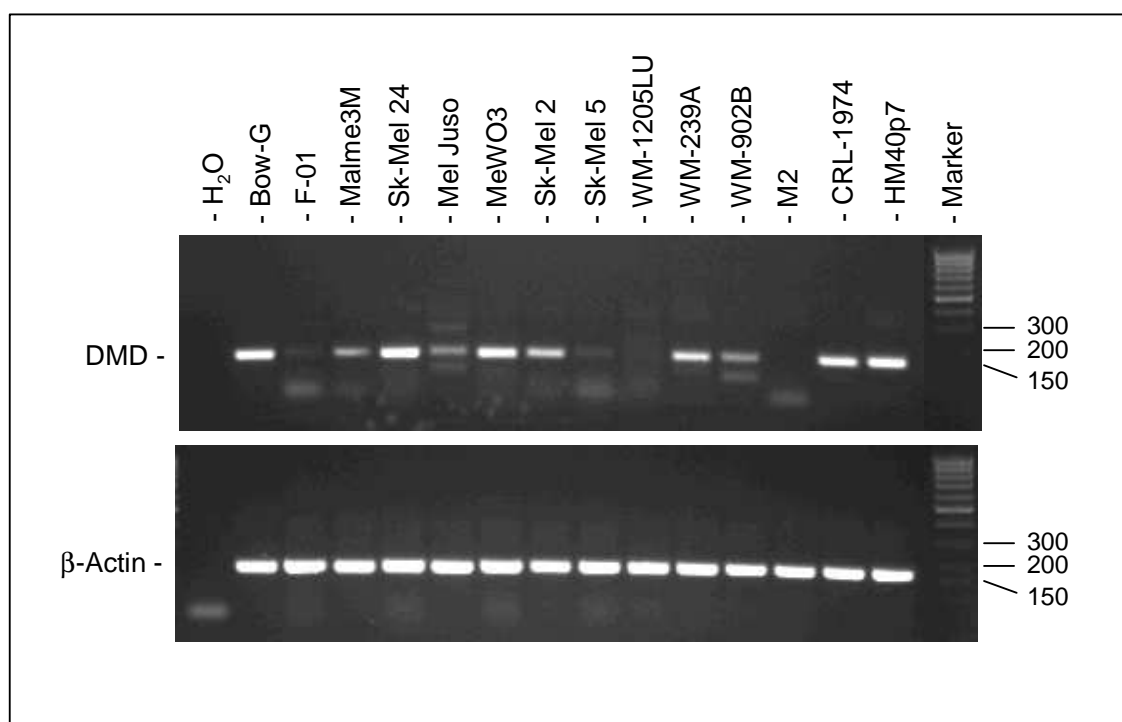


Figure 15 Representative examples of *DMD* mRNA expression. cDNA from different melanoma cell lines and primary melanocytes (HM40p7) was analyzed by qPCR for expression of *DMD*. Quantification was done using crossing point differences between primary melanocytes and melanoma samples normalized to β -actin. Afterwards, LightCycler PCR products were visualized on a 2% agarose gel. Expected sizes of PCR products: *DMD* (187 bp), β -actin (213 bp).

A good correlation was observed when comparing the amount of *DMD* mRNA with the protein level in each cell line. For cell lines with 50-100% of *DMD* expression compared to primary melanocytes, dystrophin protein could also be detected in Western blot analysis, whereas in most cell lines with low *DMD* expression no dystrophin protein was observed. General information about all cell lines together with expression levels of *DMD* mRNA and protein is listed in Supplementary Table 2.

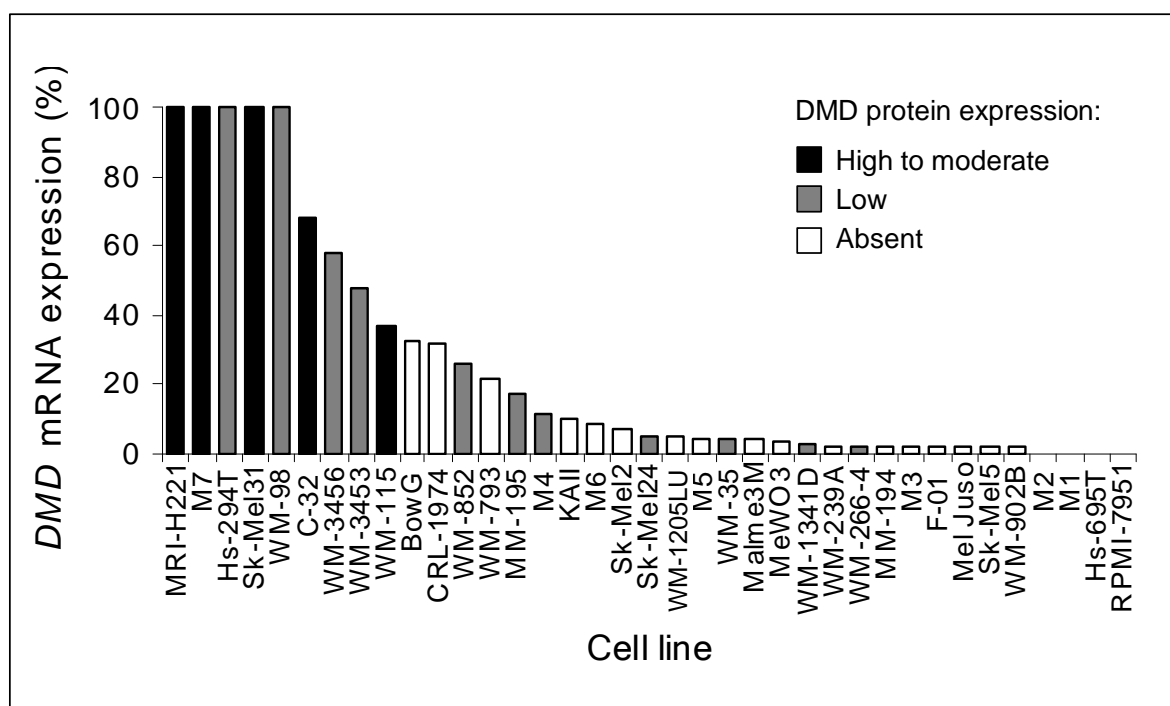


Figure 16 Correlation of *DMD* mRNA and protein expression. *DMD* mRNA expression was determined by quantitative PCR and compared to dystrophin protein expression assessed by Western blot analysis. Expression of *DMD* in each cell line is indicated by its ratio to that of the mean expression of primary melanocytes from three different donors. Protein levels were determined by Western blot analysis and classified as high to moderate expression (black bars), low expression (gray bars) and no expression (white bars).

5.3.4 Functional analysis of dystrophin

5.3.4.1 Analysis of the components of the dystrophin-glycoprotein complex

In muscle cells, dystrophin acts as a linker between the muscle basement membrane and the inner cytoskeleton through binding to cytoskeletal F-actin and β -dystroglycan, which together with α -dystroglycan forms a complex at the muscle cell membrane (for details see chapter 1.3.5). In addition, the sarcoglycan complex and several other proteins are associated with the dystrophin-glycoprotein complex (DGC) in muscle tissue. In most non-muscle cells the full-length dystrophin isoform is not expressed and replaced by its homolog utrophin or shorter dystrophin isoforms. The association of other proteins with the dystroglycan complex can vary greatly in different tissues (Durbeej and Campbell, 1999; Imamura et al., 2000).

As nothing was known about the dystrophin-glycoprotein complex in primary melanocytes, the expression of several components of the DGC was analyzed. cDNA from primary melanocytes was examined by PCR with primers specific for different components of the complex. Thereby, specific products for *dystroglycan* (*DAG1*), *utrophin* (*UTRN*), *syntrophin- β 2* (*SNTB2*), *β -sarcoglycan* (*SGCB*), *ϵ -sarcoglycan* (*SGCE*), *laminin- α 2* (*LAMA2*), *sarcospan* (*SSPN*), and *nitric oxide synthase 1 (neuronal)* (*NOS1*) but not *α -dystrobrevin* (*DTNA*) were detected (Figure 17). These results show, that all the necessary components are expressed to form a functional dystrophin-dystroglycan complex in melanocytes, although no conclusions can be drawn as to the exact composition of the DGC.

It has been shown, that dystrophin deficiency in muscle leads to a secondary deficiency of all the components of the DGC either through down-regulation or mislocalization of the respective proteins (Ohlendieck and Campbell, 1991). Therefore, melanoma cell lines with and without the expression of dystrophin protein were analyzed by qPCR for down-regulation of some of the components of the DGC. The expression of *UTRN*, *DAG1*, *SGCB*, *SGCE*, *SNTB2*, and *LAMA2* was evaluated in the cell lines WM-115 (with normal dystrophin expression), RPMI-7951, WM-793, and M1, (all three with deletions in *DMD*) and compared to the expression of the

respective mRNA in the primary melanocyte sample HM40p7. For *UTRN*, *DAG1*, *SGCB*, *SGCE*, and *SNTB2* no significant changes in expression level could be detected, whereas expression of *LAMA2* was down-regulated in the cell lines M1 and RPMI-7951, and absent in WM-793. Expression of *LAMA2* was normal in WM-115. Because no specific product for *LAMA2* could be detected in WM-793, genomic DNA was analyzed but no deletion of the gene locus was observed with PCR.

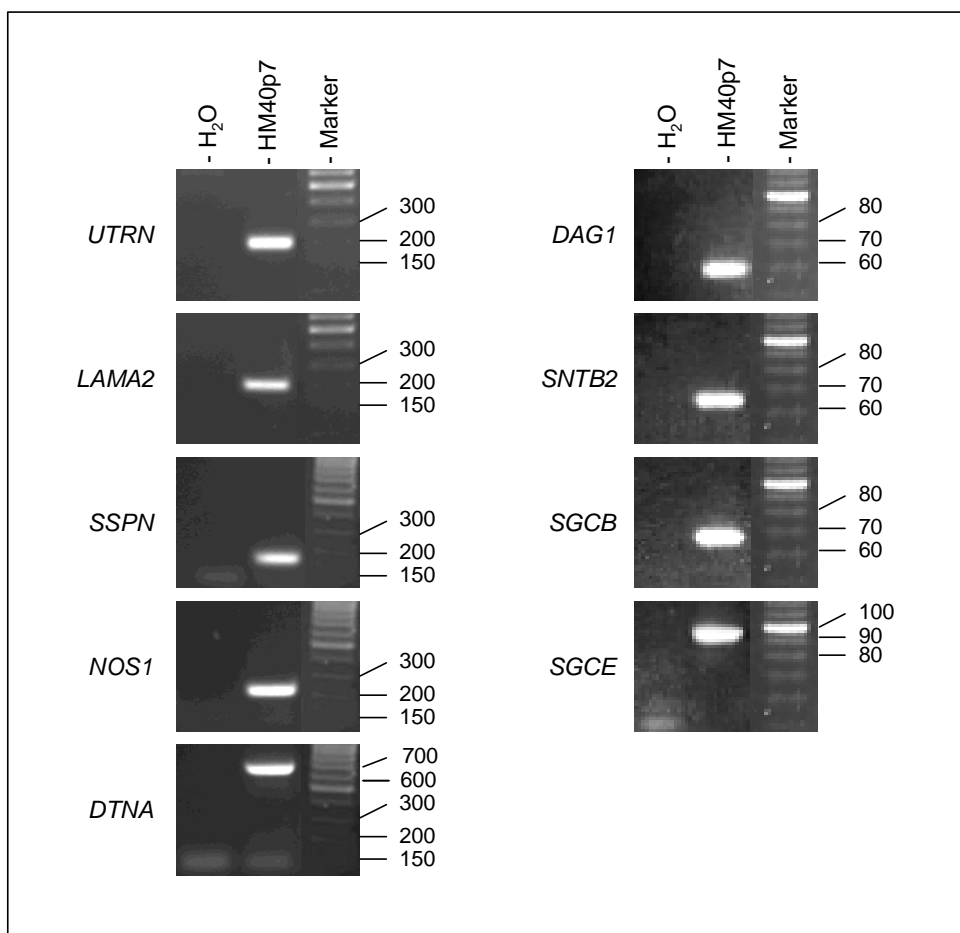


Figure 17 Expression of DGC components in primary melanocytes. cDNA from primary melanocytes (HM40p7) was analyzed by PCR for the expression of *utrophin* (*UTRN*; 180 bp), *laminin- α 2* (*LAMA2*; 185 bp), *sarcospan* (*SSPN*; 157 bp), *nitric oxide synthase 1* (*NOS1*; 211 bp), *α -dystrobrevin* (*DTNA*; 137 bp), *dystroglycan* (*DAG1*; 60 bp), *syntrophin- β 2* (*SNTB2*; 65 bp), *β -sarcoglycan* (*SGCB*; 67 bp), and *ϵ -sarcoglycan* (*SGCE*; 95 bp). Except for *DTNA*, specific products were observed for all transcripts analyzed.

Next, mRNA of 37 melanoma cell lines and two primary melanocyte samples was examined for down-regulation of *LAMA2*. Conventional PCR was employed and PCR products were evaluated on an agarose gel with β -actin as standard to ensure equal amounts of template. In 23 of 37 (62%) melanoma cell lines expression of laminin- α 2 was diminished or absent (Table 16).

Table 16 PCR analysis of *LAMA2* expression. cDNA of two primary melanocyte samples (HM40p7 and HM37p7) and 37 melanoma cell lines was analyzed for expression of *LAMA2* and compared to dystrophin protein expression. ++ strong expression; + low expression; - no expression.

Cell line	<i>LAMA2</i> cDNA expression	dystrophin protein expression
HM40p7	++	++
HM34p7	++	++
Sk-Mel 31	++	++
M7	++	++
WM-115	++	++
WM-98	++	+
Hs-294T	++	+
WM-852	++	+
MM-195	++	+
M4	++	+
Sk-Mel 24	++	+
WM-266-4	++	+
Sk-Mel 2	++	-
WM-239A	++	-
WM-902B	++	-
MRI-H 221	+	++
C-32	+	++
WM-3456	+	+
WM-3453	+	+
WM-35	+	+
CRL-1974	+	-
M5	+	-
F-01	+	-
Sk-Mel 5	+	-
M2	+	-
M1	+	-
RPMI-7951	+	-
WM-1341D	-	+
Bow-G	-	-
WM-793	-	-
KAll	-	-
M6	-	-
WM-1205LU	-	-
Malme3M	-	-
MeWO3	-	-
MM-194	-	-
M3	-	-
Mel Juso	-	-
Hs-695T	-	-

In the subset of melanoma without dystrophin protein 11 of 21 (52%) cell lines were negative for *LAMA2* expression, whereas in the 16 cell lines with dystrophin protein only one cell line (6%) was negative for *LAMA2* expression. Statistical analysis with a X^2 test proved this finding to be significant with $P < 0.0036$, which indicates a correlation between the loss of expression of the dystrophin protein and absence of *LAMA2* mRNA.

In addition, DAG1 expression was evaluated on protein level, because for a number of cancers decreased expression of α -dystroglycan (α -DG) has been described and analysis of the mRNA suggested that this is likely regulated at a post-transcriptional level (Henry et al., 2001; Sgambato et al., 2003). Therefore, α -dystroglycan expression was evaluated by Western blot analysis with the IIH6 antibody in a panel of melanoma cell lines with and without expression of dystrophin protein (Figure 18). As this antibody recognizes a glycosylated epitope of α -dystroglycan, the protein is detected with several bands indicating a varying number of added sugar moieties. Although differences in the expression level of α -DG were detected, there was no correlation to the expression level of dystrophin protein.

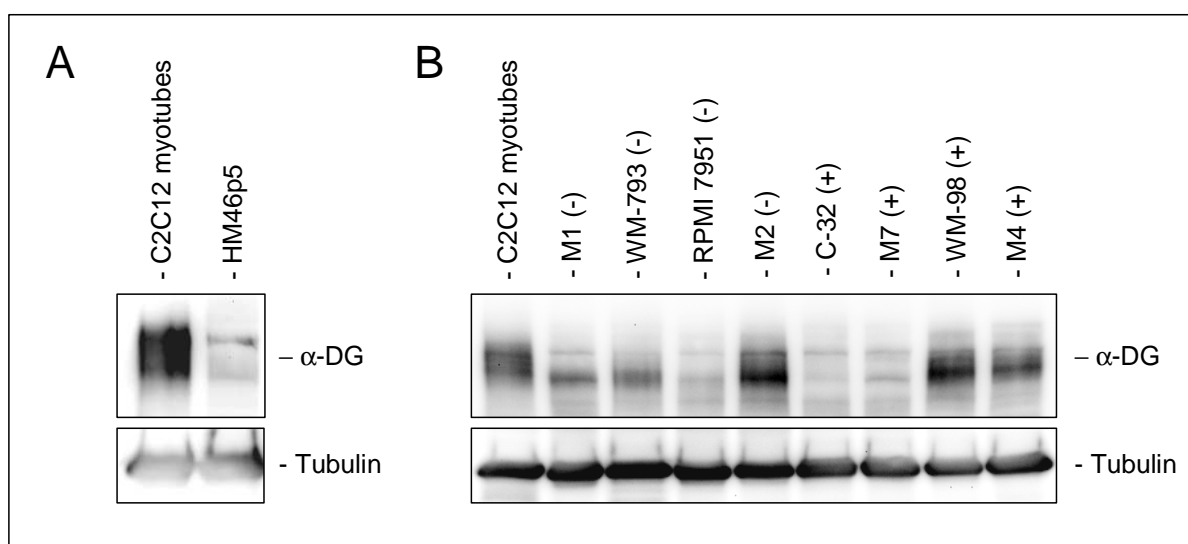


Figure 18 Western blot analysis of α -dystroglycan (α -DG) expression in primary melanocytes and melanoma cell lines. (A) Expression of α -DG in primary melanocytes (HM46p5) detected with the IIH6 antibody. Protein lysate from C2C12 mouse myotubes was used as positive control for the expression of α -DG. (B) Expression of α -DG in melanoma cell lines detected with the IIH6 antibody. Due to extensive glycosylation, multiple bands are detected for α -DG. (+) and (-) indicate presence or absence of full-length dystrophin protein expression.

In muscle and nerve cells the full-length dystrophin protein is always tightly associated with the dystroglycan complex, which is located at the cell membrane providing a link to the extracellular matrix. Visualization of endogenous dystrophin and α -DG protein in melanocytes or melanoma cell lines was not possible. This was due to the fact that none of the antibodies used for analysis of the proteins in Western blot was sensitive enough to detect them in immunofluorescence or immunohistochemistry. To analyze localization of dystrophin and α -DG in melanoma, cell lines with and without dystrophin expression were transfected with expression vectors for both proteins. Localization of full-length dystrophin was visualized by detection of eGFP fused to the N-terminus of dystrophin expressed from the attb-pDysE vector. α -DG was expressed from the pCMV-DAG1-VSV vector, which contains the *dystroglycan* gene with a C-terminal fusion to a VSV tag. Since DAG is post-translationally cleaved into α - and β -DG, only β -DG can be detected with an anti-VSV antibody. Co-expression of both proteins was not possible due to very low transfection efficiencies of the melanoma cell lines. In total, 13 cell lines (8 with dystrophin protein expression and 5 without) were analyzed. Thereby, ectopically expressed dystrophin and β -DG were mainly localized at the cell membrane as visualized by confocal microscopy (examples are shown in Figure 19). In some cell lines signals from inclusion bodies or at ER/Golgi vesicles were detected. The latter pattern is probably due to protein overexpression. Nevertheless, the correct localization suggests that a functional dystrophin-dystroglycan complex is likely to be present in melanocytes and melanoma cell lines.

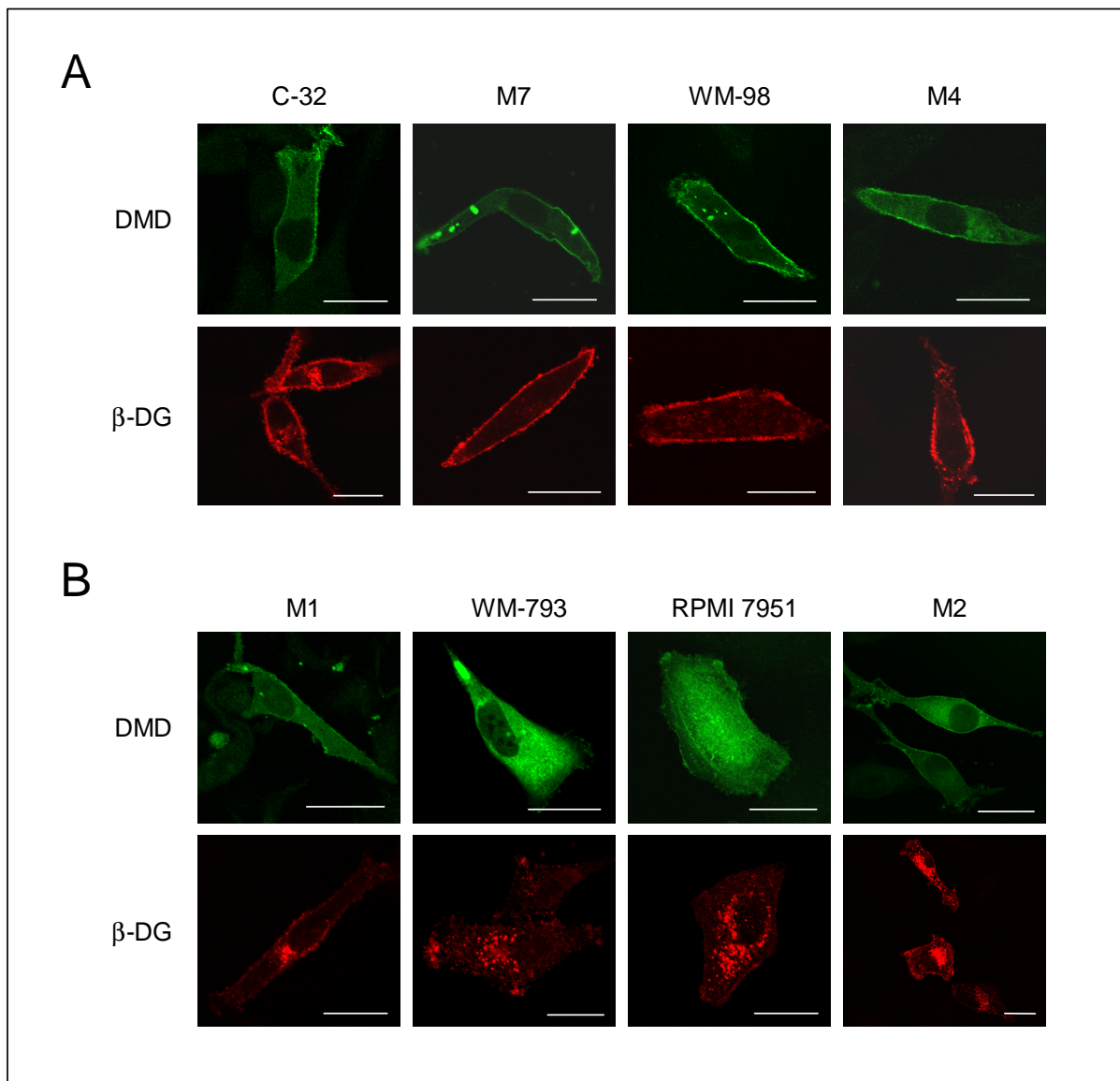


Figure 19 Localization of ectopically expressed dystrophin (DMD) and β -dystroglycan (β -DG) in melanoma cell lines. **(A)** Melanoma cell lines with expression of endogenous dystrophin protein. **(B)** Melanoma cell lines without expression of endogenous dystrophin protein. Dystrophin was directly visualized as fusion protein to eGFP, whereas β -DG was detected as VSV-fusion protein using an anti-VSV antibody. Scale bars, 80 μ m.

5.3.4.2 Knockdown of *DMD* in melanoma cell lines

In order to determine the functional consequences of *DMD* loss in melanoma, RNA interference was used to "knock down" *DMD* in melanoma cell lines. The melanoma cell lines M7 and C-32, which displayed high dystrophin expression at the mRNA and protein level were chosen (see chapter 5.3.3, Figure 16). Both cell lines were infected with a retrovirus mediating stable expression of a short hairpin RNA (shDMD) directed against the *Dp427* isoforms or empty vector as control. Single cell clones were selected with puromycin and reduced dystrophin expression was confirmed by Western blot (Figure 20A) and qPCR analyses (Figure 20B). As the DGC forms a connection between the inner cytoskeleton and the extracellular matrix, single cell clones with knockdown of *DMD* expression were tested for changes in migration and invasion behavior. Invasion was assessed by branching morphology observed after placing cells into matrigel matrix. Clones with reduced *DMD* expression from both cell lines formed branching structures after 1-2 days, which gradually extended with time (Figure 20C). In contrast, only spheroids were observed in the parental cells and control clones (Figure 20C). Next, migration of cells was tested in a scratch assay. Cells were grown to confluence and treated with mitomycin C to inhibit proliferation. Afterwards the cell layer was scratched with the sealed tip of a Pasteur pipette. Migration of cells into the wounded area was analyzed in designated areas over the indicated time period. Thereby, the ability to close an artificial wound by migration in a monolayer was significantly enhanced in cells with reduced *DMD* expression (Figure 20D, E). In addition, cellular migration was analyzed in a transwell migration assay. Cells were placed in the upper compartment of a transwell chamber and migration through a membrane with defined pore size was assessed after the indicated time points. In accordance with the results from the scratch assay, down-regulation of *DMD* expression also resulted in increased migration of cells through the membrane (Figure 20F, G).

As cells with knockdown of *DMD* showed enhanced invasion, branching morphology in matrigel was also analyzed in a panel of melanoma cell lines with (WM-98, M4) and without (M1, RPMI-7951, WM-793, M2, MM-232) dystrophin protein expression over a period of seven days. All cell lines tested showed the ability to form branching structures in matrigel. Thereby, differences were observed in onset

and structure of the branches formed but could not be correlated to expression of the dystrophin protein.

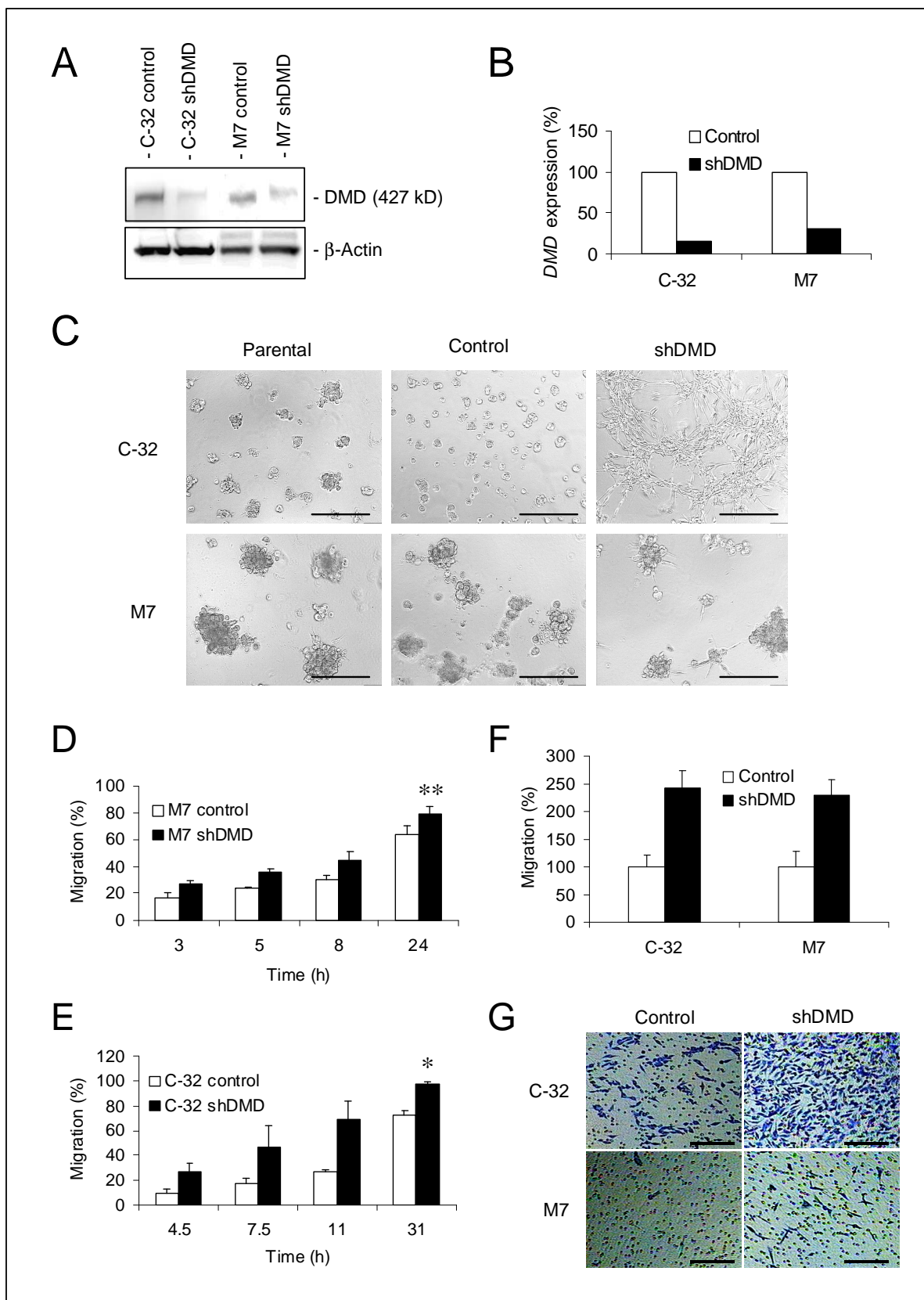


Figure 20 Knockdown of *DMD* in the melanoma cell lines C-32 and M7. **(A)** Detection of reduced dystrophin expression (shDMD) in clones of the cell lines C-32 and M7 by Western blot analysis. β -actin was used as loading control. **(B)** Detection of reduced *DMD* expression (shDMD) in clones of the cell lines C-32 and M7 by qPCR analysis. cDNA was normalized against β -actin. **(C)** Branching morphology of parental cell lines, control clones, and clones with reduced dystrophin expression (shDMD) in matrigel matrix. Pictures were taken 3 days (C-32) and 5 days (M7) after plating. Scale bars; 300 μ m. **(D)** Analysis of control clones and clones with reduced dystrophin expression (shDMD) from the cell line M7 in a scratch assay. ** $P < 0.02$. **(E)** Analysis of control clones and clones with reduced dystrophin expression (shDMD) from the cell line C-32 in a scratch assay. * $P < 0.005$. **(F)** Migration of control clones and clones with reduced *DMD* expression (shDMD) through the membrane of a transwell chamber. The y-axis shows the percentage of migrated cells from C-32 (after 18 hours) and M7 (after 24 hours). **(G)** Pictures of representative areas of migrated cells on the membrane of the transwell chamber stained with crystal violet. Scale bars; 300 μ m.

5.3.4.3 Re-expression of dystrophin in melanoma cell lines

Expression of dystrophin was restored in the melanoma cell lines RPMI-7951 and WM-793, which showed deletion of *DMD* exons 17-30 and exons 42-43, respectively, leading to a truncated *DMD* mRNA. No dystrophin protein was observed in both cell lines in Western blot analysis (see chapter 5.3.3, Figure 16). Both cell lines were transfected with the attb-pDysE vector for expression of the dystrophin protein N-terminally tagged with eGFP and as control the attb-pEGFP vector expressing eGFP only. After selection with neomycin, re-expression of dystrophin was confirmed in the pools of both cell lines by Western blot analysis (Figure 21A, D). After ectopic expression of dystrophin, morphological changes could be observed in RPMI-7951 and WM-793. Cells adopted a flattened shape and increased in size (Figure 21B, F). Next, migration of WM-793 was assessed in a scratch assay. Thereby, decreased migration was observed in cells with restored expression of dystrophin compared to control cells (Figure 21C). In RPMI-7951 ectopic expression of dystrophin induced a senescent cell-like phenotype. As cellular senescence is often accompanied by expression of β -galactosidase (pH 6.0), this can be visualized by a chemical reaction turning the cells blue (Dimri et al., 1995). In two independent transfection experiments after ectopic expression of dystrophin the frequency of cells positive for β -galactosidase (pH 6.0) increased from 3% to 26% and 7% to 14%, respectively (Figure 21E, F). This was accompanied by a decrease in cell proliferation (Figure 22A) and an increase in the amount of apoptotic cells (Figure 22B).

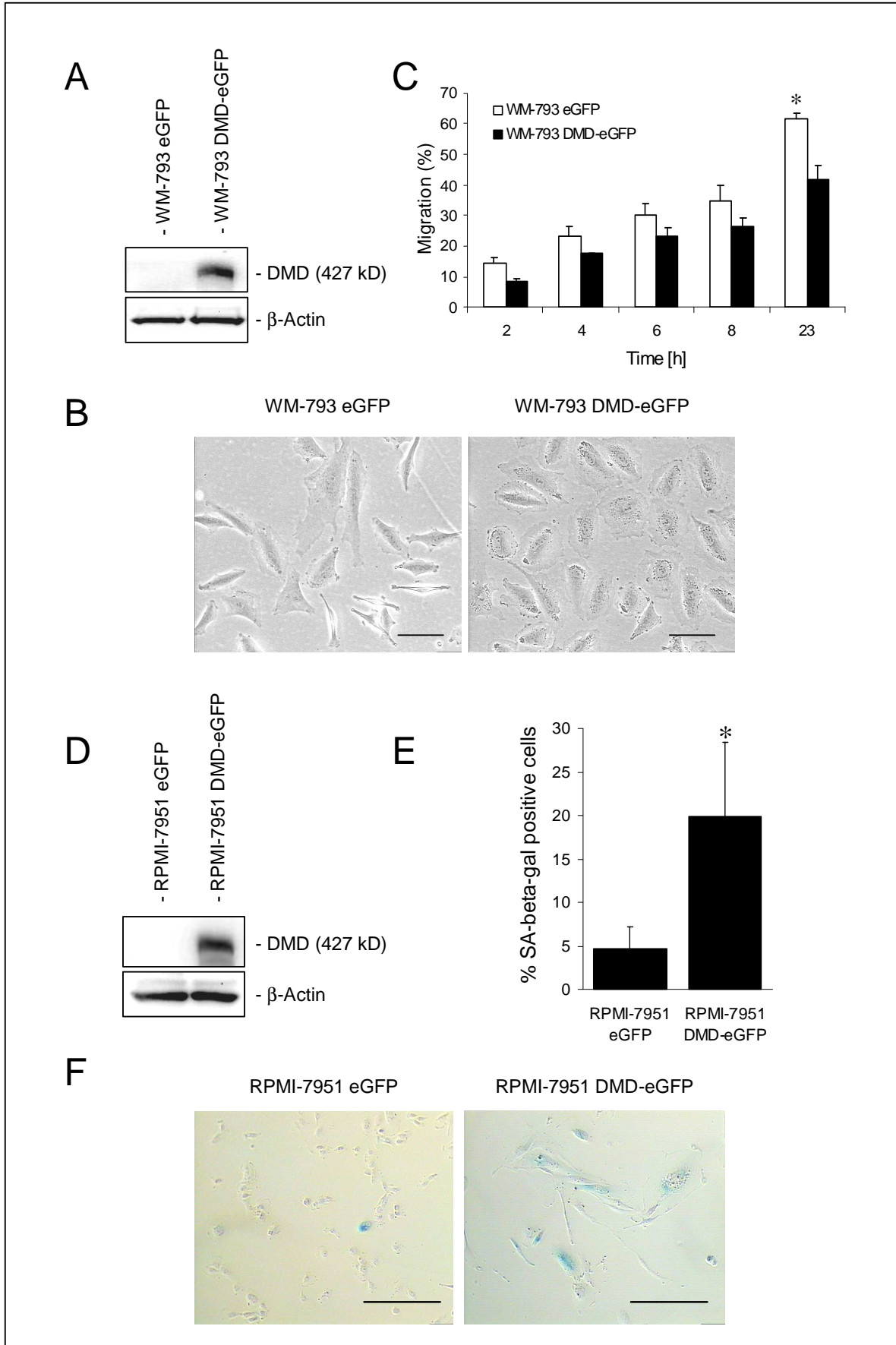


Figure 21 Re-expression of dystrophin in the melanoma cell lines WM-793 and RPMI-7951. **(A)** Analysis of dystrophin by Western blot after transfecting the cell line WM-793 with eGFP-tagged dystrophin (DMD-eGFP) or as control eGFP only. β -actin was used as control. **(B)** After ectopic expression of dystrophin, morphology of WM-793 changed. Cells adopted a flattened shape and increased in size compared to control cells. Scale bars, 200 μ m. **(C)** Analysis of cellular migration in a scratch assay in the cell line WM-793. Migration was assessed by quantifying the size of the wounded area after the indicated time points. * $P < 0.02$. **(D)** Analysis of dystrophin by Western blot after transfecting the cell line RPMI-7951 with eGFP-tagged dystrophin (DMD-eGFP) or as control eGFP only. **(E)** Quantification of blue cells (representing SA- β -gal staining) compared to total cells. The y-axis shows the average percentage of SA- β -gal positive cells of two independent transfection experiments. In total, 800 cells were counted for each condition. * $P < 0.0001$. **(F)** Representative areas of cells after senescence-associated β -galactosidase staining (SA- β -gal). Morphology of RPMI-7951 changed and cells adopted a flattened shape and increased in size after ectopic expression of dystrophin. Scale bars, 300 μ m. All experiments were performed with stable pools of cells after transfection and selection with neomycin for two weeks.

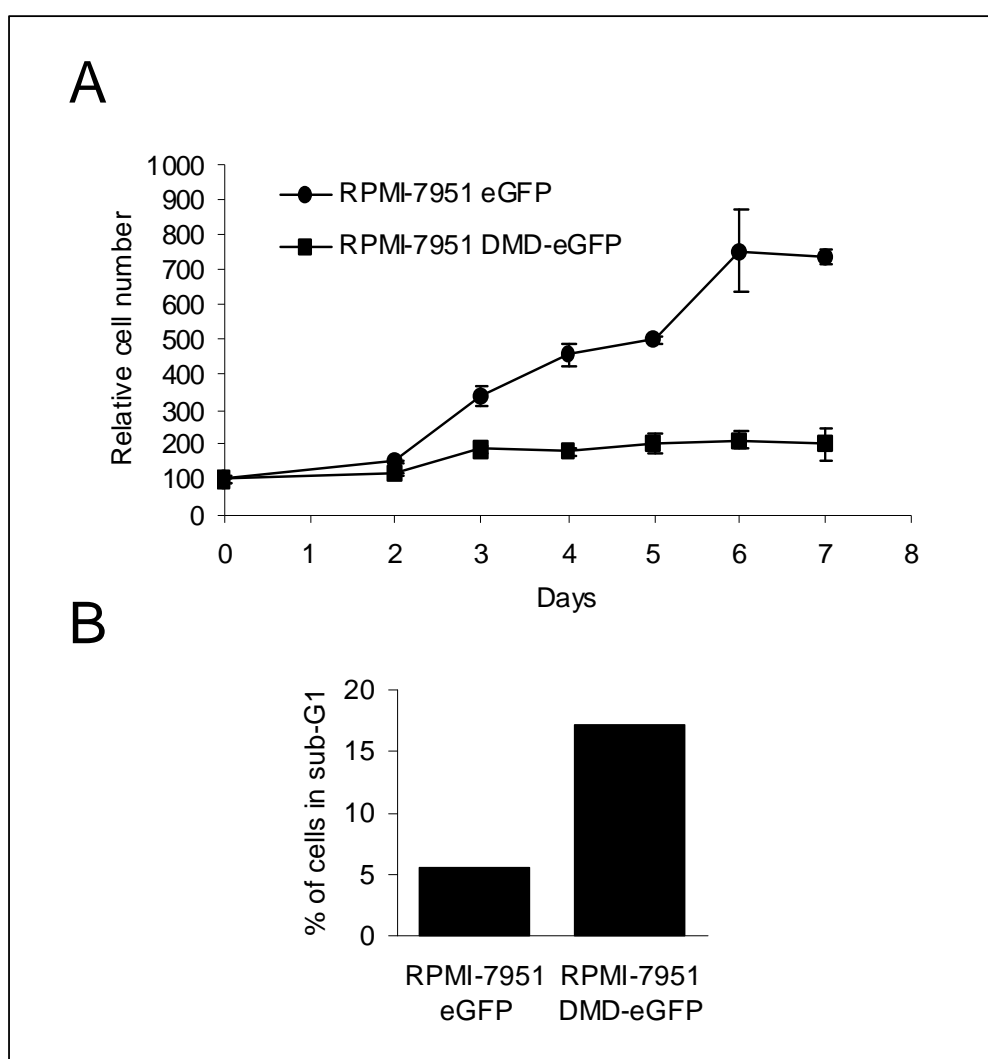


Figure 22 Proliferation and apoptosis of the melanoma cell line RPMI-7951 after re-expression of dystrophin. **(A)** Growth curve of RPMI-7951 after transfection with eGFP-tagged dystrophin (DMD-eGFP) or as control eGFP only. Relative cell number was measured in triplicates after the indicated time points. **(B)** FACS analysis of RPMI-7951 after transfection with eGFP-tagged dystrophin (DMD-eGFP) or as control eGFP only. Cells were fixed and stained with propidium iodide. Apoptosis was evaluated by comparing the percentage of cells in the sub-G1 fraction.

6 DISCUSSION

6.1 *Cytogenetic characterization of melanoma cell lines*

Cytogenetic techniques such as M-FISH and CGH are valuable tools to identify chromosomal regions important in oncogenesis and disease progression. Both techniques can be used to complement each other in the characterization of complex chromosomal changes which occur in most tumor types. M-FISH is typically applied to elucidate complex karyotypes involving numerical and structural aberrations, for example translocations, insertions or duplications. This technique also allows to detect genetic heterogeneity in a tumor cell population. CGH on the other hand allows to comprehensively analyze the average chromosomal copy number changes present in all cells of the tumor.

Both methods were applied to a panel of 9 malignant melanoma cell lines to gain an overview of chromosomal changes and genetic heterogeneity. M-FISH analysis of four melanoma cell lines showed the most complex karyotypes for M1 and M7 with 52 and 21 chromosomes with translocations together with a high clonal heterogeneity. The cell lines M2 and M3 displayed a more homogeneous karyotype. In contrast, the cell line M1 was one of the least affected by copy number alterations as detected by CGH analysis.

Analysis of chromosomal breakpoints revealed a random cluster distribution, indicating karyotypic progression in metastases of melanoma. However, chromosomes 1 and 8 were most frequently affected by rearrangements. This corresponds well with a series of melanoma studies that reported aberrations on 1p to be the most common alterations in malignant melanoma (Poetsch et al., 1998; Smedley et al., 2000; Thompson et al., 1995). Also, several structural aberrations for chromosome 8 have been detected in a case study of cutaneous metastatic melanoma (Wiltshire et al., 2001).

In addition, according to M-FISH analysis amplifications were observed most frequently for chromosomes 3 and 7. Whereas gains of chromosome 3 appear to be rather uncommon, extra copies of chromosome 7 are frequently recognized in metastatic melanoma, and this seems to be a late event in tumor progression

(Pedersen and Wang, 1989; Thompson et al., 1995). Aneuploidy of chromosome 7 has been correlated with strong *EGFR* gene expression, located on 7p12.3-p12.1 (Koprowski et al., 1985; Udart et al., 2001).

A good correlation was observed when comparing results from M-FISH with CGH in a given cell line, although differences occurred. This could in part be due to misinterpretation of aberrations caused by the complexity of the karyotypes or hybridization artifacts. For example, technical uncertainties of M-FISH were observed particularly at terminal ends and centromeric regions of chromosomes as well as at interfaces of breakpoint regions.

CGH analysis of the melanoma cell lines M1-M7, M9, and CRL-1974 showed frequent overrepresentation of regions on chromosomes 1q, 6p, 7, 20, 22 and X with losses observed on 6q, 9p, and 10q.

Gains of chromosomes 1q and 6p are frequently found in malignant melanoma (Bastian et al., 2003; Hoglund et al., 2004) and have been associated with a poorer prognosis (Namiki et al., 2005), although their prognostic significance has to be evaluated on a larger number of tumors.

As mentioned above, chromosome 7 aneuploidy has been described in the literature in melanoma metastases using the FISH technique and correlated with increased expression of *EGFR* (Udart et al., 2001). Nevertheless, other genes residing on chromosome 7, which have been shown to be overexpressed in primary melanoma or metastases, might also be involved in tumor development; namely BRAF (Brose et al., 2002), PDGF-A (Barnhill et al., 1996), PAI-1 (van Muijen et al., 1995), or MET (Natali et al., 1993).

Amplification of chromosome 20q has been found in metastatic breast cancer (Tanner et al., 1994) and was also detected in malignant melanoma by FISH analysis (Barks et al., 1997). No potential candidate genes contributing to melanoma have been identified on this chromosome so far, although three uncharacterized genes located on 20q were isolated that are highly amplified in breast cancer (Guan et al., 1996).

Amplifications of chromosome 22 have been detected most frequently in acral melanoma (Bastian et al., 2000), whereas gains of the X chromosome have not been described.

Cytogenetic studies have shown that especially the long arm of chromosome 6 is preferentially lost during the progression of the majority of melanoma (Morita et al., 1998; Trent et al., 1989). The importance of chromosome 6 in melanoma has been confirmed by the introduction of a normal chromosome 6 into melanoma cell lines, leading to suppression of metastatic growth (Trent et al., 1990; Welch et al., 1994). Several candidate tumor-suppressor genes have been mapped to chromosome 6q, for example *THW* (now named *PERP*) (Hildebrandt et al., 2001), but further investigations refining the affected regions need to be carried out.

At chromosome 9p the *CDKN2A* locus, encoding *p16INK4A* and *p14ARF*, is not only a melanoma susceptibility gene in familial melanoma, but also a candidate tumor-suppressor gene in sporadic malignant melanoma. The expression of p16 is significantly decreased from melanocytes over RGP and VGP to metastatic lesions (Keller-Melchior et al., 1998), although the frequency of *p16* inactivation in uncultured tumors is much lower than in melanoma cell lines (Healy et al., 1996; Ohta et al., 1994). This and the high frequency of LOH on 9p suggests the existence of other tumor-suppressor genes mapping to the same region (Ohta et al., 1996).

Aberrations in the long arm of chromosome 10 have been frequently described in malignant melanoma of the skin (Thompson et al., 1995) and mainly associated with inactivation of the tumor-suppressor gene *PTEN* (Steck et al., 1997). Investigations revealed several aberrations of this gene in melanoma cell lines (Guldberg et al., 1997), but the analysis of a larger number of primary tumors and metastases limited the importance of *PTEN* to advanced tumor stages (Poetsch et al., 2001).

Apart from aberrations involving larger chromosomal regions, high level amplifications found by CGH analysis were analyzed. Thereby, genomic amplification of *hTERT*, *C-MYC*, and *AKT3* could be confirmed. *hTERT* together with *hTERC* compose the telomerase holoenzyme, which is essential for maintaining telomere length. Acquisition of telomerase activity is believed to be a decisive step in immortalization of human cells and thus seems to be a critical event in cancer development (for review see (Shay et al., 2001)). In cell lines from cutaneous malignant melanoma, especially from SSM primary tumors or local subcutaneous metastases, *hTERT* was found to be amplified (Pirker et al., 2003). Also, telomerase activity has been detected in the majority of melanoma samples (Villa et al., 2001)

and dysplastic nevi (Glaessl et al., 1999), which are believed to be precursor lesions for CMM.

The proto-oncogene *C-MYC* encodes a transcription factor that is implicated in various cellular processes, such as cell growth, proliferation, loss of differentiation and apoptosis. Therefore, it is not surprising that deregulated expression of *C-MYC* has been reported in a broad range of human cancers (for review see (Pelengaris et al., 2002)). CGH and FISH analyses have also detected extra copies of the *C-MYC* gene in primary and metastatic melanoma (Balazs et al., 2001; Kraehn et al., 2001).

The Akt serine/threonine protein kinases consist of three members – Akt1, Akt2, and Akt3, which regulate divergent cellular processes including apoptosis, proliferation, differentiation, and metabolism (for review see (Nicholson and Anderson, 2002)). Increased levels of total phosphorylated Akt were reported in several dysplastic nevi and metastatic melanomas (Dhawan et al., 2002). The predominant Akt isoform responsible for elevated pAkt levels in melanoma has been shown to be Akt3 (Stahl et al., 2004). Increased Akt3 activation also plays a significant role in progression to more advanced tumors (Stahl et al., 2004).

Taken together, the results obtained by FISH and CGH analysis strongly correlate with previous findings of aberrations detected in melanoma as reported in the literature.

6.2 Digital karyotyping of melanoma cell lines

Digital karyotyping has been developed for a genome-wide analysis of DNA copy number alterations at high resolution (Wang et al., 2002). Since then, a small number of laboratories have demonstrated the remarkable power of digital karyotyping in detecting amplifications of several specific tumor-related genes in different cancer cell lines (Boon et al., 2005; Di et al., 2005; Park et al., 2006; Wang et al., 2004). In this work, two malignant melanoma cell lines were analyzed with the digital karyotyping technique in addition to CGH and M-FISH analyses. Thereby, a good correlation was observed between CGH and digital karyotyping concerning subchromosomal changes. However, as digital karyotyping allows for a much better resolution than CGH, additional subchromosomal changes of less than 10 Mbp were detected. In the cell line M2 a homozygous deletion of 1.9 Mbp containing the

CDKN2A locus was found, whereas in one of the two additional digital karyotyping experiments carried out by Alex Epanchintsev an even smaller homozygous deletion of 570 kbp located in the *DMD* gene was detected.

With digital karyotyping it is not only possible to detect small scale genomic alterations, but with the completion of the sequencing of the human genome it is also possible to precisely map those tags that are over- or underrepresented and might correspond to regions containing novel oncogenes or tumor-suppressor genes. Currently, however, the resolution for the detection of gene dosage alterations is limited by the number of experimentally derived tags that can be sequenced economically. Wang et al. demonstrated that although the digital karyotyping shows exquisite sensitivity and specificity for detecting genomic amplifications and deletions, the positive predictive value of detection was significant only for resolutions of 0.1 Mbp for amplifications, 0.6 Mbp for homozygous deletions, and 4 Mbp for heterozygous deletions if 100,000 experimental tags were sequenced (Wang et al., 2002). In accordance with those predictions a homozygous deletion of 250 kbp inside the *p16INK4A* gene in the cell line M3 was not detected by digital karyotyping.

No high level amplifications could be observed in any of the malignant melanoma cell lines analyzed by digital karyotyping. Probable reasons could be the small number of libraries created or that in melanoma oncogenes are activated rather through point mutations than amplifications as in the case of BRAF (Davies et al., 2002).

6.3 Down-regulation of *DMD* in melanoma cell lines

In primary melanocytes expression of the *Dp427m*, *Dp116*, and *Dp71* dystrophin isoforms was observed. The full-length *Dp427m* isoform normally shows strong expression in skeletal and cardiac muscle (Muntoni et al., 1995), and to a lesser extend in glial cells (Yaffe et al., 1992). So far, no full-length dystrophin isoform has been detected in non-muscle or non-neuronal tissues. Instead, in those tissues dystroglycan is linked to utrophin, a homolog of dystrophin (Haenggi and Fritschy, 2006) or shorter dystrophin isoforms (Jung et al., 1995; Saito et al., 1999). *Dp116* is exclusively found in Schwann cells and seems to play an important role in

peripheral myelination (Comi et al., 1995). The shortest dystrophin isoform Dp71 is almost ubiquitously expressed except for skeletal muscle (Bar et al., 1990). In this work, the expression of dystrophin and dystroglycan has been described in melanocytes for the first time. Further experiments are needed to elucidate their function in this specific cell type. It can be speculated, that a dystroglycan complex binding the Dp427m isoform serves a similar purpose in melanocytes as in epithelial cells. However, no conclusions can be drawn concerning the function of the Dp116 and Dp71 isoforms. Both isoforms lack the N-terminal actin-binding domain but retain the binding sites for dystroglycan, dystrobrevin, and syntrophin. Interestingly, in the majority of melanoma cell lines analyzed concomitant loss of the Dp427m and Dp116 isoforms was observed, whereas Dp71 was expressed.

The analysis of 55 melanoma cell lines by Alex Epanchintsev showed homozygous deletions in the *DMD* gene in three cases. As the *DMD* gene spans more than 2.5 Mbp it is one of the largest human genes and located close to or even inside the FRA3C region on Xp21.1. Almost half of the 20 largest human genes are located within common fragile site (CFS) regions, and because of their localization are uniquely susceptible to genomic instability such as occurs during the development of many different cancers (Smith et al., 2006). Several of the large CFS genes appear to function as tumor suppressors, even if they are not mutational targets in cancer, for example the *FHIT* gene in FRA3B (Druck et al., 1998; Vecchione et al., 2004), the *WWOX* gene in FRA16D (Bednarek et al., 2001; Driouch et al., 2002), or the *Parkin* gene in FRA6E (Wang et al., 2004).

Arguing against a common genomic instability at the *DMD* locus is the fact, that although in a few publications homozygous deletions in the *DMD* gene have been described, they occurred with a much lower frequency than in the melanoma cell lines analyzed in this work and no conclusions can be drawn as to their effect on dystrophin expression. In a recent study, homozygous deletions within the *DMD* gene were detected in 2 of 636 (0.3%) cancer cell lines (Cox et al., 2005). Analysis of SNP genotype data obtained by the International HapMap Project identified an exon spanning deletion in *DMD* in 1 of 60 (1.7%) (Conrad et al., 2006) and a small intronic deletion in 1 of 269 genomes analyzed (0.4%) (McCarroll et al., 2006), but none of the deletions were verified by PCR. In contrast, the relatively high frequency of 3

homozygous deletions in 55 (5.5%) melanoma cell lines in the *DMD* gene suggests, that this might be a non-random event specific for melanoma progression.

Furthermore, the expression of the full-length dystrophin protein is completely lost in 69% and significantly reduced in another 18% of melanoma cell lines. Sequencing of the respective cDNAs by Alex Epanchintsev did not reveal any nonsense mutations, which could mediate accelerated decay of the mRNA (Kerr et al., 2001). Also, the promoter regions of all 427 kD *DMD* isoforms do not contain any CpG islands, which may mediate silencing by hypermethylation. Therefore, further analyses are necessary to identify the mechanisms responsible for the loss of dystrophin expression in malignant melanoma cells without *DMD* deletions or nonsense mutations. In addition, it would be of interest to study expression of dystrophin at different stages of melanoma progression – from primary melanomas to RGP, VGP, and metastases. Unfortunately, until now it was not possible to visualize the dystrophin protein with immunohistochemical methods in primary melanocytes or melanoma samples probably due to its low expression level.

The enhanced migration and invasiveness of melanoma cells observed after inactivation of dystrophin could be mediated through functional impairment of the dystroglycan complex. It has been shown, that reduction or absence of dystrophin protein concomitantly leads to loss of function of the dystroglycan complex (Ervasti et al., 1990), which plays important roles in adhesion (Ervasti and Campbell, 1993), basement membrane assembly (Durbeej et al., 1995), and epithelial polarization (Muschler et al., 2002) in a variety of cell types. Importantly, the alteration of dystroglycan function has been implicated not only in muscular dystrophies (Rando, 2001) and neuronal disorders (Moore et al., 2002), but also in cancer progression (Henry et al., 2001).

Reintroduction of dystrophin into melanoma cell lines in one case led to the opposite effect as down-regulation, namely decreased migration. In another cell line reintroduction of dystrophin induced a senescent phenotype, which is a phenomenon that has commonly been observed after introduction of tumor-suppressor genes into tumor cells (Schwarze et al., 2001; Xu et al., 1997). These results strongly suggest, that the *DMD* gene may play a role in the pathogenesis or progression of malignant melanoma.

Another means to link loss of dystrophin to melanoma development could be the analysis of epidemiological data from DMD patients or heterozygous female carriers. However, as male Duchenne Muscular Dystrophy patients die in their early twenties, it is difficult to determine whether an increased incidence of melanoma is linked to an inherited loss of dystrophin function. In addition, loss of dystrophin may be a late event during the progression of malignant melanoma and therefore its inherited loss may have no significant effect on the timing and frequency of melanoma occurrence. Analysis of the occurrence of melanoma in female carriers of a mutant *DMD* gene, which normally do not show a DMD phenotype, is complicated by the random inactivation of the X chromosome in the majority of cases. Also, analysis of the mdx mouse, which lacks full-length dystrophin, for a predisposition to melanoma is complicated by differences in DMD biology between mouse and human, as mdx mice only show a mild DMD phenotype compared to humans (Nowak and Davies, 2004). In addition, melanocyte biology and melanoma development significantly differ between humans and mice (Yang et al., 2001).

6.4 *The dystrophin-glycoprotein complex in melanocytes and melanoma cell lines*

In striated muscle cells, three major functions can be assigned to the dystrophin-glycoprotein complex (DGC): (i) the actin binding domain of dystrophin or utrophin which links the complex to the cytoskeleton; (ii) the dystroglycans (DGs) with the transmembrane protein β -DG and the peripheral protein α -DG anchoring the DGC to the cell membrane and providing contact with the ECM; (iii) the binding sites to signaling proteins located on β -DG, syntrophin, and dystrobrevin (Ervasti and Campbell, 1993; Rando, 2001).

In non-muscle tissues, the DGC typically contains fewer components associated with a short C-terminal isoform of dystrophin or with utrophin and is usually concentrated at membranes facing a basal lamina (Imamura et al., 2000). Although the functional role of non-muscle DGC needs to be clarified, there is compelling evidence for its involvement in adhesion (Ervasti and Campbell, 1993), basement membrane assembly (Durbeej et al., 1995), epithelial polarization

(Muschler et al., 2002), brain development (Nico et al., 2004), synapse formation and plasticity (Mehler, 2000), as well as water and ion homeostasis (Nicchia et al., 2004).

In order to verify the existence of a dystrophin-glycoprotein complex in primary melanocytes and melanoma cell lines, the expression of several components of the DGC was analyzed. cDNA from primary melanocytes was examined by PCR and mRNAs encoding *dystroglycan* (*DAG1*; α - and β -dystroglycan are produced through post-translational cleavage from a single polypeptide), *utrophin* (*UTRN*), *syntrophin* $\beta 2$ (*SNTB2*), *β -sarcoglycan* (*SGCB*), *ϵ -sarcoglycan* (*SGCE*), *laminin- $\alpha 2$* (*LAMA2*), *sarcospan* (*SSPN*), and *nitric oxide synthase 1 (neuronal)* (*NOS1*) but not *α -dystrobrevin* (*DTNA*) were detected.

The expression of both dystrophin and utrophin suggests that different dystroglycan complexes could potentially be formed in melanocytes with either dystrophin or utrophin as intracellular binding partner for β -dystroglycan (James et al., 1996). It has been shown that binding of utrophin and dystrophin to dystroglycan is mutually exclusive and that both complexes are differentially localized in muscle and nerve cells, suggesting different functions (Bewick et al., 1992; Nguyen et al., 1991).

Two components of the sarcoglycan complex were found to be expressed, but no conclusions can be drawn as to the association of this complex with the DGC in melanocytes. It has been shown that in contrast to muscle cells both complexes are not associated in epithelial cells (Durbeej and Campbell, 1999). Likewise, sarcospan and NOS1 interact only indirectly with the dystroglycan complex. Sarcospan is associated with the DGC through its binding to the sarcoglycan complex in skeletal muscle (Crosbie et al., 1999) and smooth muscle (Coral-Vazquez et al., 1999), whereas NOS1 is associated with the DGC through interaction with syntrophin (Abdelmoity et al., 2000). On the other hand, all members of the syntrophin family interact with various members of the dystrophin family (including dystrophin, utrophin and dystrobrevin), with the binding being influenced by calmodulin (Newbell et al., 1997) and phosphorylation of dystrophin (Michalak et al., 1996). Laminin- $\alpha 2$ is one of the three subunits of laminin-2, which serves as extracellular matrix substrate for α -dystroglycan in muscle cells. But so far neither the DGC nor potential binding partners for α -dystroglycan have been analyzed in melanocytes.

In melanoma cell lines the expression of *UTRN*, *DAG1*, *SGCB*, *SGCE*, *SNTB2*, and *LAMA2* was analyzed by PCR and compared to the levels in primary melanocytes. Thereby, significant changes in expression level were detected only for *LAMA2*, which was diminished or absent in 62% of melanoma cell lines significantly correlating with absence of dystrophin protein. Laminin-2 belongs to a family of at least 10 to 15 different laminin isoforms distinguished by their differences in subunit composition. Various laminins and their degradation products have been described to contribute to cancer progression by promoting cell adhesion or by regulating proteolytic cascades via matrix metalloproteases (MMPs) (Pasco et al., 2004; Tran et al., 2005). In a small number of melanoma cell lines expression of *LAMA2* has been shown to promote cell adhesion and to correlate with a more metastatic phenotype (Jenq et al., 1994). In this work down-regulation of *LAMA2* was observed. In addition, in melanoma cell lines with low or absent expression of dystrophin rapid attachment to fibronectin and to a lesser degree to laminin-1 was observed, but not to laminin-2 (data not shown). As the functional consequences of down-regulation of *LAMA2* were not investigated further, no final conclusions can be drawn. Also, it is not clear whether the DGC in melanoma cell lines preferentially binds to laminin-2 and to what extent other laminin receptors, for example integrins, contribute to melanocyte attachment.

Localization of β -dystroglycan and dystrophin was evaluated by overexpression of both proteins in melanoma cell lines with and without endogenous dystrophin protein expression. Using confocal microscopy localization of both proteins to the cell membrane was observed. Due to low transfection efficiency of both plasmids into melanoma cell lines no co-localization studies could be performed. Nevertheless, in the literature interaction of dystrophin with β -dystroglycan has always been confirmed when both proteins were found to be expressed in the same tissue. Therefore, a functional dystrophin-dystroglycan complex is presumably present in melanocytes and melanoma cells, which could mediate interactions of melanocytes with extracellular matrix proteins of the basement membrane.

7 SUMMARY

Malignant melanoma is a highly metastatic cancer whose incidence has increased markedly over the past decade in the white skinned population. Only a few genes have been shown to predispose to melanoma or to contribute to melanoma development and progression. To identify additional genetic alterations, several whole-genome analyses were applied to a panel of malignant melanoma cell lines. First, M-FISH and CGH analyses were carried out to gain a general overview of genomic, structural and numerical aberrations. Thereby, chromosomal alterations commonly found in melanoma were detected. Most frequently, overrepresentation of chromosomes 1q, 6p, 7, 20, 22, and X together with underrepresentation of chromosomes 6q, 9p, and 10q were observed. In addition, high-level amplifications of *C-MYC*, *hTERT*, and *AKT3* together with frequent loss of *p16INK4A* were identified and confirmed by PCR.

In order to detect additional single-gene genetic alterations, the digital karyotyping technique was employed. With this method, two digital karyotyping libraries were generated each comprising ~100,000 sequence tags. Thereby, a homozygous deletion of the *CDKN2A* locus was identified in the cell line M2. In additional digital karyotyping analyses by Alex Epanchintsev a homozygous deletion inside the *DMD* gene was observed in the melanoma cell line M1. By genomic PCR analysis, carried out by Alex Epanchintsev, two additional deletions, one homozygous and one hemizygous, were identified in the *DMD* gene in a total of 55 melanoma cell lines.

To evaluate the relevance of this finding, primary melanocytes were analyzed for the expression of *DMD* mRNA. RT-PCR analysis confirmed expression of the *Dp427m*, *Dp116*, and *Dp71 DMD* isoforms. In addition to homozygous deletion of *DMD*, the *Dp427* protein was absent in 69% and present at very low levels in 18% of melanoma cell lines. This correlated well with *DMD* mRNA expression analyzed in a subset of melanoma cell lines. Furthermore, there was a concomitant loss of expression of the *Dp116* and *Dp427* isoforms in melanoma cell lines, whereas expression of *Dp71* remained unchanged.

In all tissues analyzed, dystrophin normally resides at the cell membrane in a complex with dystroglycans and F-actin, thereby providing a link between

extracellular matrix components and the intracellular cytoskeleton. Several components of this dystrophin-glycoprotein complex (DGC) were analyzed in primary melanocytes and expression of *dystroglycan*, *utrophin*, *syntrophin-β2*, *β-* and *ε-sarcoglycan*, *laminin-α2*, *sarcospan*, and *nitric oxide synthase 1* could be confirmed. As loss of dystrophin frequently leads to down-regulation of components of the DGC, their expression was also analyzed in melanoma cell lines. Thereby, down-regulation of *laminin-α2* was observed which significantly correlated with loss of dystrophin protein.

In order to evaluate functional consequences of loss of dystrophin, short hairpin RNAs directed against *DMD* were stably expressed in the melanoma cell lines M7 and C-32. Upon down-regulation of *DMD* by RNA interference, clones of both cell lines showed enhanced migration and invasion compared to control clones. In addition, dystrophin was stably re-expressed in the cell lines WM-793 and RPMI-7951, which were characterized by homozygous deletion of several exons of this gene. In both cell lines morphological changes were observed; cells became flattened and increased in size, displaying a senescent phenotype. This was accompanied with a higher rate of apoptosis and reduced proliferation in the cell line RPMI-7951. Also, in the cell line WM-793 migration was reduced. Taken together, these results suggest that the loss of dystrophin expression might be involved in the pathogenesis or progression of malignant melanoma.

8 REFERENCES

Abdelmoity, A., Padre, R. C., Burzynski, K. E., Stull, J. T., and Lau, K. S. (2000). Neuronal nitric oxide synthase localizes through multiple structural motifs to the sarcolemma in mouse myotubes. *FEBS Lett* 482, 65-70.

Aitken, J., Welch, J., Duffy, D., Milligan, A., Green, A., Martin, N., and Hayward, N. (1999). CDKN2A variants in a population-based sample of Queensland families with melanoma. *J Natl Cancer Inst* 91, 446-452.

Albino, A. P., Nanus, D. M., Mentle, I. R., Cordon-Cardo, C., McNutt, N. S., Bressler, J., and Andreeff, M. (1989). Analysis of ras oncogenes in malignant melanoma and precursor lesions: correlation of point mutations with differentiation phenotype. *Oncogene* 4, 1363-1374.

Anderson, J. T., Rogers, R. P., and Jarrett, H. W. (1996). Ca²⁺-calmodulin binds to the carboxyl-terminal domain of dystrophin. *J Biol Chem* 271, 6605-6610.

Armstrong, B. K., and Krickler, A. (1993). How much melanoma is caused by sun exposure? *Melanoma Res* 3, 395-401.

Armstrong, B. K., and Krickler, A. (2001). The epidemiology of UV induced skin cancer. *J Photochem Photobiol B* 63, 8-18.

Arning, L., Jagiello, P., Schara, U., Vorgerd, M., Dahmen, N., Gencikova, A., Mortier, W., Epplen, J. T., and Gencik, M. (2004). Transcriptional profiles from patients with dystrophinopathies and limb girdle muscular dystrophies as determined by qRT-PCR. *J Neurol* 251, 72-78.

Azofeifa, J., Fauth, C., Kraus, J., Maierhofer, C., Langer, S., Bolzer, A., Reichman, J., Schuffenhauer, S., and Speicher, M. R. (2000). An optimized probe set for the detection of small interchromosomal aberrations by use of 24-color FISH. *Am J Hum Genet* 66, 1684-1688.

Bai, C., Connolly, B., Metzker, M. L., Hilliard, C. A., Liu, X., Sandig, V., Soderman, A., Galloway, S. M., Liu, Q., Austin, C. P., and Caskey, C. T. (2000). Overexpression of M68/DcR3 in human gastrointestinal tract tumors independent of gene amplification and its location in a four-gene cluster. *Proc Natl Acad Sci U S A* 97, 1230-1235.

Balazs, M., Adam, Z., Treszl, A., Begany, A., Hunyadi, J., and Adany, R. (2001). Chromosomal imbalances in primary and metastatic melanomas revealed by comparative genomic hybridization. *Cytometry* 46, 222-232.

Bar, S., Barnea, E., Levy, Z., Neuman, S., Yaffe, D., and Nudel, U. (1990). A novel product of the Duchenne muscular dystrophy gene which greatly differs from the known isoforms in its structure and tissue distribution. *Biochem J* 272, 557-560.

Barks, J. H., Thompson, F. H., Taetle, R., Yang, J. M., Stone, J. F., Wymer, J. A., Khavari, R., Guan, X. Y., Trent, J. M., Pinkel, D., and Nelson, M. A. (1997). Increased chromosome 20 copy number detected by fluorescence in situ hybridization (FISH) in malignant melanoma. *Genes Chromosomes Cancer* 19, 278-285.

Barnhill, R. L., Xiao, M., Graves, D., and Antoniades, H. N. (1996). Expression of platelet-derived growth factor (PDGF)-A, PDGF-B and the PDGF-alpha receptor, but not the PDGF-beta receptor, in human malignant melanoma in vivo. *Br J Dermatol* 135, 898-904.

Bastian, B. C., Kashani-Sabet, M., Hamm, H., Godfrey, T., Moore, D. H., 2nd, Brocker, E. B., LeBoit, P. E., and Pinkel, D. (2000). Gene amplifications characterize acral melanoma and permit the detection of occult tumor cells in the surrounding skin. *Cancer Res* 60, 1968-1973.

Bastian, B. C., LeBoit, P. E., Hamm, H., Brocker, E. B., and Pinkel, D. (1998). Chromosomal gains and losses in primary cutaneous melanomas detected by comparative genomic hybridization. *Cancer Res* 58, 2170-2175.

- Bastian, B. C., Olshen, A. B., LeBoit, P. E., and Pinkel, D. (2003). Classifying melanocytic tumors based on DNA copy number changes. *Am J Pathol* 163, 1765-1770.
- Bataille, V., Bishop, J. A., Sasieni, P., Swerdlow, A. J., Pinney, E., Griffiths, K., and Cuzick, J. (1996). Risk of cutaneous melanoma in relation to the numbers, types and sites of naevi: a case-control study. *Br J Cancer* 73, 1605-1611.
- Bednarek, A. K., Keck-Waggoner, C. L., Daniel, R. L., Laflin, K. J., Bergsagel, P. L., Kiguchi, K., Brenner, A. J., and Aldaz, C. M. (2001). WWOX, the FRA16D gene, behaves as a suppressor of tumor growth. *Cancer Res* 61, 8068-8073.
- Beggs, A. H., Koenig, M., Boyce, F. M., and Kunkel, L. M. (1990). Detection of 98% of DMD/BMD gene deletions by polymerase chain reaction. *Hum Genet* 86, 45-48.
- Bentz, M., Huck, K., du Manoir, S., Joos, S., Werner, C. A., Fischer, K., Dohner, H., and Lichter, P. (1995). Comparative genomic hybridization in chronic B-cell leukemias shows a high incidence of chromosomal gains and losses. *Blood* 85, 3610-3618.
- Bentz, M., Plesch, A., Stilgenbauer, S., Dohner, H., and Lichter, P. (1998). Minimal sizes of deletions detected by comparative genomic hybridization. *Genes Chromosomes Cancer* 21, 172-175.
- Bewick, G. S., Nicholson, L. V., Young, C., O'Donnell, E., and Slater, C. R. (1992). Different distributions of dystrophin and related proteins at nerve-muscle junctions. *Neuroreport* 3, 857-860.
- Bies, R. D., Friedman, D., Roberts, R., Perryman, M. B., and Caskey, C. T. (1992). Expression and localization of dystrophin in human cardiac Purkinje fibers. *Circulation* 86, 147-153.
- Bies, R. D., Phelps, S. F., Cortez, M. D., Roberts, R., Caskey, C. T., and Chamberlain, J. S. (1992). Human and murine dystrophin mRNA transcripts are

differentially expressed during skeletal muscle, heart, and brain development. *Nucleic Acids Res* 20, 1725-1731.

Blake, D. J., Tinsley, J. M., Davies, K. E., Knight, A. E., Winder, S. J., and Kendrick-Jones, J. (1995). Coiled-coil regions in the carboxy-terminal domains of dystrophin and related proteins: potentials for protein-protein interactions. *Trends Biochem Sci* 20, 133-135.

Blake, D. J., Weir, A., Newey, S. E., and Davies, K. E. (2002). Function and genetics of dystrophin and dystrophin-related proteins in muscle. *Physiol Rev* 82, 291-329.

Boon, K., Eberhart, C. G., and Riggins, G. J. (2005). Genomic amplification of orthodenticle homologue 2 in medulloblastomas. *Cancer Res* 65, 703-707.

Bottaro, D. P., Rubin, J. S., Faletto, D. L., Chan, A. M., Kmieciak, T. E., Vande Woude, G. F., and Aaronson, S. A. (1991). Identification of the hepatocyte growth factor receptor as the c-met proto-oncogene product. *Science* 251, 802-804.

Box, N. F., Duffy, D. L., Chen, W., Stark, M., Martin, N. G., Sturm, R. A., and Hayward, N. K. (2001). MC1R genotype modifies risk of melanoma in families segregating CDKN2A mutations. *Am J Hum Genet* 69, 765-773.

Brenman, J. E., Chao, D. S., Gee, S. H., McGee, A. W., Craven, S. E., Santillano, D. R., Wu, Z., Huang, F., Xia, H., Peters, M. F., *et al.* (1996). Interaction of nitric oxide synthase with the postsynaptic density protein PSD-95 and alpha1-syntrophin mediated by PDZ domains. *Cell* 84, 757-767.

Brose, M. S., Volpe, P., Feldman, M., Kumar, M., Rishi, I., Gerrero, R., Einhorn, E., Herlyn, M., Minna, J., Nicholson, A., *et al.* (2002). BRAF and RAS mutations in human lung cancer and melanoma. *Cancer Res* 62, 6997-7000.

Brummelkamp, T. R., Bernards, R., and Agami, R. (2002). A system for stable expression of short interfering RNAs in mammalian cells. *Science* 296, 550-553.

- Busca, R., Abbe, P., Mantoux, F., Aberdam, E., Peyssonnaud, C., Eychene, A., Ortonne, J. P., and Ballotti, R. (2000). Ras mediates the cAMP-dependent activation of extracellular signal-regulated kinases (ERKs) in melanocytes. *Embo J* 19, 2900-2910.
- Busca, R., and Ballotti, R. (2000). Cyclic AMP a key messenger in the regulation of skin pigmentation. *Pigment Cell Res* 13, 60-69.
- Byers, T. J., Lidov, H. G., and Kunkel, L. M. (1993). An alternative dystrophin transcript specific to peripheral nerve. *Nat Genet* 4, 77-81.
- Campbell, K. P., and Kahl, S. D. (1989). Association of dystrophin and an integral membrane glycoprotein. *Nature* 338, 259-262.
- Carreira, S., Goodall, J., Aksan, I., La Rocca, S. A., Galibert, M. D., Denat, L., Larue, L., and Goding, C. R. (2005). Mitf cooperates with Rb1 and activates p21Cip1 expression to regulate cell cycle progression. *Nature* 433, 764-769.
- Caspersson, T., Farber, S., Foley, G. E., Kudynowski, J., Modest, E. J., Simonsson, E., Wagh, U., and Zech, L. (1968). Chemical differentiation along metaphase chromosomes. *Exp Cell Res* 49, 219-222.
- Caspersson, T., Zech, L., and Johansson, C. (1970). Analysis of human metaphase chromosome set by aid of DNA-binding fluorescent agents. *Exp Cell Res* 62, 490-492.
- Castellano, M., Pollock, P. M., Walters, M. K., Sparrow, L. E., Down, L. M., Gabrielli, B. G., Parsons, P. G., and Hayward, N. K. (1997). CDKN2A/p16 is inactivated in most melanoma cell lines. *Cancer Res* 57, 4868-4875.
- Chapdelaine, P., Moisset, P. A., Campeau, P., Asselin, I., Vilquin, J. T., and Tremblay, J. P. (2000). Functional EGFP-dystrophin fusion proteins for gene therapy vector development. *Protein Eng* 13, 611-615.

- Chin, L., Pomerantz, J., Polsky, D., Jacobson, M., Cohen, C., Cordon-Cardo, C., Horner, J. W., 2nd, and DePinho, R. A. (1997). Cooperative effects of INK4a and ras in melanoma susceptibility in vivo. *Genes Dev* 11, 2822-2834.
- Chung, W., and Campanelli, J. T. (1999). WW and EF hand domains of dystrophin-family proteins mediate dystroglycan binding. *Mol Cell Biol Res Commun* 2, 162-171.
- Cohen, C., Zavala-Pompa, A., Sequeira, J. H., Shoji, M., Sexton, D. G., Cotsonis, G., Cerimele, F., Govindarajan, B., Macaron, N., and Arbiser, J. L. (2002). Mitogen-activated protein kinase activation is an early event in melanoma progression. *Clin Cancer Res* 8, 3728-3733.
- Comi, G. P., Ciafaloni, E., de Silva, H. A., Prella, A., Bardoni, A., Rigoletto, C., Robotti, M., Bresolin, N., Moggio, M., and Fortunato, F. (1995). A G+1-->A transversion at the 5' splice site of intron 69 of the dystrophin gene causing the absence of peripheral nerve Dp116 and severe clinical involvement in a DMD patient. *Hum Mol Genet* 4, 2171-2174.
- Comi, G. P., Prella, A., Bresolin, N., Moggio, M., Bardoni, A., Gallanti, A., Vita, G., Toscano, A., Ferro, M. T., Bordoni, A., and et al. (1994). Clinical variability in Becker muscular dystrophy. Genetic, biochemical and immunohistochemical correlates. *Brain* 117 (Pt 1), 1-14.
- Conrad, D. F., Andrews, T. D., Carter, N. P., Hurles, M. E., and Pritchard, J. K. (2006). A high-resolution survey of deletion polymorphism in the human genome. *Nat Genet* 38, 75-81.
- Coral-Vazquez, R., Cohn, R. D., Moore, S. A., Hill, J. A., Weiss, R. M., Davisson, R. L., Straub, V., Barresi, R., Bansal, D., Hrstka, R. F., et al. (1999). Disruption of the sarcoglycan-sarcospan complex in vascular smooth muscle: a novel mechanism for cardiomyopathy and muscular dystrophy. *Cell* 98, 465-474.

Cox, C., Bignell, G., Greenman, C., Stabenau, A., Warren, W., Stephens, P., Davies, H., Watt, S., Teague, J., Edkins, S., *et al.* (2005). A survey of homozygous deletions in human cancer genomes. *Proc Natl Acad Sci U S A* 102, 4542-4547.

Crawford, G. E., Faulkner, J. A., Crosbie, R. H., Campbell, K. P., Froehner, S. C., and Chamberlain, J. S. (2000). Assembly of the dystrophin-associated protein complex does not require the dystrophin COOH-terminal domain. *J Cell Biol* 150, 1399-1410.

Cremer, T., Lichter, P., Borden, J., Ward, D. C., and Manuelidis, L. (1988). Detection of chromosome aberrations in metaphase and interphase tumor cells by in situ hybridization using chromosome-specific library probes. *Hum Genet* 80, 235-246.

Crosbie, R. H., Lebakken, C. S., Holt, K. H., Venzke, D. P., Straub, V., Lee, J. C., Grady, R. M., Chamberlain, J. S., Sanes, J. R., and Campbell, K. P. (1999). Membrane targeting and stabilization of sarcospan is mediated by the sarcoglycan subcomplex. *J Cell Biol* 145, 153-165.

D'Souza, V. N., Nguyen, T. M., Morris, G. E., Karges, W., Pillers, D. A., and Ray, P. N. (1995). A novel dystrophin isoform is required for normal retinal electrophysiology. *Hum Mol Genet* 4, 837-842.

Davies, H., Bignell, G. R., Cox, C., Stephens, P., Edkins, S., Clegg, S., Teague, J., Woffendin, H., Garnett, M. J., Bottomley, W., *et al.* (2002). Mutations of the BRAF gene in human cancer. *Nature* 417, 949-954.

Demunter, A., Stas, M., Degreef, H., De Wolf-Peeters, C., and van den Oord, J. J. (2001). Analysis of N- and K-ras mutations in the distinctive tumor progression phases of melanoma. *J Invest Dermatol* 117, 1483-1489.

Dhawan, P., Singh, A. B., Ellis, D. L., and Richmond, A. (2002). Constitutive activation of Akt/protein kinase B in melanoma leads to up-regulation of nuclear factor-kappaB and tumor progression. *Cancer Res* 62, 7335-7342.

- Di, C., Liao, S., Adamson, D. C., Parrett, T. J., Broderick, D. K., Shi, Q., Lengauer, C., Cummins, J. M., Velculescu, V. E., Fults, D. W., *et al.* (2005). Identification of OTX2 as a medulloblastoma oncogene whose product can be targeted by all-trans retinoic acid. *Cancer Res* 65, 919-924.
- Dimri, G. P., Lee, X., Basile, G., Acosta, M., Scott, G., Roskelley, C., Medrano, E. E., Linskens, M., Rubelj, I., Pereira-Smith, O., and *et al.* (1995). A biomarker that identifies senescent human cells in culture and in aging skin in vivo. *Proc Natl Acad Sci U S A* 92, 9363-9367.
- Ding, H., Schertzer, M., Wu, X., Gertsenstein, M., Selig, S., Kammori, M., Pourvali, R., Poon, S., Vulto, I., Chavez, E., *et al.* (2004). Regulation of murine telomere length by Rtel: an essential gene encoding a helicase-like protein. *Cell* 117, 873-886.
- Driouch, K., Prydz, H., Monese, R., Johansen, H., Lidereau, R., and Frengen, E. (2002). Alternative transcripts of the candidate tumor suppressor gene, WWOX, are expressed at high levels in human breast tumors. *Oncogene* 21, 1832-1840.
- Druck, T., Berk, L., and Huebner, K. (1998). FHITness and cancer. *Oncol Res* 10, 341-345.
- Du, J., Widlund, H. R., Horstmann, M. A., Ramaswamy, S., Ross, K., Huber, W. E., Nishimura, E. K., Golub, T. R., and Fisher, D. E. (2004). Critical role of CDK2 for melanoma growth linked to its melanocyte-specific transcriptional regulation by MITF. *Cancer Cell* 6, 565-576.
- du Manoir, S., Speicher, M. R., Joos, S., Schrock, E., Popp, S., Dohner, H., Kovacs, G., Robert-Nicoud, M., Lichter, P., and Cremer, T. (1993). Detection of complete and partial chromosome gains and losses by comparative genomic in situ hybridization. *Hum Genet* 90, 590-610.
- Durbeej, M., and Campbell, K. P. (1999). Biochemical characterization of the epithelial dystroglycan complex. *J Biol Chem* 274, 26609-26616.

- Durbeej, M., Jung, D., Hjalt, T., Campbell, K. P., and Ekblom, P. (1997). Transient expression of Dp140, a product of the Duchenne muscular dystrophy locus, during kidney tubulogenesis. *Dev Biol* 181, 156-167.
- Durbeej, M., Larsson, E., Ibraghimov-Beskrovnaya, O., Roberds, S. L., Campbell, K. P., and Ekblom, P. (1995). Non-muscle alpha-dystroglycan is involved in epithelial development. *J Cell Biol* 130, 79-91.
- Emery, A. E. H. (1993). *Duchenne Muscular Dystrophy*, 2nd edition edn (Oxford: Oxford University Press).
- Ervasti, J. M., and Campbell, K. P. (1991). Membrane organization of the dystrophin-glycoprotein complex. *Cell* 66, 1121-1131.
- Ervasti, J. M., and Campbell, K. P. (1993). A role for the dystrophin-glycoprotein complex as a transmembrane linker between laminin and actin. *J Cell Biol* 122, 809-823.
- Ervasti, J. M., Ohlendieck, K., Kahl, S. D., Gaver, M. G., and Campbell, K. P. (1990). Deficiency of a glycoprotein component of the dystrophin complex in dystrophic muscle. *Nature* 345, 315-319.
- Fauth, C., Zhang, H., Harabacz, S., Brown, J., Saracoglu, K., Lederer, G., Rittinger, O., Rost, I., Eils, R., Kearney, L., and Speicher, M. R. (2001). A new strategy for the detection of subtelomeric rearrangements. *Hum Genet* 109, 576-583.
- Feener, C. A., Koenig, M., and Kunkel, L. M. (1989). Alternative splicing of human dystrophin mRNA generates isoforms at the carboxy terminus. *Nature* 338, 509-511.
- Fountain, J. W., Bale, S. J., Housman, D. E., and Dracopoli, N. C. (1990). Genetics of melanoma. *Cancer Surv* 9, 645-671.
- Friedberg, E. C. (2003). DNA damage and repair. *Nature* 421, 436-440.

- Gardner, R. J., Bobrow, M., and Roberts, R. G. (1995). The identification of point mutations in Duchenne muscular dystrophy patients by using reverse-transcription PCR and the protein truncation test. *Am J Hum Genet* 57, 311-320.
- Gavet, O., Ozon, S., Manceau, V., Lawler, S., Curmi, P., and Sobel, A. (1998). The stathmin phosphoprotein family: intracellular localization and effects on the microtubule network. *J Cell Sci* 111 (Pt 22), 3333-3346.
- Gee, S. H., Montanaro, F., Lindenbaum, M. H., and Carbonetto, S. (1994). Dystroglycan-alpha, a dystrophin-associated glycoprotein, is a functional agrin receptor. *Cell* 77, 675-686.
- Glaessl, A., Bosserhoff, A. K., Buettner, R., Hohenleutner, U., Landthaler, M., and Stolz, W. (1999). Increase in telomerase activity during progression of melanocytic cells from melanocytic naevi to malignant melanomas. *Arch Dermatol Res* 291, 81-87.
- Goldstein, A. M., Struewing, J. P., Chidambaram, A., Fraser, M. C., and Tucker, M. A. (2000). Genotype-phenotype relationships in U.S. melanoma-prone families with CDKN2A and CDK4 mutations. *J Natl Cancer Inst* 92, 1006-1010.
- Gorecki, D. C., Monaco, A. P., Derry, J. M., Walker, A. P., Barnard, E. A., and Barnard, P. J. (1992). Expression of four alternative dystrophin transcripts in brain regions regulated by different promoters. *Hum Mol Genet* 1, 505-510.
- Grange, F., Chompret, A., Guilloud-Bataille, M., Guillaume, J. C., Margulis, A., Prade, M., Demenais, F., and Avril, M. F. (1995). Comparison between familial and nonfamilial melanoma in France. *Arch Dermatol* 131, 1154-1159.
- Guan, X. Y., Xu, J., Anzick, S. L., Zhang, H., Trent, J. M., and Meltzer, P. S. (1996). Hybrid selection of transcribed sequences from microdissected DNA: isolation of genes within amplified region at 20q11-q13.2 in breast cancer. *Cancer Res* 56, 3446-3450.

Guldberg, P., thor Straten, P., Birck, A., Ahrenkiel, V., Kirkin, A. F., and Zeuthen, J. (1997). Disruption of the MMAC1/PTEN gene by deletion or mutation is a frequent event in malignant melanoma. *Cancer Res* 57, 3660-3663.

Haenggi, T., and Fritschy, J. M. (2006). Role of dystrophin and utrophin for assembly and function of the dystrophin glycoprotein complex in non-muscle tissue. *Cell Mol Life Sci*.

Halaban, R., Rubin, J. S., Funasaka, Y., Cobb, M., Boulton, T., Faletto, D., Rosen, E., Chan, A., Yoko, K., White, W., and et al. (1992). Met and hepatocyte growth factor/scatter factor signal transduction in normal melanocytes and melanoma cells. *Oncogene* 7, 2195-2206.

Hanahan, D., and Weinberg, R. A. (2000). The hallmarks of cancer. *Cell* 100, 57-70.

Healy, E., Flannagan, N., Ray, A., Todd, C., Jackson, I. J., Matthews, J. N., Birch-Machin, M. A., and Rees, J. L. (2000). Melanocortin-1-receptor gene and sun sensitivity in individuals without red hair. *Lancet* 355, 1072-1073.

Healy, E., Sikkink, S., and Rees, J. L. (1996). Infrequent mutation of p16INK4 in sporadic melanoma. *J Invest Dermatol* 107, 318-321.

Henry, M. D., and Campbell, K. P. (1998). A role for dystroglycan in basement membrane assembly. *Cell* 95, 859-870.

Henry, M. D., Cohen, M. B., and Campbell, K. P. (2001). Reduced expression of dystroglycan in breast and prostate cancer. *Hum Pathol* 32, 791-795.

Herzog, C., Has, C., Franzke, C. W., Echtermeyer, F. G., Schlotzer-Schrehardt, U., Kroger, S., Gustafsson, E., Fassler, R., and Bruckner-Tuderman, L. (2004). Dystroglycan in skin and cutaneous cells: beta-subunit is shed from the cell surface. *J Invest Dermatol* 122, 1372-1380.

Hildebrandt, T., van Dijk, M. C., van Muijen, G. N., and Weidle, U. H. (2001). Loss of heterozygosity of gene THW is frequently found in melanoma metastases. *Anticancer Res* 21, 1071-1080.

Hoeijmakers, J. H. (2001). Genome maintenance mechanisms for preventing cancer. *Nature* 411, 366-374.

Hoglund, M., Gisselsson, D., Hansen, G. B., White, V. A., Sall, T., Mitelman, F., and Horsman, D. (2004). Dissecting karyotypic patterns in malignant melanomas: temporal clustering of losses and gains in melanoma karyotypic evolution. *Int J Cancer* 108, 57-65.

Hsu, M. Y., Meier, F., and Herlyn, M. (2002). Melanoma development and progression: a conspiracy between tumor and host. *Differentiation* 70, 522-536.

Hsu, M. Y., Wheelock, M. J., Johnson, K. R., and Herlyn, M. (1996). Shifts in cadherin profiles between human normal melanocytes and melanomas. *J Investig Dermatol Symp Proc* 1, 188-194.

Hugnot, J. P., Gilgenkrantz, H., Vincent, N., Chafey, P., Morris, G. E., Monaco, A. P., Berwald-Netter, Y., Koulakoff, A., Kaplan, J. C., Kahn, A., and et al. (1992). Distal transcript of the dystrophin gene initiated from an alternative first exon and encoding a 75-kDa protein widely distributed in nonmuscle tissues. *Proc Natl Acad Sci U S A* 89, 7506-7510.

Hussussian, C. J., Struewing, J. P., Goldstein, A. M., Higgins, P. A., Ally, D. S., Sheahan, M. D., Clark, W. H., Jr., Tucker, M. A., and Dracopoli, N. C. (1994). Germline p16 mutations in familial melanoma. *Nat Genet* 8, 15-21.

Hwang, P. H., Yi, H. K., Kim, D. S., Nam, S. Y., Kim, J. S., and Lee, D. Y. (2001). Suppression of tumorigenicity and metastasis in B16F10 cells by PTEN/MMAC1/TEP1 gene. *Cancer Lett* 172, 83-91.

- Ibraghimov-Beskrovnaya, O., Ervasti, J. M., Leveille, C. J., Slaughter, C. A., Sernett, S. W., and Campbell, K. P. (1992). Primary structure of dystrophin-associated glycoproteins linking dystrophin to the extracellular matrix. *Nature* 355, 696-702.
- Ibraghimov-Beskrovnaya, O., Milatovich, A., Ozcelik, T., Yang, B., Koepnick, K., Francke, U., and Campbell, K. P. (1993). Human dystroglycan: skeletal muscle cDNA, genomic structure, origin of tissue specific isoforms and chromosomal localization. *Hum Mol Genet* 2, 1651-1657.
- Imamura, M., Araishi, K., Noguchi, S., and Ozawa, E. (2000). A sarcoglycan-dystroglycan complex anchors Dp116 and utrophin in the peripheral nervous system. *Hum Mol Genet* 9, 3091-3100.
- Isola, J. J., Kallioniemi, O. P., Chu, L. W., Fuqua, S. A., Hilsenbeck, S. G., Osborne, C. K., and Waldman, F. M. (1995). Genetic aberrations detected by comparative genomic hybridization predict outcome in node-negative breast cancer. *Am J Pathol* 147, 905-911.
- Jafari, M., Papp, T., Kirchner, S., Diener, U., Henschler, D., Burg, G., and Schiffmann, D. (1995). Analysis of ras mutations in human melanocytic lesions: activation of the ras gene seems to be associated with the nodular type of human malignant melanoma. *J Cancer Res Clin Oncol* 121, 23-30.
- James, M., Nguyen, T. M., Wise, C. J., Jones, G. E., and Morris, G. E. (1996). Utrophin-dystroglycan complex in membranes of adherent cultured cells. *Cell Motil Cytoskeleton* 33, 163-174.
- Jennekens, F. G., ten Kate, L. P., de Visser, M., and Wintzen, A. R. (1991). Diagnostic criteria for Duchenne and Becker muscular dystrophy and myotonic dystrophy. *Neuromuscul Disord* 1, 389-391.
- Jenq, W., Wu, S. J., and Kefalides, N. A. (1994). Expression of the alpha 2-subunit of laminin correlates with increased cell adhesion and metastatic propensity. *Differentiation* 58, 29-36.

Johnson, G. L., and Lapadat, R. (2002). Mitogen-activated protein kinase pathways mediated by ERK, JNK, and p38 protein kinases. *Science* 298, 1911-1912.

Jones, P. A., and Baylin, S. B. (2002). The fundamental role of epigenetic events in cancer. *Nat Rev Genet* 3, 415-428.

Jung, D., Yang, B., Meyer, J., Chamberlain, J. S., and Campbell, K. P. (1995). Identification and characterization of the dystrophin anchoring site on beta-dystroglycan. *J Biol Chem* 270, 27305-27310.

Kallioniemi, A., Kallioniemi, O. P., Sudar, D., Rutovitz, D., Gray, J. W., Waldman, F., and Pinkel, D. (1992). Comparative genomic hybridization for molecular cytogenetic analysis of solid tumors. *Science* 258, 818-821.

Keller-Melchior, R., Schmidt, R., and Piepkorn, M. (1998). Expression of the tumor suppressor gene product p16INK4 in benign and malignant melanocytic lesions. *J Invest Dermatol* 110, 932-938.

Kerr, T. P., Sewry, C. A., Robb, S. A., and Roberts, R. G. (2001). Long mutant dystrophins and variable phenotypes: evasion of nonsense-mediated decay? *Hum Genet* 109, 402-407.

Koenig, M., Beggs, A. H., Moyer, M., Scherpf, S., Heindrich, K., Bettecken, T., Meng, G., Muller, C. R., Lindlof, M., Kaariainen, H., and et al. (1989). The molecular basis for Duchenne versus Becker muscular dystrophy: correlation of severity with type of deletion. *Am J Hum Genet* 45, 498-506.

Koenig, M., and Kunkel, L. M. (1990). Detailed analysis of the repeat domain of dystrophin reveals four potential hinge segments that may confer flexibility. *J Biol Chem* 265, 4560-4566.

Koenig, M., Monaco, A. P., and Kunkel, L. M. (1988). The complete sequence of dystrophin predicts a rod-shaped cytoskeletal protein. *Cell* 53, 219-226.

- Koprowski, H., Herlyn, M., Balaban, G., Parmiter, A., Ross, A., and Nowell, P. (1985). Expression of the receptor for epidermal growth factor correlates with increased dosage of chromosome 7 in malignant melanoma. *Somat Cell Mol Genet* 11, 297-302.
- Kraehn, G. M., Utikal, J., Udart, M., Greulich, K. M., Bezold, G., Kaskel, P., Leiter, U., and Peter, R. U. (2001). Extra c-myc oncogene copies in high risk cutaneous malignant melanoma and melanoma metastases. *Br J Cancer* 84, 72-79.
- Kraemer, K. H., and Greene, M. H. (1985). Dysplastic nevus syndrome. Familial and sporadic precursors of cutaneous melanoma. *Dermatol Clin* 3, 225-237.
- Krimpenfort, P., Quon, K. C., Mooi, W. J., Loonstra, A., and Berns, A. (2001). Loss of p16Ink4a confers susceptibility to metastatic melanoma in mice. *Nature* 413, 83-86.
- Kumar, R., Sauroja, I., Punnonen, K., Jansen, C., and Hemminki, K. (1998). Selective deletion of exon 1 beta of the p19ARF gene in metastatic melanoma cell lines. *Genes Chromosomes Cancer* 23, 273-277.
- Kumar, R., Smeds, J., Berggren, P., Straume, O., Rozell, B. L., Akslen, L. A., and Hemminki, K. (2001). A single nucleotide polymorphism in the 3'untranslated region of the CDKN2A gene is common in sporadic primary melanomas but mutations in the CDKN2B, CDKN2C, CDK4 and p53 genes are rare. *Int J Cancer* 95, 388-393.
- Lederfein, D., Levy, Z., Augier, N., Mornet, D., Morris, G., Fuchs, O., Yaffe, D., and Nudel, U. (1992). A 71-kilodalton protein is a major product of the Duchenne muscular dystrophy gene in brain and other nonmuscle tissues. *Proc Natl Acad Sci U S A* 89, 5346-5350.
- Lengauer, C., Kinzler, K. W., and Vogelstein, B. (1998). Genetic instabilities in human cancers. *Nature* 396, 643-649.
- Lengauer, C., Speicher, M. R., Popp, S., Jauch, A., Taniwaki, M., Nagaraja, R., Riethman, H. C., Donis-Keller, H., D'Urso, M., Schlessinger, D., and et al. (1993).

Chromosomal bar codes produced by multicolor fluorescence in situ hybridization with multiple YAC clones and whole chromosome painting probes. *Hum Mol Genet* 2, 505-512.

Li, G., and Herlyn, M. (2000). Dynamics of intercellular communication during melanoma development. *Mol Med Today* 6, 163-169.

Li, G., Schaider, H., Satyamoorthy, K., Hanakawa, Y., Hashimoto, K., and Herlyn, M. (2001). Downregulation of E-cadherin and Desmoglein 1 by autocrine hepatocyte growth factor during melanoma development. *Oncogene* 20, 8125-8135.

Lichter, P., Cremer, T., Borden, J., Manuelidis, L., and Ward, D. C. (1988). Delineation of individual human chromosomes in metaphase and interphase cells by in situ suppression hybridization using recombinant DNA libraries. *Hum Genet* 80, 224-234.

Lidov, H. G., Selig, S., and Kunkel, L. M. (1995). Dp140: a novel 140 kDa CNS transcript from the dystrophin locus. *Hum Mol Genet* 4, 329-335.

Liechti-Gallati, S., Koenig, M., Kunkel, L. M., Frey, D., Boltshauser, E., Schneider, V., Braga, S., and Moser, H. (1989). Molecular deletion patterns in Duchenne and Becker type muscular dystrophy. *Hum Genet* 81, 343-348.

Liu, L., Dilworth, D., Gao, L., Monzon, J., Summers, A., Lassam, N., and Hogg, D. (1999). Mutation of the CDKN2A 5' UTR creates an aberrant initiation codon and predisposes to melanoma. *Nat Genet* 21, 128-132.

Love, D. R., Flint, T. J., Marsden, R. F., Bloomfield, J. F., Daniels, R. J., Forrest, S. M., Gabrielli, O., Giorgi, P., Novelli, G., and Davies, K. E. (1990). Characterization of deletions in the dystrophin gene giving mild phenotypes. *Am J Med Genet* 37, 136-142.

- Madhavan, R., Massom, L. R., and Jarrett, H. W. (1992). Calmodulin specifically binds three proteins of the dystrophin-glycoprotein complex. *Biochem Biophys Res Commun* 185, 753-759.
- Markowitz, S. (2000). DNA repair defects inactivate tumor suppressor genes and induce hereditary and sporadic colon cancers. *J Clin Oncol* 18, 75S-80S.
- McCarroll, S. A., Hadnott, T. N., Perry, G. H., Sabeti, P. C., Zody, M. C., Barrett, J. C., Dallaire, S., Gabriel, S. B., Lee, C., Daly, M. J., *et al.* (2006). Common deletion polymorphisms in the human genome. *Nat Genet* 38, 86-92.
- Mehler, M. F. (2000). Brain dystrophin, neurogenetics and mental retardation. *Brain Res Brain Res Rev* 32, 277-307.
- Michalak, M., Fu, S. Y., Milner, R. E., Busaan, J. L., and Hance, J. E. (1996). Phosphorylation of the carboxyl-terminal region of dystrophin. *Biochem Cell Biol* 74, 431-437.
- Michaloglou, C., Vredeveld, L. C., Soengas, M. S., Denoyelle, C., Kuilman, T., van der Horst, C. M., Majoor, D. M., Shay, J. W., Mooi, W. J., and Peeper, D. S. (2005). BRAFE600-associated senescence-like cell cycle arrest of human naevi. *Nature* 436, 720-724.
- Micheli, A., Mugno, E., Krogh, V., Quinn, M. J., Coleman, M., Hakulinen, T., Gatta, G., Berrino, F., and Capocaccia, R. (2002). Cancer prevalence in European registry areas. *Ann Oncol* 13, 840-865.
- Monaco, A. P., Bertelson, C. J., Liechti-Gallati, S., Moser, H., and Kunkel, L. M. (1988). An explanation for the phenotypic differences between patients bearing partial deletions of the DMD locus. *Genomics* 2, 90-95.
- Monaco, A. P., Bertelson, C. J., Middlesworth, W., Colletti, C. A., Aldridge, J., Fischbeck, K. H., Bartlett, R., Pericak-Vance, M. A., Roses, A. D., and Kunkel, L. M.

(1985). Detection of deletions spanning the Duchenne muscular dystrophy locus using a tightly linked DNA segment. *Nature* 316, 842-845.

Monni, O., Oinonen, R., Elonen, E., Franssila, K., Teerenhovi, L., Joensuu, H., and Knuutila, S. (1998). Gain of 3q and deletion of 11q22 are frequent aberrations in mantle cell lymphoma. *Genes Chromosomes Cancer* 21, 298-307.

Montanaro, F., Gee, S. H., Jacobson, C., Lindenbaum, M. H., Froehner, S. C., and Carbonetto, S. (1998). Laminin and alpha-dystroglycan mediate acetylcholine receptor aggregation via a MuSK-independent pathway. *J Neurosci* 18, 1250-1260.

Moore, S. A., Saito, F., Chen, J., Michele, D. E., Henry, M. D., Messing, A., Cohn, R. D., Ross-Barta, S. E., Westra, S., Williamson, R. A., *et al.* (2002). Deletion of brain dystroglycan recapitulates aspects of congenital muscular dystrophy. *Nature* 418, 422-425.

Morita, R., Fujimoto, A., Hatta, N., Takehara, K., and Takata, M. (1998). Comparison of genetic profiles between primary melanomas and their metastases reveals genetic alterations and clonal evolution during progression. *J Invest Dermatol* 111, 919-924.

Morrison, C., Radmacher, M., Mohammed, N., Suster, D., Auer, H., Jones, S., Rigganbach, J., Kelbick, N., Bos, G., and Mayerson, J. (2005). MYC amplification and polysomy 8 in chondrosarcoma: array comparative genomic hybridization, fluorescent in situ hybridization, and association with outcome. *J Clin Oncol* 23, 9369-9376.

Muntoni, F., Melis, M. A., Ganau, A., and Dubowitz, V. (1995). Transcription of the dystrophin gene in normal tissues and in skeletal muscle of a family with X-linked dilated cardiomyopathy. *Am J Hum Genet* 56, 151-157.

Muntoni, F., Torelli, S., and Ferlini, A. (2003). Dystrophin and mutations: one gene, several proteins, multiple phenotypes. *Lancet Neurol* 2, 731-740.

Muschler, J., Levy, D., Boudreau, R., Henry, M., Campbell, K., and Bissell, M. J. (2002). A role for dystroglycan in epithelial polarization: loss of function in breast tumor cells. *Cancer Res* 62, 7102-7109.

Namiki, T., Yanagawa, S., Izumo, T., Ishikawa, M., Tachibana, M., Kawakami, Y., Yokozeki, H., Nishioka, K., and Kaneko, Y. (2005). Genomic alterations in primary cutaneous melanomas detected by metaphase comparative genomic hybridization with laser capture or manual microdissection: 6p gains may predict poor outcome. *Cancer Genet Cytogenet* 157, 1-11.

Natali, P. G., Nicotra, M. R., Di Renzo, M. F., Prat, M., Bigotti, A., Cavaliere, R., and Comoglio, P. M. (1993). Expression of the c-Met/HGF receptor in human melanocytic neoplasms: demonstration of the relationship to malignant melanoma tumour progression. *Br J Cancer* 68, 746-750.

Nevo, Y., Muntoni, F., Sewry, C., Legum, C., Kutai, M., Harel, S., and Dubowitz, V. (2003). Large in-frame deletions of the rod-shaped domain of the dystrophin gene resulting in severe phenotype. *Isr Med Assoc J* 5, 94-97.

Newbell, B. J., Anderson, J. T., and Jarrett, H. W. (1997). Ca²⁺-calmodulin binding to mouse alpha1 syntrophin: syntrophin is also a Ca²⁺-binding protein. *Biochemistry* 36, 1295-1305.

Nguyen, T. M., Ellis, J. M., Love, D. R., Davies, K. E., Gatter, K. C., Dickson, G., and Morris, G. E. (1991). Localization of the DMDL gene-encoded dystrophin-related protein using a panel of nineteen monoclonal antibodies: presence at neuromuscular junctions, in the sarcolemma of dystrophic skeletal muscle, in vascular and other smooth muscles, and in proliferating brain cell lines. *J Cell Biol* 115, 1695-1700.

Nicchia, G. P., Nico, B., Camassa, L. M., Mola, M. G., Loh, N., Dermietzel, R., Spray, D. C., Svelto, M., and Frigeri, A. (2004). The role of aquaporin-4 in the blood-brain barrier development and integrity: studies in animal and cell culture models. *Neuroscience* 129, 935-945.

Nicholson, K. M., and Anderson, N. G. (2002). The protein kinase B/Akt signalling pathway in human malignancy. *Cell Signal* 14, 381-395.

Nico, B., Paola Nicchia, G., Frigeri, A., Corsi, P., Mangieri, D., Ribatti, D., Svelto, M., and Roncali, L. (2004). Altered blood-brain barrier development in dystrophic MDX mice. *Neuroscience* 125, 921-935.

Nishio, H., Takeshima, Y., Narita, N., Yanagawa, H., Suzuki, Y., Ishikawa, Y., Minami, R., Nakamura, H., and Matsuo, M. (1994). Identification of a novel first exon in the human dystrophin gene and of a new promoter located more than 500 kb upstream of the nearest known promoter. *J Clin Invest* 94, 1037-1042.

Nowak, K. J., and Davies, K. E. (2004). Duchenne muscular dystrophy and dystrophin: pathogenesis and opportunities for treatment. *EMBO Rep* 5, 872-876.

Nudel, U., Zuk, D., Einat, P., Zeelon, E., Levy, Z., Neuman, S., and Yaffe, D. (1989). Duchenne muscular dystrophy gene product is not identical in muscle and brain. *Nature* 337, 76-78.

Ohlendieck, K., and Campbell, K. P. (1991). Dystrophin-associated proteins are greatly reduced in skeletal muscle from mdx mice. *J Cell Biol* 115, 1685-1694.

Ohta, M., Berd, D., Shimizu, M., Nagai, H., Cotticelli, M. G., Mastrangelo, M., Shields, J. A., Shields, C. L., Croce, C. M., and Huebner, K. (1996). Deletion mapping of chromosome region 9p21-p22 surrounding the CDKN2 locus in melanoma. *Int J Cancer* 65, 762-767.

Ohta, M., Nagai, H., Shimizu, M., Rasio, D., Berd, D., Mastrangelo, M., Singh, A. D., Shields, J. A., Shields, C. L., Croce, C. M., and et al. (1994). Rarity of somatic and germline mutations of the cyclin-dependent kinase 4 inhibitor gene, CDK4I, in melanoma. *Cancer Res* 54, 5269-5272.

Palmer, J. S., Duffy, D. L., Box, N. F., Aitken, J. F., O'Gorman, L. E., Green, A. C., Hayward, N. K., Martin, N. G., and Sturm, R. A. (2000). Melanocortin-1 receptor

polymorphisms and risk of melanoma: is the association explained solely by pigmentation phenotype? *Am J Hum Genet* 66, 176-186.

Papp, T., Pemsel, H., Rollwitz, I., Schipper, H., Weiss, D. G., Schiffmann, D., and Zimmermann, R. (2003). Mutational analysis of N-ras, p53, CDKN2A (p16(INK4a)), p14(ARF), CDK4, and MC1R genes in human dysplastic melanocytic naevi. *J Med Genet* 40, E14.

Park, J. T., Li, M., Nakayama, K., Mao, T. L., Davidson, B., Zhang, Z., Kurman, R. J., Eberhart, C. G., Shih Ie, M., and Wang, T. L. (2006). Notch3 gene amplification in ovarian cancer. *Cancer Res* 66, 6312-6318.

Parrett, T. J., and Yan, H. (2005). Digital karyotyping technology: exploring the cancer genome. *Expert Rev Mol Diagn* 5, 917-925.

Pasco, S., Ramont, L., Maquart, F. X., and Monboisse, J. C. (2004). Control of melanoma progression by various matrikines from basement membrane macromolecules. *Crit Rev Oncol Hematol* 49, 221-233.

Pedersen, M. I., and Wang, N. (1989). Chromosomal evolution in the progression and metastasis of human malignant melanoma. A multiple lesion study. *Cancer Genet Cytogenet* 41, 185-201.

Pelengaris, S., Khan, M., and Evan, G. (2002). c-MYC: more than just a matter of life and death. *Nat Rev Cancer* 2, 764-776.

Petrof, B. J., Shrager, J. B., Stedman, H. H., Kelly, A. M., and Sweeney, H. L. (1993). Dystrophin protects the sarcolemma from stresses developed during muscle contraction. *Proc Natl Acad Sci U S A* 90, 3710-3714.

Pfaffl, M. W. (2001). A new mathematical model for relative quantification in real-time RT-PCR. *Nucleic Acids Res* 29, e45.

- Piccinin, S., Doglioni, C., Maestro, R., Vukosavljevic, T., Gasparotto, D., D'Orazi, C., and Boiocchi, M. (1997). p16/CDKN2 and CDK4 gene mutations in sporadic melanoma development and progression. *Int J Cancer* 74, 26-30.
- Pickl, W. F., Majdic, O., Fischer, G. F., Petzelbauer, P., Fae, I., Waclavicek, M., Stockl, J., Scheinecker, C., Vidicki, T., Aschauer, H., *et al.* (1997). MUC18/MCAM (CD146), an activation antigen of human T lymphocytes. *J Immunol* 158, 2107-2115.
- Pillers, D. A., Bulman, D. E., Weleber, R. G., Sigesmund, D. A., Musarella, M. A., Powell, B. R., Murphey, W. H., Westall, C., Panton, C., Becker, L. E., and *et al.* (1993). Dystrophin expression in the human retina is required for normal function as defined by electroretinography. *Nat Genet* 4, 82-86.
- Pinkel, D., Landegent, J., Collins, C., Fuscoe, J., Segraves, R., Lucas, J., and Gray, J. (1988). Fluorescence in situ hybridization with human chromosome-specific libraries: detection of trisomy 21 and translocations of chromosome 4. *Proc Natl Acad Sci U S A* 85, 9138-9142.
- Pinkel, D., Segraves, R., Sudar, D., Clark, S., Poole, I., Kowbel, D., Collins, C., Kuo, W. L., Chen, C., Zhai, Y., *et al.* (1998). High resolution analysis of DNA copy number variation using comparative genomic hybridization to microarrays. *Nat Genet* 20, 207-211.
- Pirker, C., Holzmann, K., Spiegl-Kreinecker, S., Elbling, L., Thallinger, C., Pehamberger, H., Micksche, M., and Berger, W. (2003). Chromosomal imbalances in primary and metastatic melanomas: over-representation of essential telomerase genes. *Melanoma Res* 13, 483-492.
- Poetsch, M., Dittberner, T., and Woenckhaus, C. (2001). PTEN/MMAC1 in malignant melanoma and its importance for tumor progression. *Cancer Genet Cytogenet* 125, 21-26.
- Poetsch, M., Woenckhaus, C., Dittberner, T., Pambor, M., Lorenz, G., and Herrmann, F. H. (1998). An increased frequency of numerical chromosomal abnormalities and

1p36 deletions in isolated cells from paraffin sections of malignant melanomas by means of interphase cytogenetics. *Cancer Genet Cytogenet* 104, 146-152.

Pollock, P. M., Harper, U. L., Hansen, K. S., Yudt, L. M., Stark, M., Robbins, C. M., Moses, T. Y., Hostetter, G., Wagner, U., Kakareka, J., *et al.* (2003). High frequency of BRAF mutations in nevi. *Nat Genet* 33, 19-20.

Prior, T. W., Bartolo, C., Pearl, D. K., Papp, A. C., Snyder, P. J., Sedra, M. S., Burghes, A. H., and Mendell, J. R. (1995). Spectrum of small mutations in the dystrophin coding region. *Am J Hum Genet* 57, 22-33.

Rando, T. A. (2001). The dystrophin-glycoprotein complex, cellular signaling, and the regulation of cell survival in the muscular dystrophies. *Muscle Nerve* 24, 1575-1594.

Riopel, M. A., Spellerberg, A., Griffin, C. A., and Perlman, E. J. (1998). Genetic analysis of ovarian germ cell tumors by comparative genomic hybridization. *Cancer Res* 58, 3105-3110.

Roberts, R. G., Barby, T. F., Manners, E., Bobrow, M., and Bentley, D. R. (1991). Direct detection of dystrophin gene rearrangements by analysis of dystrophin mRNA in peripheral blood lymphocytes. *Am J Hum Genet* 49, 298-310.

Roberts, R. G., Gardner, R. J., and Bobrow, M. (1994). Searching for the 1 in 2,400,000: a review of dystrophin gene point mutations. *Hum Mutat* 4, 1-11.

Robertson, G. P. (2005). Functional and therapeutic significance of Akt deregulation in malignant melanoma. *Cancer Metastasis Rev* 24, 273-285.

Robertson, G. P., Furnari, F. B., Miele, M. E., Glendening, M. J., Welch, D. R., Fountain, J. W., Lugo, T. G., Huang, H. J., and Cavenee, W. K. (1998). In vitro loss of heterozygosity targets the PTEN/MMAC1 gene in melanoma. *Proc Natl Acad Sci U S A* 95, 9418-9423.

- Rosa, G., Ceccarini, M., Cavaldesi, M., Zini, M., and Petrucci, T. C. (1996). Localization of the dystrophin binding site at the carboxyl terminus of beta-dystroglycan. *Biochem Biophys Res Commun* 223, 272-277.
- Ruas, M., and Peters, G. (1998). The p16INK4a/CDKN2A tumor suppressor and its relatives. *Biochim Biophys Acta* 1378, F115-177.
- Rybakova, I. N., Amann, K. J., and Ervasti, J. M. (1996). A new model for the interaction of dystrophin with F-actin. *J Cell Biol* 135, 661-672.
- Sadoulet-Puccio, H. M., and Kunkel, L. M. (1996). Dystrophin and its isoforms. *Brain Pathol* 6, 25-35.
- Saito, F., Masaki, T., Kamakura, K., Anderson, L. V., Fujita, S., Fukuta-Ohi, H., Sunada, Y., Shimizu, T., and Matsumura, K. (1999). Characterization of the transmembrane molecular architecture of the dystroglycan complex in schwann cells. *J Biol Chem* 274, 8240-8246.
- Schofield, J. N., Blake, D. J., Simmons, C., Morris, G. E., Tinsley, J. M., Davies, K. E., and Edwards, Y. H. (1994). Apo-dystrophin-1 and apo-dystrophin-2, products of the Duchenne muscular dystrophy locus: expression during mouse embryogenesis and in cultured cell lines. *Hum Mol Genet* 3, 1309-1316.
- Schreiber-Agus, N., Meng, Y., Hoang, T., Hou, H., Jr., Chen, K., Greenberg, R., Cordon-Cardo, C., Lee, H. W., and DePinho, R. A. (1998). Role of Mxi1 in ageing organ systems and the regulation of normal and neoplastic growth. *Nature* 393, 483-487.
- Schrock, E., du Manoir, S., Veldman, T., Schoell, B., Wienberg, J., Ferguson-Smith, M. A., Ning, Y., Ledbetter, D. H., Bar-Am, I., Soenksen, D., *et al.* (1996). Multicolor spectral karyotyping of human chromosomes. *Science* 273, 494-497.
- Schulten, H. J., Gunawan, B., Otto, F., Hassmann, R., Hallermann, C., Noebel, A., and Fuzesi, L. (2002). Cytogenetic characterization of complex karyotypes in seven

established melanoma cell lines by multiplex fluorescence in situ hybridization and DAPI banding. *Cancer Genet Cytogenet* 133, 134-141.

Schulze, A., Zerfass, K., Spitkovsky, D., Henglein, B., and Jansen-Durr, P. (1994). Activation of the E2F transcription factor by cyclin D1 is blocked by p16INK4, the product of the putative tumor suppressor gene MTS1. *Oncogene* 9, 3475-3482.

Schwarze, S. R., Shi, Y., Fu, V. X., Watson, P. A., and Jarrard, D. F. (2001). Role of cyclin-dependent kinase inhibitors in the growth arrest at senescence in human prostate epithelial and uroepithelial cells. *Oncogene* 20, 8184-8192.

Serrano, M., Lee, H., Chin, L., Cordon-Cardo, C., Beach, D., and DePinho, R. A. (1996). Role of the INK4a locus in tumor suppression and cell mortality. *Cell* 85, 27-37.

Sgambato, A., Migaldi, M., Montanari, M., Camerini, A., Brancaccio, A., Rossi, G., Cangiano, R., Losasso, C., Capelli, G., Trentini, G. P., and Cittadini, A. (2003). Dystroglycan expression is frequently reduced in human breast and colon cancers and is associated with tumor progression. *Am J Pathol* 162, 849-860.

Sharpless, N. E., Alson, S., Chan, S., Silver, D. P., Castrillon, D. H., and DePinho, R. A. (2002). p16(INK4a) and p53 deficiency cooperate in tumorigenesis. *Cancer Res* 62, 2761-2765.

Sharpless, N. E., Kannan, K., Xu, J., Bosenberg, M. W., and Chin, L. (2003). Both products of the mouse *Ink4a/Arf* locus suppress melanoma formation in vivo. *Oncogene* 22, 5055-5059.

Shay, J. W., Zou, Y., Hiyama, E., and Wright, W. E. (2001). Telomerase and cancer. *Hum Mol Genet* 10, 677-685.

Shih le, M., and Wang, T. L. (2005). Apply innovative technologies to explore cancer genome. *Curr Opin Oncol* 17, 33-38.

- Shih, I. M., Elder, D. E., Hsu, M. Y., and Herlyn, M. (1994). Regulation of Mel-CAM/MUC18 expression on melanocytes of different stages of tumor progression by normal keratinocytes. *Am J Pathol* 145, 837-845.
- Simon, R., Burger, H., Brinkschmidt, C., Bocker, W., Hertle, L., and Terpe, H. J. (1998). Chromosomal aberrations associated with invasion in papillary superficial bladder cancer. *J Pathol* 185, 345-351.
- Simpson, L., and Parsons, R. (2001). PTEN: life as a tumor suppressor. *Exp Cell Res* 264, 29-41.
- Smedley, D., Sidhar, S., Birdsall, S., Bennett, D., Herlyn, M., Cooper, C., and Shipley, J. (2000). Characterization of chromosome 1 abnormalities in malignant melanomas. *Genes Chromosomes Cancer* 28, 121-125.
- Smith, D. I., Zhu, Y., McAvoy, S., and Kuhn, R. (2006). Common fragile sites, extremely large genes, neural development and cancer. *Cancer Lett* 232, 48-57.
- Solinas-Toldo, S., Lampel, S., Stilgenbauer, S., Nickolenko, J., Benner, A., Dohner, H., Cremer, T., and Lichter, P. (1997). Matrix-based comparative genomic hybridization: biochips to screen for genomic imbalances. *Genes Chromosomes Cancer* 20, 399-407.
- Soufir, N., Avril, M. F., Chompret, A., Demenais, F., Bombléd, J., Spatz, A., Stoppa-Lyonnet, D., Benard, J., and Bressac-de Paillerets, B. (1998). Prevalence of p16 and CDK4 germline mutations in 48 melanoma-prone families in France. The French Familial Melanoma Study Group. *Hum Mol Genet* 7, 209-216.
- Speicher, M. R., Gwyn Ballard, S., and Ward, D. C. (1996). Karyotyping human chromosomes by combinatorial multi-fluor FISH. *Nat Genet* 12, 368-375.
- St Croix, B., Rago, C., Velculescu, V., Traverso, G., Romans, K. E., Montgomery, E., Lal, A., Riggins, G. J., Lengauer, C., Vogelstein, B., and Kinzler, K. W. (2000). Genes expressed in human tumor endothelium. *Science* 289, 1197-1202.

- Stahl, J. M., Sharma, A., Cheung, M., Zimmerman, M., Cheng, J. Q., Bosenberg, M. W., Kester, M., Sandirasegarane, L., and Robertson, G. P. (2004). Deregulated Akt3 activity promotes development of malignant melanoma. *Cancer Res* *64*, 7002-7010.
- Stambolic, V., Suzuki, A., de la Pompa, J. L., Brothers, G. M., Mirtsos, C., Sasaki, T., Ruland, J., Penninger, J. M., Siderovski, D. P., and Mak, T. W. (1998). Negative regulation of PKB/Akt-dependent cell survival by the tumor suppressor PTEN. *Cell* *95*, 29-39.
- Steck, P. A., Pershouse, M. A., Jasser, S. A., Yung, W. K., Lin, H., Ligon, A. H., Langford, L. A., Baumgard, M. L., Hattier, T., Davis, T., *et al.* (1997). Identification of a candidate tumour suppressor gene, MMAC1, at chromosome 10q23.3 that is mutated in multiple advanced cancers. *Nat Genet* *15*, 356-362.
- Sugita, S., Saito, F., Tang, J., Satz, J., Campbell, K., and Sudhof, T. C. (2001). A stoichiometric complex of neurexins and dystroglycan in brain. *J Cell Biol* *154*, 435-445.
- Surono, A., Takeshima, Y., Wibawa, T., Ikezawa, M., Nonaka, I., and Matsuo, M. (1999). Circular dystrophin RNAs consisting of exons that were skipped by alternative splicing. *Hum Mol Genet* *8*, 493-500.
- Tanner, M. M., Tirkkonen, M., Kallioniemi, A., Collins, C., Stokke, T., Karhu, R., Kowbel, D., Shadravan, F., Hintz, M., Kuo, W. L., and *et al.* (1994). Increased copy number at 20q13 in breast cancer: defining the critical region and exclusion of candidate genes. *Cancer Res* *54*, 4257-4260.
- Teng, D. H., Hu, R., Lin, H., Davis, T., Iliev, D., Frye, C., Swedlund, B., Hansen, K. L., Vinson, V. L., Gumpfer, K. L., *et al.* (1997). MMAC1/PTEN mutations in primary tumor specimens and tumor cell lines. *Cancer Res* *57*, 5221-5225.
- Thompson, F. H., Emerson, J., Olson, S., Weinstein, R., Leavitt, S. A., Leong, S. P., Emerson, S., Trent, J. M., Nelson, M. A., Salmon, S. E., and *et al.* (1995).

- Cytogenetics of 158 patients with regional or disseminated melanoma. Subset analysis of near-diploid and simple karyotypes. *Cancer Genet Cytogenet* 83, 93-104.
- Thompson, J. F., Scolyer, R. A., and Kefford, R. F. (2005). Cutaneous melanoma. *Lancet* 365, 687-701.
- Tienari, J., Reima, I., Larramendy, M. L., Knuutila, S., von Boguslawsky, K., Kaartinen, M., Virtanen, I., and Lehtonen, E. (1998). A cloned human germ cell tumor-derived cell line differentiating in culture. *Int J Cancer* 77, 710-719.
- Tran, K. T., Lamb, P., and Deng, J. S. (2005). Matrikines and matricryptins: Implications for cutaneous cancers and skin repair. *J Dermatol Sci* 40, 11-20.
- Trent, J. M., Stanbridge, E. J., McBride, H. L., Meese, E. U., Casey, G., Araujo, D. E., Witkowski, C. M., and Nagle, R. B. (1990). Tumorigenicity in human melanoma cell lines controlled by introduction of human chromosome 6. *Science* 247, 568-571.
- Trent, J. M., Thompson, F. H., and Meyskens, F. L., Jr. (1989). Identification of a recurring translocation site involving chromosome 6 in human malignant melanoma. *Cancer Res* 49, 420-423.
- Trevor, K. T., Cover, C., Ruiz, Y. W., Akporiaye, E. T., Hersh, E. M., Landais, D., Taylor, R. R., King, A. D., and Walters, R. E. (2004). Generation of dendritic cell-tumor cell hybrids by electrofusion for clinical vaccine application. *Cancer Immunol Immunother* 53, 705-714.
- Tsao, H., Zhang, X., Kwitkiwski, K., Finkelstein, D. M., Sober, A. J., and Haluska, F. G. (2000). Low prevalence of germline CDKN2A and CDK4 mutations in patients with early-onset melanoma. *Arch Dermatol* 136, 1118-1122.
- Udart, M., Utikal, J., Krahn, G. M., and Peter, R. U. (2001). Chromosome 7 aneusomy. A marker for metastatic melanoma? Expression of the epidermal growth factor receptor gene and chromosome 7 aneusomy in nevi, primary malignant melanomas and metastases. *Neoplasia* 3, 245-254.

- Uhrig, S., Schuffenhauer, S., Fauth, C., Wirtz, A., Daumer-Haas, C., Apacik, C., Cohen, M., Muller-Navia, J., Cremer, T., Murken, J., and Speicher, M. R. (1999). Multiplex-FISH for pre- and postnatal diagnostic applications. *Am J Hum Genet* 65, 448-462.
- Valverde, P., Healy, E., Jackson, I., Rees, J. L., and Thody, A. J. (1995). Variants of the melanocyte-stimulating hormone receptor gene are associated with red hair and fair skin in humans. *Nat Genet* 11, 328-330.
- van der Velden, P. A., Sandkuijl, L. A., Bergman, W., Pavel, S., van Mourik, L., Frants, R. R., and Gruis, N. A. (2001). Melanocortin-1 receptor variant R151C modifies melanoma risk in Dutch families with melanoma. *Am J Hum Genet* 69, 774-779.
- van Elsas, A., Zerp, S. F., van der Flier, S., Kruse, K. M., Aarnoudse, C., Hayward, N. K., Ruiter, D. J., and Schrier, P. I. (1996). Relevance of ultraviolet-induced N-ras oncogene point mutations in development of primary human cutaneous melanoma. *Am J Pathol* 149, 883-893.
- van Muijen, G. N., Danen, E. H., de Vries, T. J., Quax, P. H., Verheijen, J. H., and Ruiter, D. J. (1995). Properties of metastasizing and nonmetastasizing human melanoma cells. *Recent Results Cancer Res* 139, 105-122.
- Vecchione, A., Seignani, C., Giarnieri, E., Zanesi, N., Ishii, H., Cesari, R., Fong, L. Y., Gomella, L. G., Croce, C. M., and Baffa, R. (2004). Inactivation of the FHIT gene favors bladder cancer development. *Clin Cancer Res* 10, 7607-7612.
- Veldman, T., Vignon, C., Schrock, E., Rowley, J. D., and Ried, T. (1997). Hidden chromosome abnormalities in haematological malignancies detected by multicolour spectral karyotyping. *Nat Genet* 15, 406-410.
- Villa, R., Porta, C. D., Folini, M., Daidone, M. G., and Zaffaroni, N. (2001). Possible regulation of telomerase activity by transcription and alternative splicing of

telomerase reverse transcriptase in human melanoma. *J Invest Dermatol* 116, 867-873.

Wang, F., Denison, S., Lai, J. P., Philips, L. A., Montoya, D., Kock, N., Schule, B., Klein, C., Shridhar, V., Roberts, L. R., and Smith, D. I. (2004). Parkin gene alterations in hepatocellular carcinoma. *Genes Chromosomes Cancer* 40, 85-96.

Wang, T. L., Diaz, L. A., Jr., Romans, K., Bardelli, A., Saha, S., Galizia, G., Choti, M., Donehower, R., Parmigiani, G., Shih le, M., *et al.* (2004). Digital karyotyping identifies thymidylate synthase amplification as a mechanism of resistance to 5-fluorouracil in metastatic colorectal cancer patients. *Proc Natl Acad Sci U S A* 101, 3089-3094.

Wang, T. L., Maierhofer, C., Speicher, M. R., Lengauer, C., Vogelstein, B., Kinzler, K. W., and Velculescu, V. E. (2002). Digital karyotyping. *Proc Natl Acad Sci U S A* 99, 16156-16161.

Welch, D. R., Chen, P., Miele, M. E., McGary, C. T., Bower, J. M., Stanbridge, E. J., and Weissman, B. E. (1994). Microcell-mediated transfer of chromosome 6 into metastatic human C8161 melanoma cells suppresses metastasis but does not inhibit tumorigenicity. *Oncogene* 9, 255-262.

Wellbrock, C., Ogilvie, L., Hedley, D., Karasarides, M., Martin, J., Niculescu-Duvaz, D., Springer, C. J., and Marais, R. (2004). V599EB-RAF is an oncogene in melanocytes. *Cancer Res* 64, 2338-2342.

Wheway, J. M., and Roberts, R. G. (2003). The dystrophin lymphocyte promoter revisited: 4.5-megabase intron, or artifact? *Neuromuscul Disord* 13, 17-20.

Widlund, H. R., and Fisher, D. E. (2003). Microphthalmia-associated transcription factor: a critical regulator of pigment cell development and survival. *Oncogene* 22, 3035-3041.

Williamson, R. A., Henry, M. D., Daniels, K. J., Hrstka, R. F., Lee, J. C., Sunada, Y., Ibraghimov-Beskrovnaya, O., and Campbell, K. P. (1997). Dystroglycan is essential

for early embryonic development: disruption of Reichert's membrane in Dag1-null mice. *Hum Mol Genet* 6, 831-841.

Wiltshire, R. N., Dennis, T. R., Sondak, V. K., Meltzer, P. S., and Trent, J. M. (2001). Application of molecular cytogenetic techniques in a case study of human cutaneous metastatic melanoma. *Cancer Genet Cytogenet* 131, 97-103.

Wolfel, T., Hauer, M., Schneider, J., Serrano, M., Wolfel, C., Klehmann-Hieb, E., De Plaen, E., Hankeln, T., Meyer zum Buschenfelde, K. H., and Beach, D. (1995). A p16INK4a-insensitive CDK4 mutant targeted by cytolytic T lymphocytes in a human melanoma. *Science* 269, 1281-1284.

Wu, H., Goel, V., and Haluska, F. G. (2003). PTEN signaling pathways in melanoma. *Oncogene* 22, 3113-3122.

Xu, H. J., Zhou, Y., Ji, W., Perng, G. S., Kruzelock, R., Kong, C. T., Bast, R. C., Mills, G. B., Li, J., and Hu, S. X. (1997). Reexpression of the retinoblastoma protein in tumor cells induces senescence and telomerase inhibition. *Oncogene* 15, 2589-2596.

Yaffe, D., Makover, A., Lederfein, D., Rapaport, D., Bar, S., Barnea, E., and Nudel, U. (1992). Multiple products of the Duchenne muscular dystrophy gene. *Symp Soc Exp Biol* 46, 179-188.

Yang, B., Jung, D., Motto, D., Meyer, J., Koretzky, G., and Campbell, K. P. (1995). SH3 domain-mediated interaction of dystroglycan and Grb2. *J Biol Chem* 270, 11711-11714.

Yang, F. C., Merlino, G., and Chin, L. (2001). Genetic dissection of melanoma pathways in the mouse. *Semin Cancer Biol* 11, 261-268.

Yoshida, M., and Ozawa, E. (1990). Glycoprotein complex anchoring dystrophin to sarcolemma. *J Biochem (Tokyo)* 108, 748-752.

Zhang, Y., Xiong, Y., and Yarbrough, W. G. (1998). ARF promotes MDM2 degradation and stabilizes p53: ARF-INK4a locus deletion impairs both the Rb and p53 tumor suppression pathways. *Cell* 92, 725-734.

Zuo, L., Weger, J., Yang, Q., Goldstein, A. M., Tucker, M. A., Walker, G. J., Hayward, N., and Dracopoli, N. C. (1996). Germline mutations in the p16INK4a binding domain of CDK4 in familial melanoma. *Nat Genet* 12, 97-99.

9 ABBREVIATIONS

ATCC	American type culture collection
bp	base pair
cAMP	cyclic adenosine monophosphate
CC domain	coiled coil domain
cDNA	complementary deoxyribonucleic acid
CFS	common fragile site
CGH	comparative genomic hybridization
CMM	cutaneous malignant melanoma
CMV	cytomegalovirus (promoter)
COOH- or C-terminal	carboxy-terminal
DGC	dystrophin-glycoprotein complex
DK	digital karyotyping
DMD/BMD	Duchenne/Becker muscular dystrophy
DNA	deoxyribonucleic acid
dNTP	deoxynucleotide triphosphate
ECM	extracellular matrix
EF-hand motif	calcium-binding motif
FRA	fragile site
HDF	human dermal fibroblast
ISCN	International System for Human Cytogenetic Nomenclature
kbp	kilo base pair
kD	kilodalton
LOH	loss of heterozygosity
MAA	melanoma-associated antigen
Mbp	mega base pair
M-FISH	multiplex fluorescence <i>in situ</i> hybridization
MMP	matrix metalloprotease
mRNA	messenger RNA
NH₂- or N-terminal	amino-terminal
NM	nodular melanoma

PCR	polymerase chain reaction
qPCR	quantitative PCR
RGP	radial growth phase
RHC	red hair color (phenotype)
RNA	ribonucleic acid
RT-PCR	reverse transcriptase PCR
shDMD	short hairpin RNA directed against <i>DMD</i>
SKY	spectral karyotyping
SSM	superficial spreading melanoma
Tris	(Hydroxymethyl)aminomethane
U	units
UV	ultraviolet
VGP	vertical growth phase
VSV	vesicular stomatitis virus (tag)
WW domain	domain with two signature tryptophan residues
ZZ domain	zinc finger domain

10 APPENDIX

Supplementary Table 1 Description of melanoma cell lines, their origin and culture conditions. Abbreviations: n. a., not available

Cell line	Description	Origin	Medium
A375P	low invasive malignant melanoma	Dr. A. Ullrich ¹⁾	DMEM high glucose, 5 % FBS
Bow-G	melanosarcoma	Dr. A. Ullrich ¹⁾	DMEM low glucose, 10 % FBS
C-32	amelanotic melanoma	Dr. A. Ullrich ¹⁾	MEM, non-essential amino acids, sodium pyruvate, L-glutamine, 10 % FBS
C-8161	metastatic melanoma	Dr. A. Ullrich ¹⁾	DMEM high glucose, 5 % FBS
CRL-1974	malignant melanoma	ATCC	RPMI 1640, 10 % FBS, sodium pyruvate, L-glutamine, sodium bicarbonate
F-01	metastatic melanoblastoma	Dr. A. Ullrich ¹⁾	RPMI 1640, 10 % FBS, L-glutamine
G-361	malignant melanoma	Dr. A. Ullrich ¹⁾	McCoy's 5A, 10 % FBS
Hs-294T	metastatic malignant melanoma	Dr. A. Ullrich ¹⁾	DMEM high glucose, 10 % FBS
Hs-695T	metastatic malignant melanoma	Dr. A. Ullrich ¹⁾	MEM, 10 % FBS, L-glutamine
HT-144	metastatic malignant melanoma	Dr. A. Ullrich ¹⁾	McCoy's 5A, 10 % FBS
IGR-39	n. a.	Dr. A. Ullrich ¹⁾	RPMI 1640, 10 % FBS, L-glutamine
Malme3M	metastatic malignant melanoma	Dr. A. Ullrich ¹⁾	Leibovitz L15, 10 % FBS
Mel Gerlach	n. a.	Dr. A. Ullrich ¹⁾	RPMI 1640, 10 % FBS, L-glutamine
Mel Juso	primary melanoma	Dr. A. Ullrich ¹⁾	RPMI 1640, 10 % FBS, L-glutamine
MeWO3	metastatic malignant melanoma	Dr. A. Ullrich ¹⁾	DMEM low glucose, 10 % FBS
MRI-H 221	metastatic malignant melanoma	Dr. A. Ullrich ¹⁾	RPMI 1640, 10 % FBS, L-glutamine
RPMI-7951	metastatic malignant melanoma	Dr. A. Ullrich ¹⁾	MEM, non-essential amino acids, sodium pyruvate, L-glutamine, 10 % FBS
SBCL2	metastatic malignant melanoma	Dr. A. Ullrich ¹⁾	MCDB 153/L15 (4:1), 2 % FBS, 5 µg/ml insulin
Sk-Mel 1	metastatic malignant melanoma	Dr. A. Ullrich ¹⁾	MEM, non-essential amino acids, sodium pyruvate, L-glutamine , 10 % FBS
Sk-Mel 2	metastatic malignant melanoma	Dr. A. Ullrich ¹⁾	MEM, non-essential amino acids, sodium pyruvate, L-glutamine, 10 % FBS
Sk-Mel 24	metastatic malignant melanoma	Dr. A. Ullrich ¹⁾	MEM, non-essential amino acids, sodium pyruvate, L-glutamine , 10 % FBS

Supplementary Table 1 continued.

Cell line	Description	Origin	Medium
Sk-Mel 28	malignant melanoma	Dr. A. Ullrich ¹⁾	MEM, non-essential amino acids, sodium pyruvate, L-glutamine , 10 % FBS
Sk-Mel 3	metastatic malignant melanoma	Dr. A. Ullrich ¹⁾	McCoy's 5A, 10 % FBS
Sk-Mel 31	malignant melanoma	Dr. A. Ullrich ¹⁾	MEM, non-essential amino acids, sodium pyruvate, L-glutamine , 15 % FBS
Sk-Mel 5	metastatic malignant melanoma	Dr. A. Ullrich ¹⁾	MEM, non-essential amino acids, sodium pyruvate, L-glutamine , 10 % FBS
WM-115	primary melanoma	Dr. A. Ullrich ¹⁾	MEM, non-essential amino acids, sodium pyruvate, L-glutamine , 10 % FBS
WM-1205LU	n. a.	Dr. A. Ullrich ¹⁾	MCDB 153/L15 (4:1), 2 % FBS, 5 µg/ml insulin
WM-1341D	RGP/VGP melanoma	Dr. A. Ullrich ¹⁾	RPMI 1640, 10 % FBS, 0.04 i.U./ml h-insulin, L-glutamine
WM-239A	metastatic melanoma from WM-115	Dr. A. Ullrich ¹⁾	RPMI 1640, 10 % FBS, 0.04 i.U./ml h-insulin, L-glutamine
WM-266-4	metastatic melanoma from WM-115	Dr. A. Ullrich ¹⁾	RPMI 1640, 10 % FBS, L-glutamine
WM-35	RGP/VGP melanoma	Dr. A. Ullrich ¹⁾	MCDB 153/L15 (4:1), 2 % FBS, 5 µg/ml insulin
WM-793	RGP/VGP melanoma	Dr. A. Ullrich ¹⁾	MCDB 153/L15 (4:1), 2 % FBS, 5 µg/ml insulin
WM-852	metastatic melanoma	Dr. A. Ullrich ¹⁾	MCDB 153/L15 (4:1), 2 % FBS, 5 µg/ml insulin
WM-902B	VGP melanoma	Dr. A. Ullrich ¹⁾	RPMI 1640, 10 % FBS, 0.04 IU/ml h-insulin, L-glutamine
WM-98	n. a.	Dr. D. Herlyn ²⁾	MCDB 153/L15 (4:1), 2 % FBS, 5 µg/ml insulin
WM-3450	n. a.	Dr. D. Herlyn ²⁾	RPMI 1640, 10 % FBS, L-glutamine
WM-3451	n. a.	Dr. D. Herlyn ²⁾	RPMI 1640, 10 % FBS, L-glutamine
WM-3453	n. a.	Dr. D. Herlyn ²⁾	RPMI 1640, 10 % FBS, L-glutamine
WM-3456	n. a.	Dr. D. Herlyn ²⁾	RPMI 1640, 10 % FBS, L-glutamine
MM-031	metastatic malignant melanoma	Dr. L. Füzési ³⁾	RPMI 1640, 10 % FBS, L-glutamine
MM-194	metastatic malignant melanoma	Dr. L. Füzési ³⁾	RPMI 1640, 10 % FBS, L-glutamine
MM-195	metastatic malignant melanoma	Dr. L. Füzési ³⁾	RPMI 1640, 10 % FBS, L-glutamine
MM-201	metastatic malignant melanoma	Dr. L. Füzési ³⁾	RPMI 1640, 10 % FBS, L-glutamine

Supplementary Table 1 continued.

Cell line	Description	Origin	Medium
MM-232	metastatic malignant melanoma	Dr. L. Füzési ³⁾	RPMI 1640, 10 % FBS, L-glutamine
MM-254	metastatic malignant melanoma	Dr. L. Füzési ³⁾	RPMI 1640, 10 % FBS, L-glutamine
MM-358	metastatic malignant melanoma	Dr. L. Füzési ³⁾	RPMI 1640, 10 % FBS, L-glutamine
KAlI	metastatic malignant melanoma	Dr. L. Füzési ³⁾	RPMI 1640, 10 % FBS, L-glutamine
M1	metastatic malignant melanoma	Dr. B. Schuler-Thurner ⁴⁾	RPMI 1640, 10 % FBS, L-glutamine
M2	metastatic malignant melanoma	Dr. B. Schuler-Thurner ⁴⁾	RPMI 1640, 10 % FBS, L-glutamine
M3	metastatic malignant melanoma	Dr. B. Schuler-Thurner ⁴⁾	RPMI 1640, 10 % FBS, L-glutamine
M4	metastatic malignant melanoma	Dr. B. Schuler-Thurner ⁴⁾	MCDB 153/L15 (4:1), 2 % FBS, 5 µg/ml insulin
M5	metastatic malignant melanoma	Dr. B. Schuler-Thurner ⁴⁾	RPMI 1640, 10 % FBS, L-glutamine
M6	metastatic malignant melanoma	Dr. B. Schuler-Thurner ⁴⁾	RPMI 1640, 10 % FBS, L-glutamine
M7	metastatic malignant melanoma	Dr. B. Schuler-Thurner ⁴⁾	MCDB 153/L15 (4:1), 2 % FBS, 5 µg/ml insulin
M8	metastatic malignant melanoma	Dr. B. Schuler-Thurner ⁴⁾	RPMI 1640, 10 % FBS, L-glutamine
M9	metastatic malignant melanoma	Dr. B. Schuler-Thurner ⁴⁾	RPMI 1640, 10 % FBS, L-glutamine

¹⁾Department of Molecular Biology, MPI of Biochemistry, Martinsried, Germany

²⁾Wistar Institute, Philadelphia, USA

³⁾Department of Pathology, Georg August University, Goettingen, Germany (Schulten et al., 2002)

⁴⁾Department of Dermatology, University Hospital of Erlangen, Erlangen, Germany

Supplementary Table 2 Description of gender and expression levels of DMD mRNA and protein in melanoma cell lines. Also listed is the deletion status of *DMD* on genomic DNA as analyzed by Alex Epanchintsev. The *DMD* mRNA expression was calculated relative to expression in primary melanocytes. If unspecific PCR products together with a PCR product specific for DMD were observed, no exact calculation was possible and expression was denoted with <. Dystrophin protein was classified as expressed (+) or not expressed (-). n. a., not available; n. d., not determined.

Melanoma cell line	Sex	% <i>DMD</i> mRNA expression	Dystrophin protein expression	<i>DMD</i> deletion on genomic DNA
primary melanocytes HM40p7	male	100	+	
primary melanocytes HM9p6	male	100	+	
A375P	female	n. d.	-	
BOW-G	n. a.	33	-	
C-32	male	68	+	
C-8161	female	n. d.	-	
CRL-1974	male	32	-	
F-01	male	<1	-	
G-361	male	n. d.	-	
Hs-294T	male	100	+	
Hs-695T	male	0	-	
HT-144	male	n. d.	-	
IGR-39	n. a.	n. d.	-	
KAll	n. a.	10	-	
M1	female	0	-	exons 3-29
M2	female	0	-	
M3	male	1	-	
M4	male	12	+	
M5	female	4	-	
M6	female	<8	-	
M7	female	100	+	
M9	female	n. d.	-	
Malme3M	male	<4	-	
Mel-Gerlach	n. a.	n.d.	-	
Mel-Juso	female	<1	-	
MM-031	male	n. d.	-	
MM-194	male	1	-	
MM-195	male	<17	+	
MM-201	female	n. d.	-	
MM-232	female	n. d.	-	
MM-254	female	n. d.	-	

Supplementary Table 2 continued.

Melanoma cell line	Sex	% <i>DMD</i> RNA expression	Dystrophin protein expression	DMD deletion on genomic DNA
MM-358	female	n. d.	-	
MeWO3	male	3	-	
MRI-H 221	female	100	+	
RPMI-7951	female	0	-	exons 17-30
SBCL2	n. a.	n. d.	-	
Sk-Mel 1	male	n. d.	+	
Sk-Mel 2	male	7	-	
Sk-Mel 24	male	5	+	
Sk-Mel 28	male	n. d.	-	
Sk-Mel 3	female	n. d.	-	
Sk-Mel 31	female	100	+	
Sk-Mel 5	female	<1	-	
WM-115	female	37	+	
WM-1205LU	male	<5	-	
WM-1341D	male	3	+	
WM-239A	female	1	-	
WM-266-4	female	1	+	
WM-3450	n. a.	n. d.	-	
WM-3451	n. a.	n. d.	+	
WM-3453	n. a.	48	-	
WM-3456	n. a.	58	+	
WM-35	female	4	+	
WM-793	male	21	-	exons 42-43
WM-852	male	26	+	
WM-902B	n. a.	<1	-	
WM-98	n. a.	100	+	

11 PUBLICATION LIST

Kaetzke, A., Körner, H., Kneist, S., Eschrich, K. Oral *Actinomyces* isolates forming red colonies on brain heart blood agar can be unambiguously classified as *A. odontolyticus* by macroscopic examination. *J Clin Microbiol* **41**, 3729-31 (2003).

Körner, H., Epanchintsev, A., Berking, C., Schuler-Thurner, B., Speicher, M. R., Menssen, A., Hermeking, H. Digital Karyotyping reveals frequent inactivation of the *dystrophin/DMD* gene in malignant melanoma. *Cell Cycle* **6**(2), 189-98 (2007).

12 ACKNOWLEDGEMENT

I want to thank PD Dr. Heiko Hermeking for the opportunity to do my PhD thesis in his laboratory, for the supervision of my work, helpful discussions and the organization of excellent collaborations with other scientists.

I am sincerely grateful to Dr. Carola Berking not only for providing me with primary melanocytes but also for her enthusiasm and encouragement, for fruitful discussions and her expert advise on melanocytes and melanoma. I also want to include Ursula Nägele who cultured the primary melanocytes and carried out immunohistochemical stainings for dystrophin.

I want to thank Dr. Michael Speicher for the great collaboration with M-FISH and CGH analyses, for letting me work in his laboratory, providing me with all the necessary equipment, and last but not least for sorting chromosomes and analyzing data with me. Cora Beier, Dr. Sabine Langer, and Dr. Jürgen Kraus for excellent help with chromosome preparation, hybridization, and image acquisition.

I want to thank Dr. Bettina Kempkes for supporting me during my PhD thesis and participating in my thesis committee.

I am grateful to all my lab colleagues for their daily help and communication. Alex Epanchintsev for the many hours of working together on the dystrophin project and for the sharing of tricks for the generation of the digital karyotyping libraries. Heike Koch and Anne Benzinger for teaching me not only the differences between Schwaben and Franken, the subtleties with Spätzle, Knödel, and Schafkopf but also for becoming true friends.

My special gratitude goes to my sister Christine Körner for patiently leading me through the jungle of statistics and my husband Dima for his love and wonderful cooking.

13 CURRICULUM VITAE**Henrike Körner**

Born 2nd of March, 1978 (Leipzig, Germany)

School Education

1984-1994 Elementary and High School, Leipzig
1994-1995 Foreign exchange student, Chesterland, Ohio, USA
1995-1997 High School, Leipzig

University Education

1997-2002 Studies of Biochemistry, University of Leipzig
Diploma in Biochemistry

2001-2002 Diploma Thesis, University of Leipzig, Medical Faculty, Institute
of Biochemistry
Title: "Charakterisierung von oral-pathogenen Bakterien mit
MALDI-TOF Massenspektrometrie"

Research Experience

1999-2001 University of Leipzig, Medical Faculty, Institute of Biochemistry
Student worker

07-08/2000 Case Western Reserve University, Cleveland, Ohio
Subject: Establishment of a yeast-two-hybrid approach to
investigate the interactions between polyglutamine-containing
proteins

Doctoral Thesis

since 05/2002 Max-Planck Institute of Biochemistry, Molecular Oncology Junior
Research Group, Martinsried, Germany
Title: "Analysis of genomic alterations in malignant melanoma"